VOLUME 35 JANUARY 1957 NUMBER 1

Canadian Journal of Chemistry

Published by THE NATIONAL RESEARCH COUNCIL

OTTAWA CANADA

CANADIAN JOURNAL OF CHEMISTRY

(*Formerly Section B, Canadian Journal of Research*)

Under the authority of the Chairman of the Committee of the Privy Council of Scientific and Industrial Research, the National Research Council issues THE CANADIAN JOURNAL OF CHEMISTRY and six other journals devoted to the publication, in English or French, of the results of original scientific research. Matters of general policy concerning these journals are the responsibility of a joint Editorial Board consisting of: members representing the National Research Council of Canada; the Editors of the Journals; and members representing the Royal Society of Canada and four other scientific societies.

The Chemical Institute of Canada has chosen the Canadian Journal of Chemistry and the Canadian Journal of Technology as its medium of publication for scientific papers.

Manuscripts for publication should be submitted to Dr. Léo Marion, Editor-in-Chief, Canadian Journal of Chemistry, National Research Council, Ottawa 2, Canada.
(For instructions on preparation of copy, see **Notes to Contributors** (inside back cover).)

Proof, correspondence concerning proof, and orders for reprints should be sent to the Manager, Editorial Office (Research Journals), Division of Administration, National Research Council, Ottawa 2, Canada.

Subscriptions, renewals, requests for single or back numbers, and all remittances should be sent to Division of Administration, National Research Council, Ottawa 2, Canada. Remittances should be made payable to the Receiver General of Canada, credit National Research Council.

The journals published, frequency of publication, and prices are:

Canadian Journal of Biochemistry and Physiology	Monthly	$3.00 a year
Canadian Journal of Botany	Bimonthly	$4.00 a year
Canadian Journal of Chemistry	Monthly	$5.00 a year
Canadian Journal of Microbiology	Bimonthly	$3.00 a year
Canadian Journal of Physics	Monthly	$4.00 a year
Canadian Journal of Technology	Bimonthly	$3.00 a year
Canadian Journal of Zoology	Bimonthly	$3.00 a year

The price of single numbers of all journals is 75 cents.

VOLUME 35 1957

Canadian Journal of Chemistry

Published by THE NATIONAL RESEARCH COUNCIL

OTTAWA CANADA

Canadian Journal of Chemistry

Issued by THE NATIONAL RESEARCH COUNCIL OF CANADA

VOLUME 35 JANUARY 1957 NUMBER 1

BIOGENESIS OF ALKALOIDS

XVIII. THE FORMATION OF HORDENINE FROM PHENYLALANINE IN BARLEY[1]

JACQUES MASSICOT[2] AND LÉO MARION

ABSTRACT

When phenylalanine-2-C^{14} was fed to sprouting barley the hordenine isolated from the plant was radioactive. The activity in the hordenine was shown by degradation of the alkaloid to be located on the carbon of the side chain β to the aromatic ring. A fraction of the fatty acids present in the roots was more strongly radioactive than the hordenine and must have arisen by the breakdown of the amino acid. The gramine isolated from the shoots was inert. Phenylalanine does not take part in the synthesis of gramine, but it is a precursor of hordenine and, hence, must be converted to tyrosine in barley. This conclusion is supported by the simultaneous synthesis of a radioactive aliphatic acid.

It has already been shown that in barley tyrosine is decarboxylated to tyramine, which is methylated by methionine first to N-methyltyramine and then to hordenine (5, 6, 7). It is known that in animals phenylalanine is transformed into tyrosine (8, 12) and if this were to occur in barley, then phenylalanine would be a precursor of hordenine. Since the metabolism of phenylalanine can follow other pathways (10) it was of interest to investigate its fate in barley.

When D,L-phenylalanine-2-C^{14} was fed to sprouting barley, the N-methyltyramine and hordenine isolated from the roots were radioactive. Hordenine was converted to O-methylhordenine methiodide, which was subjected to the Hofmann degradation and oxidized to radioactive anisic acid as previously described (5).

It has been shown previously that *p*-vinylanisole containing a C^{14} in the β-position to the vinyl group gives, on oxidation with potassium permanganate, inert anisic acid. If, on the other hand, it is oxidized first with mercuric oxide and iodine, and the oxime of the product further oxidized with potassium permanganate, radioactive anisic acid is obtained (5). This anomaly is due to a well-known rearrangement taking place under the conditions of the mercuric oxide oxidation (5). It can be concluded, therefore, that the C^{14} was present in the side chain of the hordenine in the β-position to the aromatic ring.[3]

The N-methyltyramine isolated with the hordenine was not further examined.

The fraction of the root extract containing the non-nitrogenous acids was much more

[1]*Manuscript received September 11, 1956.*
Contribution from the Division of Pure Chemistry, National Research Council, Ottawa, Canada.
Issued as N.R.C. No. 4148.

[2]*National Research Council of Canada Postdoctorate Fellow, 1955–1956. Attaché de Recherches, C.N.R.S., Lyon, France, on leave of absence.*

[3]*Because of the definite proof of the location of C^{14} in hordenine derived from tyrosine (6) and from tyramine (5), it has been assumed that the label in the present instance would be similarly located, although the proof offered is not as rigorous as previously.*

radioactive than the alkaloids. By chromatography on silica gel, this yielded a fraction eluted by chloroform which had an equivalent weight of 442. It seems to contain a carbonyl as well as one or more carboxyl. It was readily converted to a methyl ester with diazomethane but could not be crystallized nor properly characterized, since it gradually decomposed on standing. Its activity was 6×10^3 d.p.m. per mg.

It has been shown that, in barley, tryptophan is the precursor of gramine (1), and it is known that in *Neurospora*, tryptophan is synthesized from indole and serine (11, 13). Gramine was therefore isolated from the extract of the shoots of the barley to ascertain whether phenylalanine could be a precursor of the indole nucleus. The gramine, however, was inert.

EXPERIMENTAL

Administration of D,L-Phenylalanine-2-C^{14} to the Barley

Barley (Charlottetown No. 80, 720 g.) was evenly divided among 12 Pyrex trays containing glass wool and grown as previously described (4). On the 6th day of sprouting, a solution of D,L-phenylalanine-2-C^{14} (110 mg.) in distilled water (600 ml.) containing hydrochloric acid (0.1 ml.) was fed to the barley. The amino acid administered had a total activity of 1.1×10^8 disintegrations per minute, or a specific activity of 1.6×10^8 d.p.m. per millimole.[4]

Isolation of the Alkaloids from the Roots

The barley was harvested on the 11th day of sprouting, the roots separated from the shoots and extracted with methanol for 48 hours. The evaporated extract was dissolved in 2 *N* sulphuric acid, the solution filtered, extracted with ether (Extract A), and treated as previously described for the isolation of the alkaloids (5). The N-methyltyramine separated from the hordenine by chromatography was not further examined. The hordenine (254 mg., m.p. 117°) was diluted with inactive hordenine, methylated, and subjected to the Hofmann degradation, and the resulting *p*-vinylanisole oxidized with mercuric oxide and iodine, all as previously described (6). The oxime of the homoanisaldehyde produced (m.p. 116–118°) was oxidized with potassium permanganate to radioactive anisic acid (5). Anisic acid was characterized by comparison with an authentic specimen and by preparation of its *p*-toluidide, which was identical with a sample prepared from authentic anisic acid. The activities of the various products are listed in Table I.

TABLE I

ACTIVITIES OF DERIVATIVES AND DEGRADATION PRODUCTS OF HORDENINE

Compound	D.p.m. per millimole
Hordenine	1.78×10^4
O-Methylhordenine methiodide	1.75×10^4
Trimethylamine chloroplatinate	0
Homoanisaldehyde oxime	1.53×10^4
Anisic acid	1.47×10^4
Anisic acid *p*-toluidide	1.50×10^4

Isolation of Acids

Extract A, which had been obtained in the course of the isolation of the alkaloids, yielded on evaporation a black resin soluble in ethanol, but only partially soluble in

[4]*D,L-Phenylalanine-2-C^{14} was purchased from Tracerlab, Inc.*

benzene. The resinous residue contained no nitrogen, and was strongly radioactive. It was triturated with benzene at room temperature and the benzene-soluble fraction was chromatographed on a column of silica. The column was eluted by being washed first with carbon tetrachloride and then with chloroform. The carbon tetrachloride eluate consisted of a very small fraction containing little activity and was discarded. The main fraction with the highest radioactivity per milligram was eluted by chloroform. It consisted of a clear yellow product with an activity about forty times that of the purified hordenine. It contained no nitrogen and decomposed on standing, becoming after a few days only partially soluble in benzene. Its equivalent weight, determined by electrometric titration with alkali, was 442. The acid could not be induced to crystallize and, because of its instability, could not be characterized. Methylation with diazomethane gave rise to a methyl ester which remained oily. Found: C, 70.10; H, 10.03%. The acid discolored potassium permanganate rapidly and with 2,4-dinitrophenylhydrazine gave rise to an amorphous, insoluble product. The ultraviolet spectrum of the acid contained a maximum at 289 mμ as well as one at < 215 mμ attributable to the carboxylic group. The acid is probably a long-chain unsaturated acid containing a carbonyl group but, because of paucity of material could not be further identified.

The activities of the various fractions obtained from the root extract are given in Table II. The only two fractions studied were the alkaloids and non-nitrogenous acids.

TABLE II

ACTIVITIES OF FRACTIONS OF ROOT EXTRACT

Compound	Weight, mg.	Total activity, d.p.m.	Activity per mg., d.p.m.
Crude amines	818	2.64×10^5	320
Hordenine	254	3.4×10^4	134
Crude acids	470	1.3×10^6	2700
Main acid fraction	95	5.7×10^5	6000
Phenols	895	Not determined	
Lipids, sterols, etc.	1200	3.6×10^5	285

Gramine

The shoots of the plants, which had been separated from the roots, were extracted with methanol and the gramine was isolated from the extract by the procedure already described (1). The gramine was inactive.

DISCUSSION

In barley, phenylalanine, just like tyrosine (6) and tyramine (5), is a precursor of hordenine. It is known that in animals phenylalanine is converted to tyrosine (8, 12) and, further, it has been shown that tyrosine is decarboxylated in the plant and that the resulting tyramine is methylated by methionine first to N-methyltyramine and then to hordenine (5, 6, 7). It can be presumed, therefore, that, in barley, phenylalanine is first converted to tyrosine.

Gramine isolated from the shoots of the barley was not radioactive and it can be concluded that phenylalanine is not a precursor of the indole nucleus in barley or at least of the tryptophan since it is known that tryptophan is the precursor of gramine (1).

Phenylalanine is the precursor of a long-chain acid in barley. Although the identity of this acid has not been established, it appears to be an unsaturated keto acid in which

no aromatic groups seem to be present. Phenylalanine can be metabolized via tyrosine with scission of the aromatic ring to produce the intermediates homogentisic acid and fumarylacetoacetic acid, which finally give rise to acetoacetic acid (3, 9). Acetoacetic acid derived from phenylalanine could then be a precursor of the long-chain acid. Indeed, it has been shown that acetoacetic acid can give rise to fatty acids without going through acetic acid (2). In the absence of more exact knowledge of the identity of the radioactive acid, any suggestion as to the intermediate steps between it and phenylalanine or tyrosine is mere speculation. The relatively high radioactivity of the acid, however, seems to indicate that it is very actively synthesized during the early growth of the plant. The formation of the aliphatic acid supports the conclusion derived from the biosynthesis of hordenine that in barley phenylalanine is converted to tyrosine.

ACKNOWLEDGMENT

The authors are indebted to Mr. R. B. MacLaren of the Experimental Station, Charlottetown, P.E.I., for supplying the barley used in these experiments.

REFERENCES

1. Bowden, K. and Marion, L. Can. J. Chem. **29**, 1037 (1951).
2. Buchanan, J. M., Sakami, W., and Gurin, S. J. Biol. Chem. **169**, 411 (1947).
3. Dische, R. and Rittenberg, D. J. Biol. Chem. **211**, 199 (1954).
4. Kirkwood, S. and Marion, L. Can. J. Chem. **29**, 30 (1951).
5. Leete, E., Kirkwood, S., and Marion, L. Can. J. Chem. **30**, 749 (1952).
6. Leete, E. and Marion, L. Can. J. Chem. **31**, 126 (1953).
7. Matchett, T. J., Marion, L., and Kirkwood, S. Can. J. Chem. **31**, 488 (1953).
8. Moss, A. R. and Schoenheimer, P. J. Biol. Chem. **135**, 415 (1940).
9. Ravdin, R. G. and Crandall, D. I. J. Biol. Chem. **189**, 137 (1951).
10. Shambaugh, N. F., Lewis, H. B., and Tourtellotte, D. J. Biol. Chem. **192**, 499 (1951).
11. Tatum, E. L. and Bonner, D. M. Proc. Natl. Acad. Sci. U.S. **30**, 30 (1944).
12. Udenfriend, S. and Cooper, J. R. J. Biol. Chem. **194**, 503 (1952).
13. Umbreit, W. W., Wood, W. A., and Gunsalus, I. C. J. Biol. Chem. **165**, 731 (1946).

THE SOLUBILITY OF URANIUM(IV) HYDROXIDE IN SOLUTIONS OF SODIUM HYDROXIDE AND PERCHLORIC ACID AT 25° C.[1]

K. H. GAYER AND H. LEIDER

ABSTRACT

The solubility of uranium(IV) hydroxide has been measured in sodium hydroxide, water, and perchloric acid solutions. A possible reaction in sodium hydroxide solutions is evaluated.

The purpose of this investigation was to measure the solubility of uranium(IV) hydroxide in dilute basic and dilute acidic media. Information pertaining to this subject is not available at this time in the literature except for the following:

Kraus and Nelson (3) investigated the hydrolytic behavior of uranium(IV) ions in excess perchloric acid (above 0.2 *M*) and in solutions of constant ionic strength ($\mu = 0.5$). They concluded that the simple ion U^{+4} exists in excess acid and is associated with eight water molecules, $U(H_2O)_8^{+4}$, and that the principal hydrolysis reaction is

$$U^{+4} + H_2O \rightleftharpoons U(OH)^{+3} + H^+.$$

$$pK = 1.44$$

where $pK = -\log [IV]_1$, and $[IV]_1 = [UOH^{+3}][H^+]/[U^{+4}]$.

Their results did not indicate an ion type such as UO^{++}.

They also found that uranium(IV) ions show a tendency to form rather stable polymeric solutions on hydrolysis, where the polymeric form has an approximate composition of $U(OH)_4$. When uranium(IV) hydroxide is dissolved in a non-complexing acid, such as perchloric, solutions containing polymeric products result. The difference in color between the simple solution and the polymeric form is very marked, being bright green for the former and almost black for the latter.

PROCEDURE

The general procedure is similar to that described by Garrett and Heiks (2). An all glass apparatus was used.

Water.—Conductivity water was prepared in a Barnstead conductivity still, degassed by being boiled with nitrogen bubbling through it, and then stored under nitrogen.

Perchloric acid solutions.—Approximately 1 molar acid was prepared from 70% G. F. Smith purified perchloric acid with degassed conductivity water and stored under nitrogen. Standard acid solutions were also made with conductivity water and standardized against standard sodium hydroxide.

Sodium hydroxide solutions.—Approximately 1 molar solutions of base were prepared under nitrogen by dissolving Baker and Adamson reagent pellets in degassed conductivity water in a paraffined flask. Barium hydroxide was added to just precipitate any carbonate, and the solutions were stored under nitrogen. Standard base solutions were also prepared with conductivity water and standardized against potassium acid phthalate using phenolphthalein indicator.

[1]*Manuscript received July 16, 1956.*

Contribution from the Department of Chemistry, Wayne State University, Detroit, Michigan. From a dissertation submitted by Mr. Herman Leider in partial fulfillment of the requirements for the Doctor of Philosophy degree at Wayne University.

Uranium(IV) sulphate.—Crystalline uranium(IV) sulphate was prepared by the reduction of acid solutions of uranyl sulphate with Eastman Kodak sodium dithionite (1). The precipitated sulphur was filtered off and uranium(IV) hydroxide was precipitated with excess sodium hydroxide. The product was washed with distilled water until the absence of a sodium flame test, and then dissolved in Baker and Adamson A. C. S. standard sulphuric acid, and filtered. The sulphate solution was evaporated until crystals of $U(SO_4)_2.4H_2O$ deposited. The crystals were filtered, dried, analyzed for uranium by 8-hydroxyquinoline precipitation, and ignited to U_3O_8. Calculated % uranium is 47.4; found % uranium equals 47.6. Solutions of the sulphate were made by dissolving the crystals in degassed conductivity water and then stored under nitrogen.

Colorimetric reagents.—A standard uranium solution was prepared by dissolving stoichiometric $UO_3.H_2O$ (prepared from hydrolysis of uranyl acetate by boiling) in perchloric acid. Aliquot portions of this solution were used to prepare the color standards. A 10% sodium hydroxide solution was prepared from Baker and Adamson reagent pellets and distilled water. A 20% sodium carbonate solution was prepared with Baker and Adamson anhydrous reagent and distilled water. Baker and Adamson 30% hydrogen peroxide was used in preparing colorimetric solutions.

Uranium(IV) hydroxide.—The hydroxide used in making samples for the acid series was precipitated from the sulphate solution with sodium hydroxide and washed with degassed conductivity water. Absence of a sodium flame test indicated completed washing.

Uranium(IV) hydroxide used in preparing basic samples was made by reacting sodium hydroxide with crystalline $U(SO_4)_2.4H_2O$. In all other respects the treatment was the same as that just described. Such a preparation was necessary because the gelatinous hydroxide precipitated from solution was extremely sensitive to oxidation in alkaline medium. The dense hydroxide prepared from crystalline sulphate proved much more stable to oxidation and could be handled more easily. In order to eliminate any possibility of oxidation the system was kept under a nitrogen pressure of 4 to 5 lb. above that of the atmosphere.

Analysis showed that the solid phase was unchanged after equilibration with acid or base.

Equilibration.—Pairs of 100 ml. samples of the hydroxide in acid or base were collected in 125 ml. sample flasks under nitrogen. One of each pair was agitated in a 35° thermostat for 5 to 7 days, followed by agitation in a 25° thermostat for 5 to 7 days. The other member of each pair was directly agitated in the 25° thermostat for 5 to 7 days. After the agitation in the 25° C. thermostat, the samples were allowed to settle for 3 to 5 days.

Uranium analyses.—The uranium analyses was made with a Beckman Model B spectrophotometer using the $NaOH–Na_2CO_3–H_2O_2$ method described in *Analytical Chemistry of the Manhattan Project* (4).

THE DATA

The data are collected in Tables I and II. Owing to the polymeric nature of the acid solubility products no definite reactions or ionic species can be evaluated and proved to occur.

Assuming that the formula for solid uranium(IV) hydroxide can be represented by

TABLE I

SOLUBILITY OF URANIUM(IV) HYDROXIDE IN $HClO_4$ SOLUTIONS AT 25° C.*

Initial moles $HClO_4$/ 1000 g. H_2O	Moles uranium/1000 g. H_2O at equilibrium
3.9×10^{-2}	2.2×10^{-2}
9.6	5.7
1.4×10^{-1}	6.7
1.9	9.5
2.9	1.5×10^{-1}
3.9	2.1

**Each set of values is actually the average of two experiments which agreed within 10% or less.*

TABLE II

SOLUBILITY OF URANIUM(IV) HYDROXIDE IN NaOH SOLUTIONS AT 25° C.*

Moles NaOH/1000 g. H_2O at equilibrium	Moles uranium/1000 g. H_2O at equilibrium	$K\times10^4$
0	3.0×10^{-4}	—
0.080	6.3×10^{-4}	—
0.144	2.7×10^{-4}	1.9
0.215	4.1	1.9
0.266	4.5	1.7
0.484	7.0	1.4
0.632	5.9	—
		Average $K = 1.7\times10^{-4}$

**Each set of values is actually the average of two experiments which agreed within 10% or less.*

$U(OH)_4$, we believe that the reaction in basic solution over the range studied (0.1 molal to 0.5 molal) can be written as follows:

$$U(OH)_4 + OH^- \rightleftarrows H_3UO_4^- + H_2O.$$

Evidence for this reaction comes from (1) the fair constancy of the equilibrium constant, (2) the extremely low solubility of the oxide, and (3) the high equilibrium sodium hydroxide concentrations.

In calculating the equilibrium constant it was assumed
(1) that

$$\gamma_{H_3UO_4^-}/\gamma_{OH^-} = 1,$$

(2) that the dissolved uranium all occurred as $H_3UO_4^-$. This latter assumption is not improbable since the solubility is very low.

ACKNOWLEDGMENT

The authors gratefully wish to acknowledge the support of U.S. Atomic Energy, Project No. AT (11-1)-214 in sponsoring this work.

REFERENCES

1. ALOY AUBER, J. Bull. soc. chim. France, **1** (4), 569 (1907).
2. GARRETT, A. B. and HEIKS, R. E. J. Am. Chem. Soc. **63**, 562 (1941).
3. KRAUS, K. A. and NELSON, F. AECD-1888, March 15, 1948 (date declassified).
4. RODDEN, C. J. Analytical chemistry of the Manhattan project, McGraw-Hill Book Company, Inc., New York, 1950. p. 93.

A NEW SYNTHESIS OF 1-SUBSTITUTED-2,3,5,6-TETRAHYDRO-1-IMIDAZ(1,2-a)IMIDAZOLES[1]

A. F. McKay and D. L. Garmaise

ABSTRACT

A number of 1-(β-hydroxyethyl)-2-(substituted amino)-2-imidazolines have been prepared by the reaction of amines with 1-(β-hydroxyethyl)-2-methylmercapto-2-imidazoline. These intermediates on chlorination and dehydrochlorination give the corresponding 1-substituted-2,3,5,6-tetrahydro-1-imidaz(1,2-a)imidazoles.

Recently (2) the preparations of 1-benzyl- and 1-β-diisopropylaminoethyl-2,3,5,6-tetrahydro-1-imidaz(1,2-a)imidazoles by the reaction of benzylamine and β-diisopropylaminoethylamine with 1-(β-chloroethyl)-2-nitriminoimidazolidine were described. This work presents another new method of preparing 1-substituted-2,3,5,6-tetrahydro-1-imidaz(1,2-a)imidazoles (IV) which involves the reaction of an amine with 1-(β-hydroxyethyl)-2-methylmercapto-2-imidazoline (I) (1, 3).

1-(β-Hydroxyethyl)-2-methylmercapto-2-imidazoline (I) or its hydroiodide salt condenses with amines with the liberation of methyl mercaptan. This reaction proceeds smoothly to give good yields of the 1-(β-hydroxyethyl)-2-(substituted amino)-2-imidazolines (II). The properties of some of these intermediates and/or their derivatives are described in Table I. Some of the 1-(β-hydroxyethyl)-2-(substituted amino)-2-imidazolines could be distilled *in vacuo* without decomposition to give good yields of purified products whereas others such as 1-(β-hydroxyethyl)-2-(β-dimethylaminoethylamino)-2-imidazoline and 1-(β-hydroxyethyl)-2-(β-di-*n*-propylaminoethylamino)-2-imidazoline partially cyclized and partially decomposed. The water liberated during the cyclization reaction is thought to be responsible for the observed degradation. The crude or purified 1-(β-hydroxyethyl)-2-(substituted-amino)-imidazolines were converted into their cor-

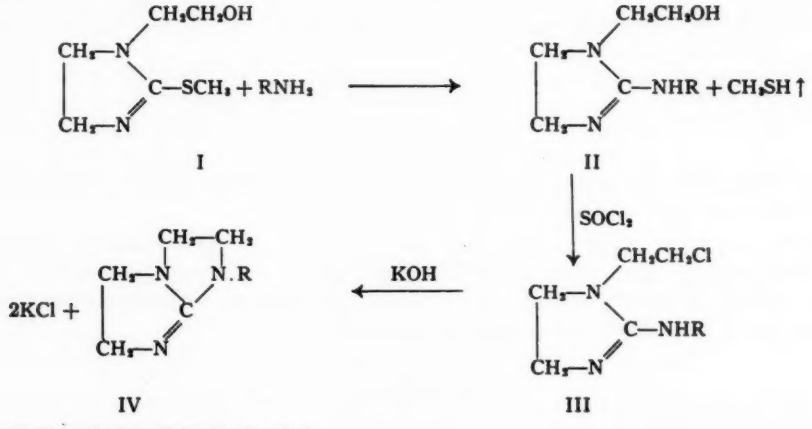

R = alkyl, aralkyl, or dialkylaminoalkyl

[1]*Manuscript received September 6, 1956.*
Contribution from the L. G. Ryan Research Laboratories of Monsanto Canada Limited, Montreal, Quebec.

TABLE I

1-(β-HYDROXYETHYL)-2-(SUBSTITUTED AMINO)-2-IMIDAZOLINES

Substituent	Yield, %	M.p., °C. or b.p., °C. (mm.)	Formula	C		H		N	
				Calc.	Found	Calc.	Found	Calc.	Found
n-Butyl	99.7	97–98	$C_9H_{19}N_3O$	58.34	58.37	10.34	10.29	22.60	22.50
	89.5	84–85[a]	$C_{15}H_{23}N_3O_8$	43.47	43.81	5.35	5.41	20.29	20.58
n-Octyl	54.5	118–119[b]	$C_{21}H_{41}N_3O_8$	62.10	62.08	6.89	6.83	7.01	6.98
n-Dodecyl	86.5	100–102[c]	$C_{28}H_{46}N_4OS$	66.61	66.61	9.32	9.38	12.95	13.15
n-Tetradecyl	100.0	114–116[b]	$C_{27}H_{53}N_3O_8$	65.00	65.01	7.80	7.85	6.14	6.05
n-Hexadecyl	99.9	110–111[b]	$C_{29}H_{57}N_3O_8$	65.88	66.17	8.07	8.29	5.91	6.01
n-Octadecyl	94.2	62–63	$C_{23}H_{47}N_3O$	72.38	72.05	12.42	12.20	11.01	11.04
Benzyl	100.0	147–148[d]	$C_{12}H_{18}ClN_3O$	56.35	56.36	7.08	7.28	16.43	16.40
		124–125[a]	$C_{18}H_{20}N_6O_8$	48.22	47.96	4.50	4.62	18.85	19.00
β-Phenylethyl	92.2	118–119[a]	$C_{19}H_{22}N_6O_8$	49.36	49.46	4.80	4.60	18.18	18.12
β-Dimethylaminoethyl	90.7	160–164(0.05)[e]							
β-Diethylaminoethyl	69.1	166–167(0.20)	$C_{11}H_{24}N_4O$	57.86	58.01	10.59	10.26	24.54	24.21
	67.0	166–167[a]	$C_{23}H_{30}N_{10}O_{15}$	40.23	40.54	4.40	4.49	20.40	20.33
γ-Dimethylamino-propyl	71.5	183–184(3.0)	$C_{10}H_{22}N_4O$	56.04	55.88	10.35	10.43	26.20	26.10
		125–126[a]	$C_{22}H_{32}N_{10}O_{14}$	39.28	39.55	4.20	4.35	20.80	20.40
γ-Diethylaminopropyl	65.0	164–165(0.20)	$C_{12}H_{26}N_4O$	59.45	59.21	10.82	11.02	23.12	22.85

[a] *Picrates.* [b] *Dibenzoyl-d-tartrates.* [c] *Phenylisothiocyanate derivative,* S *calc., 7.41; found, 7.20%.* [d] *Hydrochloride salt,* Cl *calc., 13.86; found, 13.90%.* [e] *Some cyclization occurred during distillation.*

TABLE II

1-SUBSTITUTED-2,3,5,6-TETRAHYDRO-1-IMIDAZ(1,2-a)IMIDAZOLES

Substituent	Yield, %	n_D^{25}	d_4^{22}	B.p., °C. (mm.)	Formula	C		H		N	
						Calc.	Found	Calc.	Found	Calc.	Found
n-Octyl	37.0	1.4857	0.959	115–117(0.05)	$C_{13}H_{26}N_2$	69.90	70.07	11.29	11.16	18.81	18.52
n-Dodecyl	45.2	1.4842	0.945	143–145(0.08)	$C_{17}H_{34}N_2$	73.05	73.00	11.95	11.58	15.04	14.83
n-Tetradecyl	44.7	1.4832	0.937	172–173(0.08)	$C_{19}H_{37}N_2$	74.21	74.43	12.13	11.88	13.67	13.39
n-Hexadecyl[a]	67.7	—	—	188–190(0.07)	$C_{21}H_{41}N_2$	75.16	75.01	12.34	12.34	12.52	12.35
n-Octadecyl[b]	60.0	—	—	227–228(0.2)	$C_{23}H_{46}N_2$	75.97	75.81	12.48	12.38	11.56	11.61
Benzyl[c]	70.0	1.5705	1.109	124–126(0.1)							
β-Phenylethyl	44.0	1.5609	1.101	122–214(0.05)	$C_{13}H_{17}N_2$	72.53	72.14	7.96	8.29	19.52	19.79
β-Dimethylaminoethyl	50.0	1.5008	1.018	—	$C_9H_{18}N_4$	59.29	59.22	9.95	9.58	30.74	30.50
β-Diethylaminoethyl		1.4984	1.002	100–102(0.05)	$C_{11}H_{22}N_4$	62.81	62.60	10.55	10.35	26.64	26.31
β-Di-*n*-propylaminoethyl	44.8	1.4938	0.986	106–108(0.05)	$C_{13}H_{26}N_4$	65.50	65.43	10.99	10.81	23.50	23.26
γ-Dimethylaminopropyl	52.5	1.5033	1.013	119–121(0.25)	$C_{10}H_{20}N_4$	61.17	61.01	10.27	10.26	28.54	28.32
γ-Diethylaminopropyl	39.8	1.4942	0.980	121–123(0.2)	$C_{12}H_{24}N_4$	64.26	64.09	10.77	10.97	24.98	24.70

[a]*M.p. 33–34° C.* [b]*M.p. 36–37° C.* [c]*M.p. 40.5° C. (3).*

TABLE III

PICRATES OF 1-SUBSTITUTED-2,3,5,6-TETRAHYDRO-1-IMIDAZ(1,2-a)IMIDAZOLES

Substituent	M.p., °C.	Formula	C		H		N	
			Calc.	Found	Calc.	Found	Calc.	Found
n-Octyl	75–76	$C_{19}H_{28}N_6O_7$	50.43	50.48	6.24	6.14	18.57	18.27
n-Dodecyl	65–66	$C_{23}H_{36}N_6O_7$	54.30	54.50	7.13	7.35	16.52	16.69
n-Tetradecyl	75–76	$C_{25}H_{40}N_6O_7$	55.94	56.16	7.51	7.58	15.66	15.56
n-Hexadecyl	78–79	$C_{27}H_{44}N_6O_7$	57.42	57.53	7.85	7.87	14.88	14.60
n-Octadecyl	86–87	$C_{29}H_{48}N_6O_7$	58.78	58.83	8.16	8.15	14.15	14.01
Benzyl	123–124	$C_{19}H_{18}N_6O_7$	50.13	49.97	4.21	4.40	19.53	19.70
β-Phenylethyl	145–146	$C_{20}H_{20}N_6O_7$	51.35	51.61	4.54	4.76	18.92	19.11
β-Dimethylaminoethyl	172–173	$C_{21}H_{24}N_{10}O_{14}$	39.36	39.81	3.78	3.98	21.87	22.30
β-Diethylaminoethyl	172–173	$C_{23}H_{28}N_{10}O_{14}$	41.30	41.33	4.22	4.26	20.95	21.29
β-Di-*n*-propylaminoethyl	169–170	$C_{25}H_{32}N_{10}O_{14}$	43.12	43.31	4.63	4.72	20.11	19.84
γ-Dimethylaminopropyl	157–158	$C_{22}H_{26}N_{10}O_{14}$	40.36	40.10	4.00	4.13	21.40	21.20
γ-Diethylaminopropyl	139–140	$C_{24}H_{30}N_{10}O_{14}$	41.93	42.22	4.45	4.43	20.40	20.50

responding 1-(β-chloroethyl)-2-(substituted amino)-2-imidazolinium chlorides by chlorination with thionyl chloride. These chloro derivatives, with the exception of 1-(β-chloroethyl)-2-benzylamino-2-imidazoline, were used for the next stage of synthesis without further purification. They were dehydrochlorinated to give the 1-substituted-2,3,5,6-tetrahydro-1-imidaz(1,2-a)imidazoles (IV). Some of the yields reported in Table II are low because of the partial degradation encountered in the distillation of the intermediates. It was observed that the over-all yields of the bicyclic compounds (IV) were much higher when the intermediate 1-(β-hydroxyethyl)-2-(substituted amino)-2-imidazolines were used directly without preliminary distillation. The properties of the 1-substituted-2,3,5,6-tetrahydro-1-imidaz(1,2-a)imidazoles and their picrates are given in Tables II and III respectively.

1-(β-Dimethylaminoethyl)- and 1-(β-diethylaminoethyl)-2,3,5,6-tetrahydro-1-imidaz(1,2-a)imidazoles were methylated with methyl iodide. These compounds combined with 2 mole equivalents of methyl iodide to give derivatives whose analytical values are in good agreement with those calculated for structure (V).

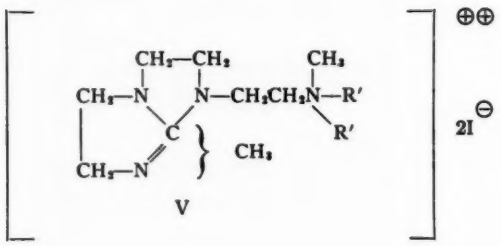

V

R′ = CH_3 or C_2H_5

EXPERIMENTAL[1]

1-(β-Hydroxyethyl)-2-methylmercapto-2-imidazolinium Iodide

1-(β-Hydroxyethyl)-2-methylmercapto-2-imidazolinium iodide (m.p. 120–121° C.) was prepared in 95% yield as previously (3) described.

1-Substituted-2,3,5,6-tetrahydro-1-imidaz(1,2-a)imidazoles

The procedures for the preparations of the 1-substituted-2,3,5,6-tetrahydro-1-imidaz(1,2-a)imidazoles are very similar and only three variations in procedure are described below in detail. Tables II and III list the physical properties of the 1-substituted-2,3,5,6-tetrahydro-1-imidaz(1,2-a)imidazoles and their picrates respectively.

1-Benzyl-2,3,5,6-tetrahydro-1-imidaz(1,2-a)imidazole

A solution of 1-(β-hydroxyethyl)-2-methylmercapto-2-imidazolinium iodide (144 g., 0.50 mole) and benzylamine (55.0 g., 0.52 mole) in 240 cc. of methanol was refluxed for 1½ hours. The methanol was removed by evaporation and the residue in water (2% solution) was passed through a column of IRA–400 (1 liter) resin. This column was washed with water and the washings and eluate were combined and acidified with hydrochloric acid solution. On evaporation of the aqueous solution 1-(β-hydroxyethyl)-2-benzylamino-2-imidazolinium chloride (m.p. 142–147° C.) was obtained in quantitative yield. A sample was prepared for analysis by crystallization twice from a methanol –

[1]*All melting points are uncorrected. Microanalyses were performed by Micro Tech Laboratories, Skokie, Illinois.*

ethyl acetate solution. The final melting point was 147–148° C. Its picrate prepared in the usual manner melted at 124° C. (3).

1-(β-Hydroxyethyl)-2-benzylamino-2-imidazolinium chloride (16.0 g., 0.062 mole) and thionyl chloride (14.0 g., 0.118 mole) in 50 cc. of chloroform were refluxed together for 3 hours. After the excess thionyl chloride and chloroform were removed by distillation, a reddish oil was obtained in quantitative yield. A portion (0.3 g.) of this oil was converted into its picrate melting at 137–138° C. This melting point was not increased on further crystallization. Calc. for $C_{18}H_{19}Cl\,N_6O_7$: C, 46.30; H, 4.11; Cl, 7.59; N, 18.24%. Found: C, 46.35; H, 4.30; Cl, 7.89; N, 18.00%.

The remainder of the reddish oil, 1-(β-chloroethyl)-2-benzylamino-2-imidazolinium chloride, was refluxed for 2 hours in a solution of potassium hydroxide (10.0 g., 0.178 mole) in absolute methanol (150 cc.). The precipitated potassium chloride was removed by filtration and the filtrate was evaporated to dryness. The residue was extracted with ether (2 × 50 cc.) and the ethereal solution on evaporation gave 8.8 gm. (70%) of oil. This oil (b.p. 124–126° C. at 0.1 mm.) was distilled *in vacuo* using a Vigreux column. Its picrate melted at 123–124° C. The picrate of 1-benzyl-2,3,5,6-tetrahydro-1-imidaz(1,2-a)imidazole was previously reported (2) to melt at 109–109.5° C. A mixture melting point determination with these two picrates gave a melting point of 123° C. When the low melting picrate was dissolved in water and then seeded with the high melting form, it gave the picrate melting at 123–124° C. It appears that this picrate is dimorphous. Both picrates gave good analytical values for the monopicrate of 1-benzyl-2,3,5,6-tetrahydro-1-imidaz(1,2-a)imidazole.

1-n-Tetradecyl-2,3,5,6-tetrahydro-1-imidaz(1,2-a)imidazole

1-(β-Hydroxyethyl)-2-methylmercapto-2-imidazolinium iodide (86.4 g., 0.30 mole) and *n*-tetradecylamine (63.9 g., 0.30 mole) were refluxed for 3 hours in 200 cc. of methanol. This solution was diluted with 600 cc. of methanol and then it was passed through a column of IRA–400 resin (1000 cc., previously washed with 800 cc. of methanol) at a rate of 8 cc. per minute. The column was washed with methanol (1200 cc.) until the eluate gave no further positive test with picric acid solution. The eluate and washing were combined and evaporated to dryness, yield 97.5 g. (100%). Part (65 g., 0.20 mole) of this residue was converted into its hydrochloride. The dry hydrochloride was dissolved in 200 cc. of dry benzene and thionyl chloride (47.6 g., 0.4 mole). After this solution had refluxed for 2 hours, the excess thionyl chloride and solvent were removed by evaporation. This procedure gave a quantitative yield of the intermediate 1-(β-chloroethyl)-2-*n*-tetradecylamino-2-imidazolinium chloride.

1-(β-Chloroethyl)-2-*n*-tetradecylamino-2-imidazolinium chloride in a solution of potassium hydroxide (24.7 g., 0.442 mole) in 425 cc. of absolute alcohol was refluxed for 3 hours. The resulting mixture was worked up as described in the procedure above for 1-benzyl-2,3,5,6-tetrahydro-1-imidaz(1,2-a)imidazole. A black oily residue was obtained, yield 50.5 g. (82.4%). Fractional distillation using a Vigreux column setup yielded 27.4 g. of colorless oil (b.p. 172–173° C. at 0.08 mm.). Its picrate melted at 75–76° C. after two crystallizations from ether.

1-(Di-n-propylaminoethyl)-2,3,5,6-tetrahydro-1-imidaz(1,2-a)imidazole

1-(β-Hydroxyethyl)-2-methylmercapto-2-imidazolinium iodide (40.0 g., 0.115 mole) was condensed with N,N′-di-*n*-propyl ethylenediamine (17.3 g., 0.12 mole) under the conditions described above for the preparation of 1-(β-hydroxyethyl)-2-benzylamino-2-imidazoline and the condensation product was dissolved in 100 cc. of water. This aqueous

solution was passed through a column of highly active IRA–400 resin (450 cc.) at a rate of 25 cc. per minute. After the column was washed with water (2000 cc.), the combined washings and eluate were evaporated to dryness, yield 29.0 g. (98%). This oily product on distillation *in vacuo* underwent extensive decomposition giving 5 g. of di-*n*-propylaminoethylamine. One fraction (b.p. 114–123° C. at 0.05 mm.) gave a picrate melting at 169–170° C., which was identified as the picrate of the bicyclic product, 1-(di-*n*-propylaminoethyl)-2,3,5,6-tetrahydro-1-imidaz(1,2-a)imidazole, yield 1.2 g.

Another fraction (b.p. > 123° C. at 0.05 mm.) (6 g.), which appeared to be a mixture of 1-(β-hydroxyethyl)-2-(di-*n*-propylaminoethylamino)-2-imidazoline and the bicyclic product, was converted into the bicyclic product by the procedure described in the above examples. The oily product (b.p. 106–108° C. at 0.05 mm.) was obtained in 44.8% yield based on the over-all conversion of 1-(β-hydroxyethyl)-2-methylmercapto-2-imidazolinium iodide into 1-(di-*n*-propylaminoethyl)-2,3,5,6-tetrahydro-1-imidaz(1,2-a)imidazole. The picrate of the latter compound formed in the usual manner melted at 169–170° C. It was purified by crystallization from ethanol.

Methylation of 1-(β-Dimethylaminoethyl)-2,3,5,6-tetrahydro-1-imidaz(1,2-a)imidazole

A solution of 4.8 g. (0.0247 mole) of 1-(β-dimethylaminoethyl)-2,3,5,6-tetrahydro-1-imidaz(1,2-a)imidazole and 14.2 g. (0.10 mole) of methyl iodide in 50 cc. of absolute alcohol was refluxed for 1 hour. This solution on evaporation of solvent and excess methyl iodide gave 11.5 g. (93.5%) of a crystalline solid (m.p. 160–170° C.). Several crystallizations from various solvents always gave crystals melting over a range (m.p. 155–170° C.). However, after drying at 64° C. *in vacuo*, the crystals had a melting point of 234–236° C. Anal. Calc. for $C_{11}H_{24}I_2N_4$: C, 28.33; H, 5.19; I, 54.45; N, 12.02%. Found: C, 28.36; H, 5.16; I, 54.29; N, 11.99%.

The dipicrate (m.p. 205–206° C.) of the dimethiodide of 1-(β-dimethylaminoethyl)-2,3,5,6-tetrahydro-1-imidaz(1,2-a)imidazole was prepared in the usual manner. Anal. Calc. for $C_{23}H_{28}N_{10}O_{14}$: C, 41.31; H, 4.22; N, 20.95%. Found: C, 41.03; H, 4.01; N, 21.39%.

Dimethiodide of 1-(β-Diethylaminoethyl)-2,3,5,6-tetrahydro-1-imidaz(1,2-a)imidazole

The dimethiodide of 1-(β-diethylaminoethyl)-2,3,5,6-tetrahydro-1-imidaz(1,2-a)imidazole (m.p. 180–200° C.) was prepared in 97% yield by the procedure described above for preparing the dimethiodide of 1-(β-dimethylaminoethyl)-2,3,5,6-tetrahydro-1-imidaz(1,2-a)imidazole. Four recrystallizations from methanol – ethyl acetate (1:3) solution raised the melting point to a constant value of 228–230° C. Anal. Calc. for $C_{13}H_{28}I_2N_4$: C, 31.59; H, 5.71; I, 51.37; N, 11.34%. Found: C, 31.71; H, 5.83; I, 51.15; N, 11.31%.

The dipicrate formed in the usual manner melted at 190–191° C. after two crystallizations from alcohol. Anal. Calc. for $C_{25}H_{32}N_{10}O_{14}$: C, 43.09; H, 4.63; N, 20.11%. Found: C, 43.12; H, 4.48; N, 19.83%.

ACKNOWLEDGMENT

The authors are pleased to acknowledge the skillful technical assistance of Miss E. Laycock of these laboratories.

REFERENCES

1. ASPINALL, S. R. and BIANCO, E. J. J. Am. Chem. Soc. **73**, 602 (1951).
2. MCKAY, A. F. and GILPIN, J. R. J. Am. Chem. Soc. **78**, 486 (1956).
3. MCKAY, A. F. and VAVASOUR, G. R. Can. J. Chem. **32**, 59 (1954).

THE STRUCTURE OF ARTIFICIAL GRAPHITES AS REVEALED BY X-RAY, ELECTRON MICROSCOPE, AND ADSORPTION STUDIES[1]

L. G. WILSON AND H. L. MCDERMOT

ABSTRACT

Three artificial graphites have been studied by X-ray, electron microscope, and adsorption techniques. Surface areas were calculated from the adsorption isotherms and from the X-ray spectra. The two sets of areas were of the same order of magnitude and varied from 18 m.²/g. for the graphite of smallest surface area to 385 m.²/g. for the graphite of largest surface area. The appearance of the graphites under the electron microscope was in qualitative agreement with the adsorption and X-ray data.

INTRODUCTION

Two previous papers (4, 5) on the adsorption of gases by graphite have shown that the artificial graphites studied were porous adsorbents which displayed Type II isotherms in the B.E.T. classification. It was also found that the graphites displayed two types of hysteresis. The first type, which was observed at high relative pressures (above $p/p_0 = 0.5$), was associated with the porous structure of the graphite. The second type, seen at relative pressures below $p/p_0 = 0.5$, was attributed to intercrystalline swelling. In every case, the isotherms were smooth Type II isotherms without any of the humps which have become associated with homogeneous surfaces (1). Hence, it was concluded that these graphites presented heterogeneous surfaces to gases at liquid nitrogen temperatures. These effects were observed with graphites varying in area from 20 m.²/g. to approximately 100 m.²/g. Finally, it was shown that the above phenomena were associated solely with the graphite and were not caused by traces of inorganic material present in the graphites.

Early X-ray studies of graphite (7) showed the crystal to be composed of layers of coplanar carbon atoms arranged in hexagons. The layers were separated by distances which were large compared with the interatomic distances within each layer. This classical structure was termed hexagonal holohedral. Atoms within the plane were 1.42 Å apart and the planes were separated by 3.34 Å.

The unit cell was hexagonal with

$a = 2.456$ Å, $c = 6.696$ Å, and the four atoms in the following two sets of special positions of $C6mc$:

(*a*) $0, 0, u; 0, 0, u+\frac{1}{2}$,

(*b*) $1/3, 2/3, v; 2/3, 1/3, v+\frac{1}{2}$ with $u \simeq 0$ and $v \not> 0.05$.

The packing in the crystal is such that half the carbon atoms in adjacent layers lie over one another (*A* atoms) while the other half (*B* atoms) lie over empty hexagon centers. This packing is designated *ABAB* . . . .

Further work revealed a second structure which could coexist with the classical hexagonal one above. This structure was composed of the same hexagonal nets of carbon atoms, but the planes were stacked differently than in the structure just described. The sequence was such that the fourth plane was identically placed to the first, i.e. *ABCABC* . . . . When this structure was indexed on the unit cell given above, fractional

[1]*Manuscript received September 21, 1956.*
Contribution from the Defence Research Chemical Laboratories, Ottawa, Canada. Also issued as D.R.C.L Report No. 224.

indices were obtained, which accounted for the extra lines observed on some graphite spectra. These indices, which contain a multiple of 2/3, are most simply explained by postulating a graphite structure with a c axis 3/2 as long as the usual one, i.e. $a = 2.456$ Å and $c = 3/2 \times 6.696 = 10.044$ Å with atoms in positions 0, 0, 0; 1/3, 2/3, 0; 0, 0, 1/3; 2/3, 1/3, 1/3; 1/3, 2/3, 2/3; and 2/3, 1/3, 2/3. This structure is rhombohedral with $a = 3.635$ Å, $\alpha = 39.49°$, atoms at $\pm u$, u, u ($u = 1/6$), and space group $R\,\bar{3}M$. This second form occurs widely in natural and artificial graphites, sometimes to as much as 15%.

It was thought to be of interest to study some of the artificial graphites by means of the X-ray camera and electron microscope and to attempt to correlate the results with adsorption data. For this purpose, graphites of widely different surface area were chosen so that differences between them would be readily discernible. The spectra of these graphites showed no evidence of the rhombohedral form and are indexed below on a hexagonal lattice.

EXPERIMENTAL AND RESULTS

Three graphites manufactured by Acheson Colloids Ltd. were used in these studies. They were designated as G–3, G–5, and GF–5. G–3 has been described in two previous papers (4, 5). G–5 was an Acheson graphite of high surface area. GF–5 was prepared by treatment of a sample of G–5 with strong hydrofluoric acid followed by washing with copious quantities of distilled water. This treatment has been found to remove effectively small quantities of inorganic ash from the graphite. The experimental work is presented under the following three headings: Adsorption, X-ray Spectroscopy, and Electron Microscopy.

Adsorption

The apparatus and procedures are exactly as described previously (4).

Isotherms for the adsorption of nitrogen by G–3, G–5, and GF–5 are presented in Fig. 1. The isotherm for G–3 has been published previously (4), but is reproduced for purposes of comparison with those of G–5 and GF–5. It is immediately obvious that G–5 and GF–5 have about the same surface area and that the surface area of G–3 is very much less than those of the other two graphites. This point is also demonstrated by the data of Table I, which gives the surface areas calculated by the B.E.T. equation (2).

TABLE I

Graphite	Surface area, $m.^2/g.$
G–3	18
G–5	380
GF–5	385

X-ray Spectroscopy

G–3, G–5, and GF–5 were already fine powders and were therefore used without pretreatment. Each powder was coated on to a glass fiber 0.09 mm. in diameter using a thin layer of white vaseline as an adhesive. The layer of carbon was formed into a uniform cylinder by means of a needle under a stereomicroscope. The specimen was then mounted in the camera. The over-all diameter of such a specimen was about 0.15 mm.

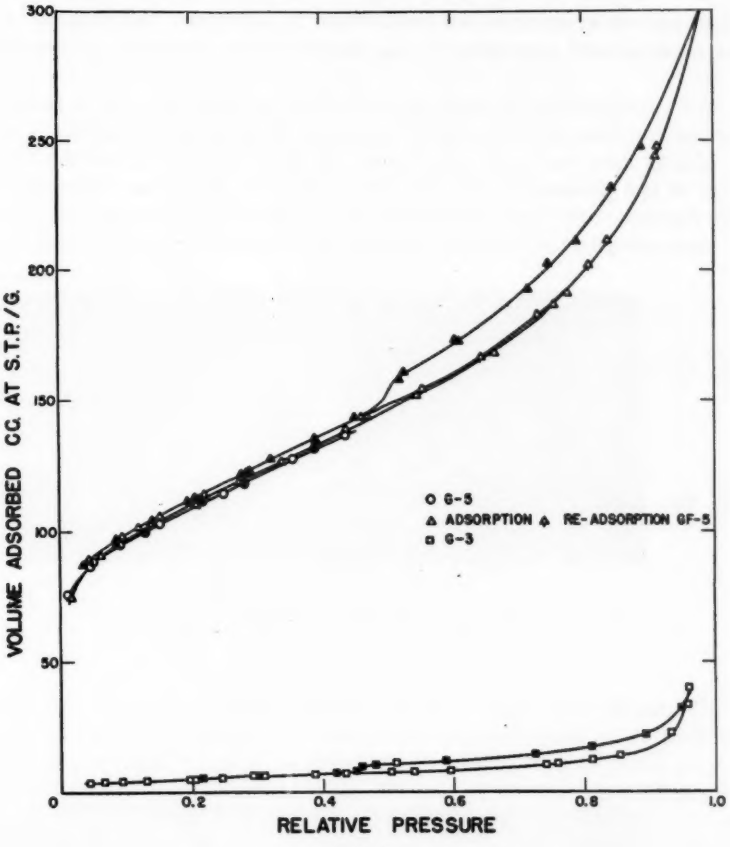

FIG. 1.

The powder spectrum was photographed using a Unicam S25 camera (30.0 mm. radius). Exposures were usually about 5 hours, and were made with both cobalt and copper radiations appropriately filtered. After the spectrum had been exposed, a density scale was printed on each negative by exposing clear parts of the film to suitable radiation intensities for a known series of times. All films were developed in a standard manner. Spectra for G–3, G–5, and GF–5 are given in Fig. 3.

After development the film was photometered using a visual split-beam photometer. Both spectrum and density scale curves were then obtained enabling relative intensities for each line to be measured. The curves were then plotted and corrected for background intensity. Finally, a curve was obtained for each graphite showing the relative intensity of each line versus its position on the film.

In order to determine the true line broadening due to particle size, the above curves had to be corrected for the doublet nature of the radiations and the broadening due to the experimental arrangement. Both of these corrections were made by taking photographs of finely-ground pure sodium chloride. This compound gave a set of clearly

resolved lines spaced at suitable intervals. From its spectrum, the natural broadening due to the experimental arrangement was measured for all values of the diffraction angle θ.

A curve was calculated for the camera used giving the peak separation to be expected for the K_{α_1} and K_{α_2} lines for each type of radiation. This curve showed that a maximum separation of 0.12 mm. was to be anticipated for the lines used. Inasmuch as the limit of resolution of the photometer was 0.1 mm. and since the above correction includes most of the doublet corrections, no further correction for K_{α_1} and K_{α_2} was made. The corrected curves are given in Fig. 2 for all three graphites. It is obvious that the lines for

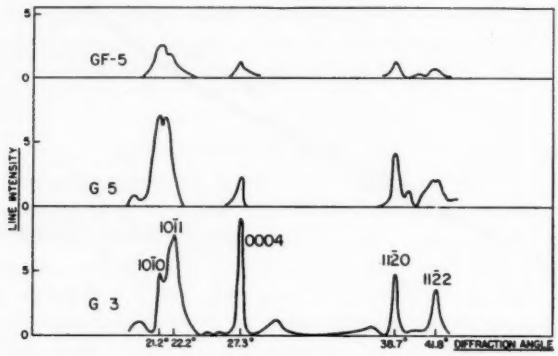

FIG. 2.

G–3 are much sharper than those for G–5, consistent with its much smaller surface area as demonstrated by its lower nitrogen adsorption. The lines for GF–5 are quite different in profile from those of G–5. They are shorter and broader indicating crystallites of different shape. This must be reconciled with the fact that both graphites have the same area as measured by nitrogen adsorption.

The procedure outlined above gives a linear measure of the true line broadening due to particle size. This broadening was converted to particle size measurements by a set of graphs relating ϵ, the particle dimension normal to the crystal planes giving a spectrum line at angle θ, and β, the angular broadening. The equation used was

$$\epsilon = \tau/\beta \cos\theta$$

where τ is the wave length.

The values of ϵ were read from these graphs corresponding to various values of τ.

The accuracy with which ϵ can be measured depends on the two factors involved in the determination of β. These factors are B, the width of the broadened line in the graphite spectrum, and b, the width of the unbroadened line in the salt spectrum. The errors inherent in determining B and b vary with the line width and angular position. The ratio b/B was converted to β/B by means of the Jones Curve (3), which has been reported to give reasonable accuracy in the case of graphite. The quantity β is obtained in linear measure from β/B and B. Conversion of β to angular measure and hence to ϵ does not introduce inaccuracies of more than a few per cent. It is obvious that the greater the broadening the less important are the instrumental errors, hence the smaller values

PLATE I

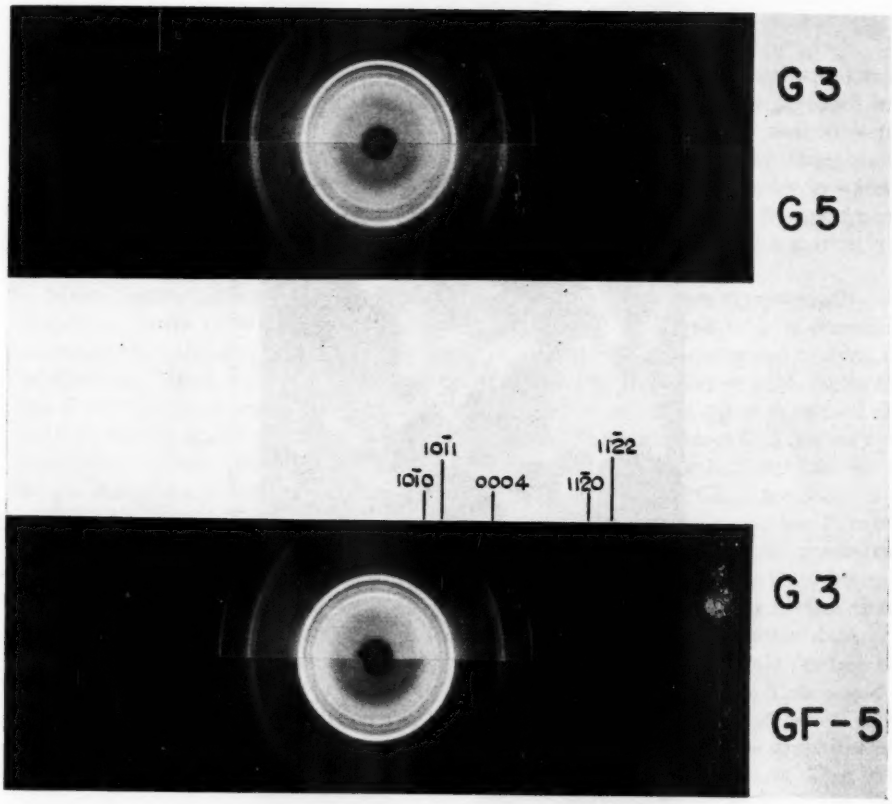

FIG. 3

PLATE II

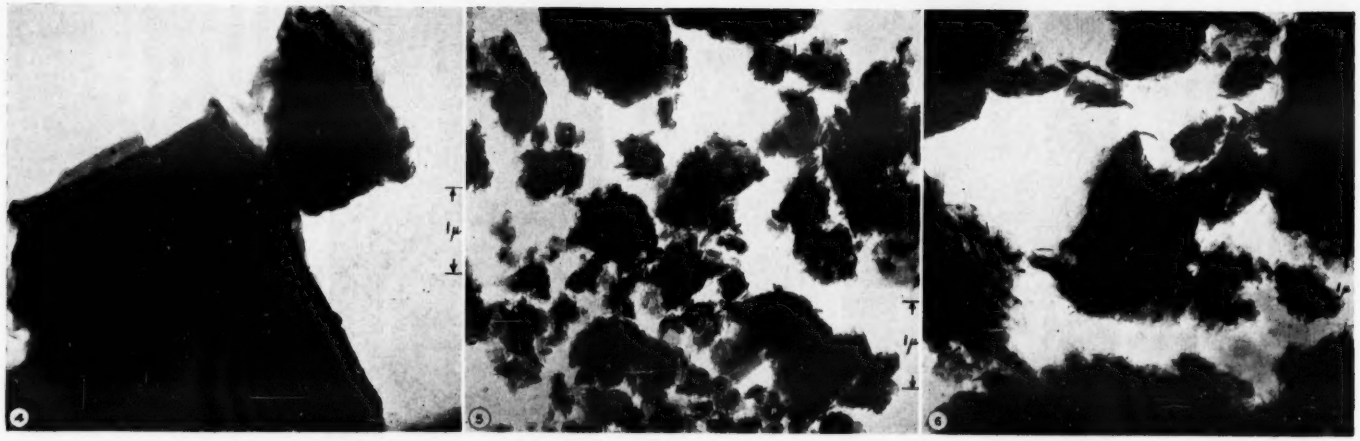

FIG. 4. G–3. FIGS. 5 and 6. G–5 and GF–5 respectively.

of ϵ are more accurate than the larger. The values of ϵ normal to three crystal planes are given in Table II.

TABLE II

Graphite	ϵ in Å taken normal to:		
	$11\bar{2}0$	$11\bar{2}2$	0004
G–3	550	110	410
G–5	112	45	165
GF–5	195	85	67

Electron Microscopy

The three graphites were photographed by means of a Philips electron microscope with a resolving power of about 20 Å. The specimens of graphite were prepared in two ways both of which gave substantially the same results. In the first method, some of the dry powder was placed on a Formvar-coated Athene specimen grid under a stereomicroscope. The second method consisted of dispersing some of the powder in water and then placing a drop of the resulting suspension on a grid. After drying, the specimen was ready for observation. The microscope field was calibrated by means of a grating replica of 1000 lines per mm.

Many photographs were taken in order to ensure that they were representative of the graphites. Three typical photographs are shown in Figs. 4, 5, and 6. It is immediately apparent that the graphite of smallest surface area (G–3) was composed of crystallites which were flatter and more regular than those of the graphites of high surface area (G–5 and GF–5). The crystallites of G–5 and GF–5 were made up of crumpled sheets with a granular appearance on a scale of about 30 Å. The particles of G–3 are very much more massive than those of G–5 and GF–5, in agreement with the X-ray data for G–3, which shows sharp *hk*0 and 00*l* lines. The particles of G–5 and GF–5 are wispy and in many cases, almost transparent to the electron beam. This is in line with the X-ray data which display broad 00*l* lines of low intensity. The particles of all the graphites are broken up and are composed of small crystallites piled in an irregular way, hence it is impossible to calculate surface areas from the photographs. However, it is clear that the observations are qualitatively in agreement with the X-ray and adsorption data.

It can be seen from the photographs that the adsorbing surfaces would contain many cracks, crevices, and wrinkles caused by crumpled-up graphite sheets. This would lead to a variety of energy states depending on the degree to which adjacent sheets of carbons gave rise to co-operative effects. Hence, it would be expected that these graphites would be energetically heterogeneous owing to the topography of the surface. This idea is supported by the adsorption isotherms which are smooth curves without the humps characteristic of homogeneous surfaces. Graphitic carbons prepared from carbon blacks may show homogeneous surfaces (1) because they presumably retain the fairly smooth topography of the parent carbon. McDermot and Lawton (6) have shown that these graphites are relatively free of chemisorbed oxygen hence the heterogeneity is likely to be exclusively of the topographic type. In this connection it was pointed out in the Introduction that removal of any ash present in the graphite left the shape of the isotherms unaffected.

DISCUSSION

The three graphites studied differ principally in degree of subdivision. The differences in surface area have been broadly indicated by all three of the methods used to study the graphites. The electron microscope photographs, while qualitatively in agreement with information from the other two methods, are not amenable to quantitative treatment. Accordingly, the following discussion will be limited to the X-ray and adsorption work.

It was impossible to calculate accurate values for the surface areas of the graphites from the X-ray data because no information was available on the distribution of particle sizes. For example, according to the method of stacking the crystallites, different 0004 profiles would be obtained for a given mass of graphite, but the $11\bar{2}2$ profile would be the same. Calculations such as the ones used, which employ dimensions calculated from the 0004 line, would tend to neglect this size distribution effect. However, as a first approximation surface areas were calculated from dimensions derived from the 0004 and the $11\bar{2}0$ lines. These are presented in Table III along with areas calculated from the adsorption data.

TABLE III

Graphite	Surface area $m.^2/g.$	
	Nitrogen adsorption	X-ray spectroscopy
G–3	18	55
G–5	380	220
GF–5	385	230

The areas calculated from the X-ray patterns are of the same order as those calculated from the adsorption data by means of the B.E.T. equation. In view of the approximations involved the agreement reached is considered to be good. It is of particular interest to note that the areas for G–5 and GF–5 derived from the X-ray data are in good agreement despite the differences in these spectra as illustrated in Fig. 2. In other words, although the crystallites are shaped differently, their surface areas are the same. This is in agreement with the fact that the B.E.T. areas are also equal, and their appearances in the electron microscope are similar.

REFERENCES

1. BEEBE, R. A. and YOUNG, D. M. J. Phys. Chem. **58**, 93 (1954).
2. BRUNAUER, S. The adsorption of gases and vapours. Princeton Univ. Press, Princeton, N.J. 1945.
3. JONES, F. W. Proc. Roy. Soc. A, **166**, 16 (1938).
4. MCDERMOT, H. L. and ARNELL, J. C. Can. J. Chem. **33**, 913 (1955).
5. MCDERMOT, H. L. and LAWTON, B. E. Can. J. Chem. **34**, 769 (1956).
6. MCDERMOT, H. L. and LAWTON, B. E. Unpublished.
7. RILEY, H. L. Fuel, **24**, 8 (1945).

PYRROLE CHEMISTRY

I. SUBSTITUTION REACTIONS OF 1-METHYLPYRROLE[1]

HUGH J. ANDERSON

ABSTRACT

An investigation of some substitution reactions of 1-methylpyrrole has indicated that the α-directing effect of the hetero nitrogen during nitration is even less than it is in pyrrole. 3-Nitro-1-methylpyrrole has been prepared together with the 2-isomer by direct nitration of 1-methylpyrrole as well as indirectly. These two compounds have been found to undergo Friedel-Crafts acylation, a reaction not previously reported among simple nitro compounds of the 5-membered heterocycles. It has been found, contrary to the results of previous workers, that direct nitration of pyrrole itself yields a mononitro product containing about 7% of the 3-isomer.

INTRODUCTION

The reactions of pyrrole and its derivatives, while generally similar to those of the corresponding furan and thiophene compounds, show a number of differences. Some of these differences are of course due to the presence in pyrrole of the acidic imino hydrogen and some are inherent in the ring system itself. We have been interested in preparing simple pyrrole derivatives that have not yet been investigated and, in order to avoid the reactions due to the imino hydrogen as well as to stabilize somewhat the compounds being prepared, we have focused our attention on 1-methylpyrrole (I) the simplest homologue not possessing the reactive hydrogen.

1-Methylpyrrole shows more similarity in physical properties to toluene and the methylthiophenes than pyrrole with its imino hydrogen does to benzene and thiophene. For instance the boiling point of pyrrole is some 40–50° higher than expected probably owing to hydrogen bonding, while that of 1-methylpyrrole is where one might predict it to be. Like thiophene, 1-methylpyrrole may be C-metalated with *n*-butyllithium (13); it undergoes Friedel-Crafts acylation (4), forms the aldehyde with phosphorus oxychloride and dimethylformamide (15), and takes part in many other reactions all leading, with the exception of nitration as reported below, to a 2-substituted product when no other functional group is present in the molecule. In all its reactions it is much more reactive than thiophene.

Thiophene, furan, and pyrrole are well known to undergo substitution primarily or exclusively in an α-position if one is open in the ring. The presence of a meta-directing group in one α-position may, however, alter this situation substantially. Thus it has been found that nitration of 2-nitrothiophene leads to 2,4-dinitrothiophene predominantly and much less of the 2,5-dinitro compound (11, 16). From 2-nitrofuran only 2,5-dinitrofuran is obtained (8), indicating the overwhelming α-directing influence of the hetero oxygen in furan. The nitration of 2-acetylthiophene gives 4- and 5-nitro-2-acetyl isomers in roughly equal amounts (11) but again with the corresponding furan compound only 2-acetyl-5-nitrofuran is isolated (10).

The situation with pyrrole, on the other hand, is somewhat different. Further nitration of 2-nitropyrrole is reported by Rinkes (12) to give about four parts of 2,4-dinitropyrrole to one of 2,5-dinitropyrrole. Similarly he found that the nitration of 2-acetylpyrrole (XI) gave more of the 2,4-isomer (IX) than of the 2,5- one (X) while with the less strongly

[1]*Manuscript received September 24, 1956.*
Contribution from the Chemistry Department, Memorial University of Newfoundland, St. John's, Nfld.

meta-directing carbomethoxy group in the 2-position roughly equal amounts of the 2,4- and 2,5-isomers were obtained on nitration. Many similar results indicate that the α-directing effect of the hetero nitrogen in pyrrole during nitration is less than that of the sulphur in thiophene, which, in turn, is much less than that of the oxygen in furan.

It was of interest to see first how the replacement of the imino hydrogen with a methyl group would change the directive influences of the pyrrole ring either through electronic or steric effects. It has now been found that nitration of 2-acetyl-1-methylpyrrole (II) following a procedure parallel to that of Rinkes (12) leads to about six parts of 2-acetyl-4-nitro-1-methylpyrrole (III) to one of the 5-nitro isomer (IV). This is a distinct change from the results for 2-acetylpyrrole where Rinkes found a ratio of roughly 2:1 in favor of the 4-isomer. The structures of III and IV have been established by repeating Rinkes' preparation of the corresponding pyrrole compounds IX and X and then methylating these two compounds on the nitrogen using sodium ethoxide and methyl sulphate in a modification of the method of Corwin and Quattlebaum (2). Formation of the sodium salt using sodium metal was found to be extremely slow even at the boiling point of toluene; however sodium ethoxide gave reasonable yields quite rapidly with these two compounds.

The synthesis of 3-nitro-1-methylpyrrole was then accomplished by subjecting the now proved 2-acetyl-4-nitro-1-methylpyrrole to a haloform reaction with alkaline sodium hypochlorite which formed the corresponding 4-nitro-1-methyl-2-pyrrole-carboxylic acid (VII). This acid was then decarboxylated to give the desired 3-nitro-1-methylpyrrole (VI), which was identical with that obtained by direct nitration as reported below and consequently proved the structure of that product. The success of the haloform reaction is an example of the stability increase caused by the N-methyl group. With simple pyrrole derivatives, alkaline hypochlorite or hypobromite causes the formation of halogenated maleimides (14). Thus it was not surprising to find that alkaline sodium hypochlorite solution gave none of the desired acid in a reaction with 2-acetyl-4-nitropyrrole, while, as reported, the 1-methyl compound gave about 40% yield of VII. With simpler N-methyl compounds there seems to be a simultaneous nuclear halogenation and this reaction is being investigated further.

Although acylation of a nitro compound has not hitherto been reported for thiophene, furan, or pyrrole, it has been found possible to acetylate 2-nitro-1-methylpyrrole (V) and the 3-nitro isomer (VI) using boron fluoride etherate as a catalyst. As might be expected from the combined meta-directing influence of the nitro group and the α-directing influence of the hetero nitrogen, only one product, 2-acetyl-4-nitro-1-methylpyrrole (III), was obtained from compound VI. With 2-nitro-1-methylpyrrole a single compound was again isolated which would be expected to be 4-acetyl-2-nitro-1-methylpyrrole (VIII). It is not the 2,5-isomer (IV) obtained above and, although we have not proved its structure, there seems little doubt of its identity.

An even more striking indication of the less intense α-directing influence in 1-methylpyrrole was found in the results of direct nitration. When furan is nitrated with acetic anhydride – nitric acid, only the 2-isomer is obtained (8) but in the nitration of thiophene roughly 5% of the 3-isomer is formed along with the 2-isomer (16). Rinkes found only 2-nitropyrrole in the mononitration product from pyrrole under these conditions (12). Following the standard procedure, nitration of 1-methylpyrrole yielded roughly two parts of 2-nitro-1-methylpyrrole (V) to one of the 3-isomer (VI). This is similar to the

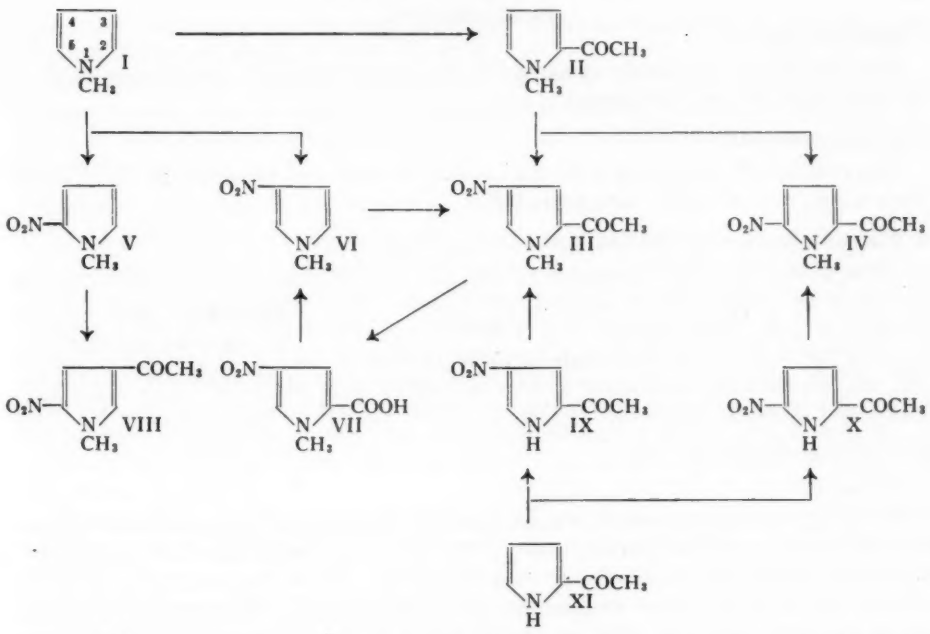

results of Dhont and Wibaut (3), who obtained about the same ratio of the 2- and 3-nitro derivatives when they nitrated 1-phenylpyrrole.

This result combined with those reported above makes it appear qualitatively that for nitration the α-directing power of the hetero atoms in these 5-membered rings decreases in the order: furan, thiophene, pyrrole, and 1-methylpyrrole. The difference between thiophene and pyrrole is not great and probably depends on the individual reaction. Nevertheless the fact that Rinkes isolated only the 2-isomer from the nitration of pyrrole now appears quite remarkable. If 5% of 3-nitrothiophene is formed, an approximately equal amount of 3-nitropyrrole would be expected. The reported properties (1) of 3-nitropyrrole are unique among the nitro derivatives of these heterocycles in that it dimerizes when heated somewhat above its melting point. It appeared possible that the conditions of isolation or purification used by Rinkes might have allowed a small percentage of the 3-isomer to escape detection if Rinkes was not actually searching for it.

Repetition of the nitration of pyrrole has confirmed this premise. Ordinary crystallization techniques applied to the crude product led only to the 2-isomer, but uncertain melting points of the partially purified material indicated that another isomer might be present. Small scale chromatography on Magnesol–Celite gave a definite but not very clear separation which enabled a small quantity of 3-nitropyrrole to be purified by further recrystallization. The amount obtained indicated that roughly 5–6% of the mononitro product was 3-nitropyrrole. A second chromatogram on an increased scale and using a proportionately larger column showed that the amount of 3-nitropyrrole was at least 6½% and probably 7%. This again places pyrrole close to thiophene in the α-directing influence of its hetero atom during nitration.

EXPERIMENTAL

1-Methylpyrrole (*I*)

This compound was kindly donated by the Electrochemicals Department of E. I. du Pont de Nemours and Company, Inc.

2-Acetylpyrrole (*XI*)

This compound was prepared by the method of Oddo and Dainotti (9). Crystallized from water, m.p. 89–89.5°. Literature 90°.

2-Acetyl-4-nitropyrrole (*IX*) *and 2-Acetyl-5-nitropyrrole* (*X*)

These compounds were prepared by the nitration of 2-acetylpyrrole following the procedure of Rinkes (12). 2-Acetyl-4-nitropyrrole (IX) was crystallized from aqueous ethanol as pale yellow prisms, m.p. 195–196°. Literature 197°. Calc. for $C_6H_6N_2O_3$: C, 46.76; H, 3.92; N, 18.18. Found: C, 46.54; H, 4.03; N, 18.15. 2-Acetyl-5-nitropyrrole (X) was crystallized from water as fibrous needles, m.p. 154.5–155°. Literature 156°. Calc. for $C_6H_6N_2O_3$: C, 46.76; H, 3.92; N, 18.18. Found: C, 46.98; H, 3.96; N, 18.09.

2-Acetyl-1-methylpyrrole (*II*)

Method A

Following the procedure used by Hartough and Kosak (5) for the acetylation of furan and thiophene, 1-methylpyrrole (16.2 g., 0.2 M.), acetic anhydride (20.4 g., 0.2 M.), and freshly fused and powdered zinc chloride (27.3 g., 0.2 M.) were stirred together in 250 ml. dry ether for 1 hour and hydrolyzed in 600 ml. cold water overnight. The two layers were separated and, after saturation with salt, the aqueous layer was extracted twice with ether. The ether was dried over magnesium sulphate and removed to give an oil which was distilled at 88–91° at 22 mm. Yield 9.8 g. (40%). Hess and Wissing (7) report b.p. 75–76° at 15 mm.

Method B

In a manner similar to that used by Heid and Levine (6) to acetylate furan and thiophene, there was added to a previously chilled mixture of 1-methylpyrrole (4.0 g., 0.05 M.) and acetic anhydride (6.0 g., 0.05 M.) 0.5 ml. of practical boron fluoride – ethyl ether. The heat evolved was not great and the mixture was warmed to about 80° and allowed to cool over 30 minutes; it was then poured into 200 ml. cold water. Several hours later the solution was steam distilled. After being neutralized with sodium carbonate and saturated with salt the distillate was extracted with ether and the product recovered as in Method A. The yield was 1.85 g. (30%).

Nitration of 2-Acetyl-1-methylpyrrole

2-Acetyl-1-methylpyrrole (6.2 g., 0.05 M.) was dissolved in 35 ml. acetic anhydride and chilled to −10°. To this was added a cold mixture of fuming nitric acid (5.6 g., 0.09 M.) in 15 ml. acetic anhydride at such a rate as to prevent the temperature from rising above 0°. The dark purple solution was poured into 300 ml. ice water and extracted three times with ether. The extract was evaporated to dryness in a vacuum and the solid taken up in benzene, washed once with 10% sodium carbonate solution, and dried. The benzene solution was concentrated twice, producing a total of roughly 3.6 g. of crude material, m.p. 120–130°. The residue after all solvent was removed was a red oil, which on steam distillation produced 0.6 g. of crude solid, m.p. 90–95°.

The first substance, 2-acetyl-4-nitro-1-methylpyrrole (III), was recrystallized from

aqueous ethanol to give needles, m.p. 141–141.5°. Calc. for $C_7H_8N_2O_3$: C, 50.00; H, 4.79; N, 16.66. Found: C, 50.23; H, 4.93; N, 16.38.

The second isomer, 2-acetyl-5-nitro-1-methylpyrrole (IV), was recrystallized from aqueous ethanol to give pale yellow prisms, m.p. 95.5–96°. Calc. for $C_7H_8N_2O_3$: C, 50.00; H, 4.79; N, 16.66. Found: C, 50.12; H, 4.83; N, 16.93. This compound is very sensitive to light.

Preparation of Compounds III and IV by N-Methylation

To a solution of 2-acetyl-5-nitropyrrole (X) (0.30 g., 0.002 M.) in 20 ml. dry toluene was added 0.5 ml. ethanol in which metallic sodium (0.05 g., 0.002 M.) had been dissolved. After the mixture had been heated for 15 minutes all the salt had precipitated; methyl sulphate (0.25 g., 0.002 M.) was then added and the solution heated at 100° for about 30 minutes. After the solution was cooled 20 ml. of 6 *N* sodium hydroxide was added and the mixture shaken vigorously; then the layers were separated. The toluene solution was dried with magnesium sulphate and evaporated to dryness under vacuum. The residue was vacuum sublimed at 3 mm., then recrystallized from water to give 0.15 g. (44%) of 2-acetyl-5-nitro-1-methylpyrrole, m.p. 94–95° and mixed m.p. with compound IV from direct nitration 94–95°.

In a similar manner 2-acetyl-4-nitropyrrole (IX) was converted to 2-acetyl-4-nitro-1-methylpyrrole, m.p. 139–140° and mixed m.p. with compound III from direct nitration 139–140°.

Haloform Reaction with 2-Acetyl-4-nitro-1-methylpyrrole

An alkaline solution of sodium hypochlorite was prepared by passing chlorine into a solution of sodium hydroxide (4.4 g., 0.11 M.) in 4 ml. water chilled by 40 g. ice until 3.6 g. (0.10 M.) had been absorbed. Then after 2 g. sodium hydroxide was added in 8 ml. water, the solution was warmed to 65° and compound III (1.8 g., 0.10 M.) was added slowly with vigorous shaking while the temperature rose to nearly 90°. When the solution had cooled to room temperature a small amount of sodium bisulphite solution was added until there was no reaction with starch–iodide paper. After an ether extraction to remove any neutral material the solution was carefully acidified with dilute hydrochloric acid solution and extracted three times with ether. The product, 4-nitro-1-methyl-2-pyrrolecarboxylic acid (VII), weighed 0.65 g. (38%) and after recrystallization from water gave thick prisms, m.p. 199–199.5°. Calc. for $C_6H_6N_2O_4$: C, 42.36; H, 3.55; N, 16.47. Found: C, 42.57; H, 3.58; N, 16.37.

Decarboxylation of Acid VII

4-Nitro-1-methyl-2-pyrrolecarboxylic acid (50 mg.) and copper powder (25 mg.) were mixed intimately and added to 3.5 ml. quinoline in a 10 ml. pear-shaped flask. The mixture was heated in an oil bath to 175°; at this temperature bubbles were evolved. After 10 minutes the temperature had reached 190° and all reaction was over. When the reaction mixture had cooled to room temperature, an excess of ether was added and the quinoline removed by washing the mixture with dilute hydrochloric acid solution. The ether extract was washed once with water, dried, and the ether removed. The dark oily residue was crystallized from petroleum hexane to give 30 mg. (80%) of 3-nitro-1-methylpyrrole (VI) as long needles, m.p. 60–62°. Another recrystallization from water gave very pale cream prisms, m.p. 62–62.5°. Calc. for $C_5H_6N_2O_2$: C, 47.62; H, 4.79; N, 22.21. Found: C, 47.25; H, 4.74; N, 21.86.

Nitration of 1-Methylpyrrole

1-Methylpyrrole (12 g., 0.15 M.) was dissolved in 60 ml. acetic anhydride and cooled to −10°, then treated slowly with a solution of fuming nitric acid (12 g., 0.19 M.) in 20 ml. acetic anhydride, the temperature being kept below 5° during the addition. After being poured into ice water and extracted with ether the extract was washed with sodium carbonate solution until no longer acidic, then dried. When the ether had been removed, the residual oil was vacuum distilled to give 5.5 g. of a yellow oil, b.p. 90–95° at 5 mm., and 4.5 g. of dark residue.

The yellow oil crystallized when cooled and, after being pressed dry on unglazed porcelain and recrystallized from petroleum pentane, yielded 4.6 g. of 2-nitro-1-methylpyrrole (V), m.p. 28–28.5°. Calc. for $C_5H_6N_2O_2$: C, 47.62; H, 4.79; N, 22.21. Found: C, 47.30; H, 4.93; N, 21.88.

The dark residue was repeatedly extracted with petroleum hexane and the crystalline solid recrystallized from water to give 2.6 g. of a compound, m.p. 62–62.5°. Mixed m.p. with 3-nitro-1-methylpyrrole (VI) from the decarboxylation was 62–62.5°.

Friedel-Crafts Acetylation of Compounds V and VI

To a solution of 3-nitro-1-methylpyrrole (VI) (0.2 g.) in 4 ml. acetic anhydride was added 0.1 ml. practical boron fluoride – ethyl ether. The solution was warmed slowly to 100° and allowed to cool again. After hydrolysis and neutralization with sodium carbonate solution the product, which was not very soluble in ether, was extracted with chloroform, dried over magnesium sulphate, and the solvent evaporated. The residue was crystallized from aqueous ethanol to give 0.16 g. of a compound, m.p. 140–141°. Mixed m.p. with 2-acetyl-4-nitro-1-methylpyrrole (III) was 140–141°.

Similarly 2-nitro-1-methylpyrrole (0.5 g.) was acetylated to give 0.35 g. of needles from water, m.p. 113.5–114°. Calc. for $C_7H_8N_2O_3$: C, 50.00; H, 4.79; N, 16.66. Found: C, 50.18; H, 4.87; N, 16.22. This compound is almost certainly 4-acetyl-2-nitro-1-methyl pyrrole (VIII).

Nitration of Pyrrole

This reaction was carried out following the procedure of Rinkes but on twice the scale. To pyrrole (10 g., 0.15 M.) in 80 ml. acetic anhydride was added fuming nitric acid (11.3 g., 0.18 M.) in 40 ml. acetic anhydride, the temperature being kept below 5°. The crude solid isolated weighed 9.8 g. Attempts to recrystallize small portions led first to crude material of wide melting range and then to pure 2-nitropyrrole, m.p. 55–56°. Literature 56°.

After a preliminary trial, 1.00 g. of crude was dissolved in 8 ml. benzene–ethanol (9: 1 by volume) and chromatographed on a column consisting of a mixture of Magnesol and Celite (3: 1 by weight) weighing 50 g. Elution was carried out with the same solvent. The first solid-containing fraction was evaporated to dryness leaving 0.18 g. solid. This was extracted repeatedly with small amounts of petroleum pentane and first 0.10 g. of 2-nitropyrrole, m.p. 50–52°, was obtained. Then 65 mg. of 3-nitropyrrole, m.p. 63–64° (literature 63°), was recovered. Fraction two contained only 2-nitropyrrole so, allowing for small losses, it appears that roughly 7% of the crude nitration product from pyrrole is 3-nitropyrrole.

To confirm its identity the 3-nitropyrrole was recrystallized from water, m.p. 100–101°. Literature 101°. Calc. for $C_4H_4N_2O_2$: C, 42.86; H, 3.60; N, 24.99. Found: C, 42.78; H, 3.62; N, 25.08.

REFERENCES

1. ANGELI, A. and ALESSANDRI, L. Atti reale accad. Lincei, **20**, 311 (1911); Chem. Abstr. **5**, 3403 (1911).
2. CORWIN, A. H. and QUATTLEBAUM, W. M. J. Am. Chem. Soc. **58**, 1081 (1936).
3. DHONT, J. and WIBAUT, J. P. Rec. trav. chim. **62**, 177 (1943).
4. FISCHER, H. and SCHUBERT, F. Hoppe-Seyler's Z. physiol. Chem. **155**, 99 (1926).
5. HARTOUGH, H. D. and KOSAK, A. I. J. Am. Chem. Soc. **69**, 1012 (1947).
6. HEID, J. V. and LEVINE, R. J. Org. Chem. **13**, 409 (1948).
7. HESS, K. and WISSING, F. Ber. **47**, 1416 (1914).
8. MARQUIS, R. Ann. chim. et phys. **4**, No. 8, 96 (1905).
9. ODDO, B. and DAINOTTI, C. Gazz. chim. ital. **42**, 727 (1912); Chem. Abstr. **6**, 2749 (1912).
10. RINKES, I. J. Rec. trav. chim. **51**, 352 (1932).
11. RINKES, I. J. Rec. trav. chim. **52**, 538 (1933).
12. RINKES, I. J. Rec. trav. chim. **53**, 1167 (1934).
13. SHIRLEY, D. A., GROSS, B. H., and ROUSSEL, P. A. J. Org. Chem. **20**, 225 (1955).
14. SIDGWICK, N. V. *In* Organic chemistry of nitrogen. *Revised by* T. W. J. Taylor and W. Baker. Oxford University Press, London. 1937. p. 479.
15. SILVERSTEIN, R. M., RYSKIEWICZ, E. E., WILLARD, C., and KOEHLER, R. C. J. Org. Chem. **20**, 668 (1955).
16. STEINKOPF, W. and HÖPNER, T. Ann. **501**, 177 (1933).

SELECTIVE SUBSTITUTION IN SUCROSE

I. THE SYNTHESIS OF 1′,4,6′-TRI-*O*-METHYL SUCROSE[1]

G. G. McKeown, R. S. E. Serenius,[2] and L. D. Hayward

ABSTRACT

Sucrose was tritylated and acetylated to give a crystalline tri-*O*-trityl-penta-*O*-acetyl sucrose derivative, and detritylation of this product by graded hydrolysis with acetic acid followed by methylation and deacetylation yielded 1′,4,6′-tri-*O*-methyl sucrose. The structure of the tri-*O*-methyl sucrose was established by periodate oxidation and by hydrolysis to the corresponding *O*-methyl ethers of glucose and fructose. Acetyl group migration from C_4 to C_6 in the glucose moiety of sucrose probably occurred during the methylation reaction.

Some aspects of syntheses involving sucrose are discussed.

INTRODUCTION

Although the molecular structure of sucrose has been carefully established (3, 21, 22, 34) and it is one of the cheapest and most abundant of the available fine organic chemicals (9), the satisfactorily characterized sucrose derivatives appear to be limited to the octa-*O*-substituted compounds which carry in each case one kind of ester or ether group (Table I). An exception is 1′,6,6′-tri-*O*-methyl sucrose, which was prepared and character-

TABLE I

FUNCTIONAL DERIVATIVES OF SUCROSE OF ESTABLISHED STRUCTURE

Derivative	M.p.	$[\alpha]_D$	n_D	Reference
Octaacetate	69–70°			
		+59.5°		23
	88–89°			
Octabenzoate	60–63°	+32.6°		26
	(+2 moles of CCl_4)	+40.6°		
Octanitrate	85.5°	+55.9°		16
Octamethyl	Sirup	+70.1°	1.4560	6
	B.p. 115°/10^{-3} mm.			
Octapropionate	45–46°	+53°		18
Octaallyl	Sirup		1.4822	27
Octamesyl	86–94 (uncorr.)	+43.7°		15
Octatosyl	82–86 (uncorr.)	+41.78°		15

ized as the penta-*O*-acetyl compound by Percival (28). Other partially *O*-substituted sucrose derivatives and sucrose compounds with mixed *O*-substituents have been reported frequently but without proof of structure (4, 15, 19).

The scant attention that sucrose derivatives have received may in some degree be attributed to the molecular structure of sucrose itself. The presence in the polyol molecule of five secondary and three primary hydroxyl groups each with a unique structural environment makes theoretically possible the synthesis of an enormous number of sucrose derivatives. Substitution of just one kind of R group for hydroxyl hydrogen could theoretically give some 255 different compounds and with mixed R groups the

[1]*Manuscript received September 4, 1956.*

Contribution from the Department of Chemistry, University of British Columbia, Vancouver, B.C. Presented in part at the second Western Regional Conference, the Chemical Institute of Canada, Vancouver, September, 1954.

[2]*Present address: Research and Development Department, Powell River Company Limited, Powell River, B.C.*

number becomes astronomical (for example 1.6×10^7 possible octa-*O*-R derivatives for eight different R groups). Synthetic preparations from sucrose are hampered by the very easy acid hydrolysis of the double glycosidic linkage (25, 32), which limits the application to sucrose of synthetic procedures commonly used with the less acid-sensitive mono- and di-saccharide compounds. Furthermore, the steric hindrance imposed on some of the hydroxyl groups as a consequence of the size and preferred conformations of the sucrose molecule makes complete substitution difficult as, for example, in the well-known case of methylation of sucrose (6).

The objective of the present work was the synthesis of a sucrose derivative with the five secondary hydroxyl groups "blocked" with acetyl groups in preparation for a study of the comparative reactivity of the free primary alcohol groups. The structure of the penta-*O*-acetyl sucrose was to be established by methylation and hydrolysis to monosaccharide derivatives. The series of preparations is outlined in Fig. 1.

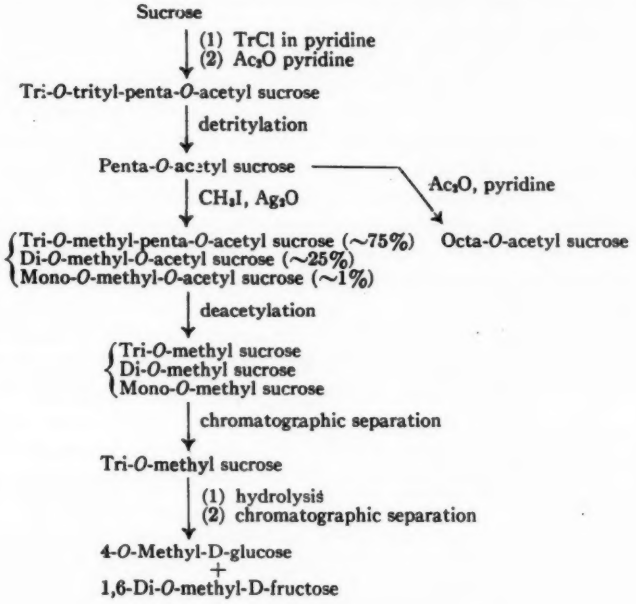

FIG. 1.

Josephson in 1929 (19) reported the synthesis of a crystalline "tritrityl sucrose" by treatment of sucrose with 3 moles of triphenylchloromethane in pyridine for 2 hours on the steam bath. The constants reported were m.p. 127–129° C. and $[\alpha]_D^{23}$ +43.4° (c = 2.4 in ethanol) and the product was analyzed for carbon and hydrogen but not for trityl content. In our attempts to reproduce these results we obtained in each case a colorless glass with a softening-point of about 125–130° C. which was a mixture of tri-*O*-trityl sucrose, products with lower trityl content, reducing sugar fragments, and tritanol. We were unable to prepare pure tri-*O*-trityl sucrose by this route and also were unable to obtain a compound corresponding to the one reported by Josephson as resulting from acetylation of his tritritylsucrose.

We found that tri-*O*-trityl-penta-*O*-acetyl sucrose was conveniently prepared in crystalline form by tritylation of sucrose in pyridine solution at room temperature followed by acetylation in the same solution (29). Tritylation at higher temperatures gave a less pure product and no substantial increase in yield. The crude yield did not exceed 50% in any of the preparations and the mother liquors were strongly reducing toward Fehling's solution, indicating that a considerable degree of hydrolysis had occurred. Our tritylated and acetylated sucrose derivative could be recrystallized from methanol in admixture with chloroform or from chloroform – petroleum ether (b.p. 30–60° C.) as beautiful six-sided prisms which melted sharply at 235–236° C. (corr.), had $[\alpha]_D^{17}$ +68.9° (c = 2.45 in chloroform), and reduced Fehling's solution only after acid hydrolysis; the composition was confirmed by the determination of the trityl and acetyl contents and the molecular weight and by the carbon and hydrogen analysis.

To effect the selective removal of the trityl groups from the tri-*O*-trityl-penta-*O*-acetyl sucrose, three methods were investigated: (*a*) the use of a hydrogen halide in an organic solvent (7, 13), (*b*) catalytic hydrogenation (24, 33), and (*c*) graded hydrolysis with aqueous acetic acid (20). Since the trityl ether and the glycosidic linkage of sucrose are both notably sensitive to acid hydrolysis (10) it was expected that competition would occur in methods (*a*) and (*c*), and indeed method (*a*) caused extensive inversion of the starting material and none of the desired product could be isolated. In method (*b*) catalyst poisoning was troublesome and the yields of penta-*O*-acetyl sucrose were low. Method (*c*) gave the acetate conveniently (43–60% yield) when optimum conditions had been established. The penta-*O*-acetyl sucrose was obtained in crystalline form (m.p. 155–156° C.; $[\alpha]_D^{22}$ +22.0° (c = 3.1 in chloroform)) and analysis indicated the compound to be a dihydrate. Acetylation of this compound gave the known octa-*O*-acetyl sucrose in 61% yield.

The progress of the methylation of the penta-*O*-acetyl sucrose with Purdie's reagents was followed by deacetylating samples with a strongly basic ion exchange resin and chromatographing the mixed sucrose ethers on paper (Table II). After five methylations

TABLE II

METHYLATION OF THE PENTA-*O*-ACETYL SUCROSE

Number of methylations	Paper chromatograms*			
	Sucrose (R_f 0.04)†	Mono-*O*-methyl sucrose (R_f 0.08)†	Di-*O*-methyl sucrose (R_f 0.20)†	Tri-*O*-methyl sucrose (R_f 0.40)†
1	Distinct	Distinct	—	—
2	Faint	Distinct	Distinct	—
3	—	Distinct	Distinct	Faint
5	—	—	Faint	Distinct

**Developer: butanol–ethanol–water (5 : 1 : 4 v/v); spray reagent: p-anisidine hydrochloride.*
†Bright yellow, U.V.-fluorescent spots.

the chromatograms indicated that substitution was essentially complete and the product was isolated as a colorless glass with the correct methoxyl and acetyl analyses. The crude tri-*O*-methyl-penta-*O*-acetyl sucrose, which did not crystallize during 6 months' standing, was deacetylated in 90% aqueous methanol solution on a column of strongly basic ion exchange resin which had previously been tested with sucrose octa-*O*-

acetate, in which case pure crystalline sucrose was obtained in better than 90% yield. The eluate from the column yielded nearly the theoretical amount of sirupy partially methylated sucrose; paper chromatography showed this product to be about 75% tri- and 25% di-*O*-methyl sucrose accompanied by a trace of mono-*O*-methyl sucrose. Pure tri-*O*-methyl sucrose was isolated from the mixture by means of a cellulose column.

When treated with an aqueous sodium metaperiodate solution the tri-*O*-methyl sucrose used up 1.8 moles of oxidant in 6 hours at room temperature and no further consumption occurred during the next 18 hours; no formic acid could be detected in the reaction mixture. Examination of the formulas of the 56 possible tri-*O*-methyl sucrose derivatives revealed that the 1′,6,6′-isomer could be expected to consume 3 moles of periodate ion and form 1 mole of formic acid while the 1′,2,6-, 2,6,6′-, 1′,2,6′-, 1′,4,6-, 4,6,6′-, and 1′,4,6′-isomers would consume 2 moles of periodate and produce no formic acid. Nine of the other isomers would consume 2 moles of periodate and produce 1 mole of formic acid and the remaining 40 isomers would consume either 1 mole or no periodate and form no formic acid. The results obtained in the periodate oxidation of our tri-*O*-methyl sucrose therefore clearly ruled out the 1′,6,6′-tri-*O*-methyl structure and pointed to one of the six compounds which carry secondary methoxyl groups on C_2 or C_4 of the glucose moiety and two other primary methoxyls.

Acid hydrolysis of the tri-*O*-methyl sucrose and chromatography of the hydrolyzate on a cellulose column yielded one mono-*O*-methyl hexose and one di-*O*-methyl hexose. The mono-*O*-methyl hexose was identified as 4-*O*-methyl-D-glucose by the optical rotation, analysis, behavior on paper chromatograms, and by its conversion to the known, crystalline 4-*O*-methyl-D-glucose phenylosazone.

The di-*O*-methyl hexose (with correct methoxyl content) was a colorless liquid with $[\alpha]_D^{24}$ +17.4° (equilibrium value) (c = 1.84 in water). It consumed 3.2 moles of periodate (constant value after 24 hours) and produced 1.71 moles of acid and no formaldehyde in 58 hours at room temperature. The R_f and R_{TG} values for this compound on paper chromatograms developed with butanol–ethanol–water (5 : 1 : 4 v/v) were larger than the corresponding values reported for the di-*O*-methyl glucose derivatives and for the known 3,4-di-*O*-methyl fructose (14). The bright yellow U.V.-fluorescent spot formed by spraying the chromatogram with *p*-anisidine hydrochloride reagent was characteristic of a ketose (17). Examination of the formulas of the possible di-*O*-methyl fructoses and their theoretical behavior toward periodate oxidation clearly indicated that our di-*O*-methyl hexose was 1,6-di-*O*-methyl fructose, which has not previously been reported (2). This conclusion was supported by the chromatographic evidence and by the equilibrium specific rotation observed, which was in good agreement with the values reported or calculated for D-fructofuranose and its *O*-methyl ethers and distinctly different from the large negative rotation given by the *O*-methyl-D-fructopyranoses (2, 22, 28, 34). The source and quantitative yield of the di-*O*-methyl hexose were also compatible with the assigned structure.

The actual isolation and identification of 4-*O*-methyl-D-glucose and 1,6-di-*O*-methyl-D-fructose established the structure of the original tri-*O*-methyl sucrose as the 1′,4,6′-tri-*O*-methyl derivative (I). Satisfactory support to this formula was given by the results of the periodate oxidation study of the tri-*O*-methyl sucrose.

If the original trityl substitution was assumed to have been at the three primary alcohol groups in the sucrose molecule (Helferich's Rule (10)), it followed that acetyl migration from C_4 to C_6 occurred in the glucose moiety during the detritylation or

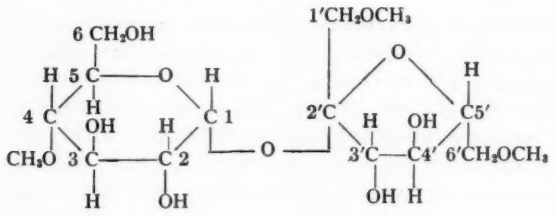

I

methylation reactions. The latter event appeared the more probable, since several cases of such migrations in monosaccharide derivatives during methylation with Purdie's reagents have previously been reported (31). The question of the original locations of the trityl groups in the tri-*O*-trityl-penta-*O*-acetyl sucrose will be examined in Part II of this series.

EXPERIMENTAL

Tri-O-trityl-penta-O-acetyl Sucrose

Commercial granulated sucrose (m.p. variable 162–177° C., $[\alpha]_D^{23}$ +65.57° (c = 26 in water)) (5.0 g.) and freshly prepared triphenylmethyl chloride (14.3 g.) (m.p. 110–111° C. (1)) were treated with 100 ml. of dry pyridine and the mixture was allowed to stand with occasional shaking at room temperature for 48 hours. Acetic anhydride (20 ml.) was then added and the pale yellow solution was stored overnight in the refrigerator. The next day a crop of colorless, hygroscopic, crystals was recovered on a filter (6.7 g., m.p. 175–177° C.). The crystalline material gave a positive test for chloride ion, an acid reaction, yielded triphenyl carbinol on hydrolysis with water, and was presumably pyridinium triphenylmethyl chloride (11, 12). The filtrate was poured in a fine stream with stirring into 1500 ml. of ice water causing the precipitation of a white amorphous solid which was recovered by filtration, washed thoroughly with water, and dried *in vacuo*. The product crystallized from solution in 20 ml. of chloroform diluted with 50 ml. of methanol (yield 8.5 g., 45%) as colorless hexagonal plates which, after repeated recrystallizations from chloroform–methanol or tetrahydrofuran–methanol, melted sharply at 235–236° C.; $[\alpha]_D^{17}$ +68.9° (c, 2.45 in chloroform). Analysis: Calc. for $C_{79}H_{74}O_{16}$: C, 74.2%; H, 5.84%; acetyl, 16.8%; trityl, 57.1%; mol. wt., 1279.5. Found: C, 73.7%; H, 5.9%;* acetyl, 16.8%; trityl, 56.4%; mol. wt., 1270 (Rast method; the lactam of *cis-p*-aminohexahydrobenzoic acid was used as solvent (30)).

The tri-*O*-trityl-penta-*O*-acetyl sucrose was soluble in acetone, chloroform, ethyl ether, and tetrahydrofuran; insoluble in water, ethanol, methanol, and petroleum ether; and reduced Fehling's solution only after acid hydrolysis.

Penta-O-acetyl Sucrose

(*a*) A solution of tri-*O*-trityl-penta-*O*-acetyl sucrose (2.0 g.) in glacial acetic acid (50 ml.) was heated to boiling and 1 ml. of water was introduced. After refluxing for 30 minutes the solution was cooled, the solvent evaporated under reduced pressure at 50° C., and the partially crystalline residue was dried *in vacuo*. Recrystallization from

*Carbon and hydrogen analyses by W. Manser, Zurich, Switzerland.

chloroform and petroleum ether acidified with acetic acid yielded colorless, needle-like crystals of penta-*O*-acetyl sucrose dihydrate (504 mg., 55%). Tritanol was recovered from the mother liquor. The penta-*O*-acetyl sucrose dihydrate was recrystallized to a constant melting point (155–156° C.) and had $[\alpha]_D^{22}$ +22.0 (c = 3.1 in chloroform). Analysis: Calc. for $C_{22}H_{32}O_{16}\,2H_2O$: acetyl, 36.6%. Found: acetyl, 36.6%. The dihydrate was soluble in methanol, acetone, chloroform; was insoluble in water and petroleum ether; gave a positive Molisch test; and reduced Fehling's solution only after acid hydrolysis. Acetylation of the compound gave octa-*O*-acetyl sucrose in 61% yield; m.p. 86–88° (23), not depressed on admixture with an authentic sample.

Some hydrolysis of the glycosidic linkage occurred during the detritylation since the reaction mixtures showed reducing action toward Fehling's solution. The effect of variation of time of reaction on the yield of penta-*O*-acetyl sucrose was as follows: 15 minutes, 23–31%; 30 minutes, 43–60%; 60 minutes, 35%; 120 minutes, 0%. Variation of the amount of water added to the glacial acetic acid solution did not greatly influence the yield: 0.25 ml., 23%; 1.0 ml., 31%; 2.0 ml., 26% (reaction time, 15 minutes).

(*b*) Catalytic hydrogenation was found to cause complete detritylation of only extremely pure samples of tri-*O*-trityl-penta-*O*-acetyl sucrose; less pure samples yielded a mixture of mono- and di-*O*-trityl sucrose derivatives (with palladized charcoal catalyst) or these compounds together with sucrose derivatives substituted with tricyclohexylmethyl groups (platinum oxide catalyst).

A 5.0 g. sample of tri-*O*-trityl-penta-*O*-acetyl sucrose which had been recrystallized 18 times alternately from chloroform–methanol and chloroform – petroleum ether (b.p. 30–60° C.) was dissolved in glacial acetic acid and hydrogenated under 4 atm. pressure in the presence of platinum oxide at 40–50° C. After 34 hours 2.55 g. of crystalline tricyclohexylmethane (83% of theor.) was recovered by filtration. Evaporation of the filtrate and crystallization of the residue yielded 0.60 g. (27%) of nearly pure penta-*O*-acetyl sucrose. In subsequent runs the yields obtained were 20, 38, 16, and 23%. Using palladized charcoal as catalyst a sample of the very pure tri-*O*-trityl compound also gave a 20% yield of the penta–*O*–acetyl sucrose accompanied in this case by triphenylmethane.

(*c*) A solution of tri-*O*-trityl-penta-*O*-acetyl sucrose (3.0 g.) in glacial acetic acid (80 ml.) was treated with 20 ml. of acetic acid saturated with hydrogen bromide (7, 13). Trityl bromide (1.7 g., m.p. 150–152° C.) precipitated immediately and was removed by filtration. The filtrate was diluted with chloroform, washed free of acid, and dried over anhydrous sodium sulphate. Evaporation of the solvent yielded a brown sirup which could not be induced to crystallize and was found to be strongly reducing toward Fehling's solution. Modifications of the procedure were applied, including the use of propionic acid or benzene as solvent, the use of hydrogen chloride as detritylating agent, and the use of buffered solutions for washing, but a non-reducing carbohydrate fraction could not be isolated from any of the reaction mixtures.

Methylation of Penta-O-acetyl Sucrose

Penta-*O*-acetyl sucrose dihydrate (1.579 g.) was dissolved in dry acetone (25 ml.) and freshly distilled methyl iodide (15 ml.), silver oxide (5 g.), and Drierite (2 g.) were added. The mixture was refluxed for 15 hours and filtered, and the filtrate was evaporated to give a viscous colorless sirup. A sample of the partially methylated sirup

was dissolved in methanol and deacetylated by heating with Dowex I strongly basic ion exchange resin for about 2 hours. The solution was then chromatographed on paper using butanol–ethanol–water (5 : 1 : 4 v/v) as developer. Treatment of the developed chromatograms with *p*-anisidine hydrochloride spray reagent (17) showed bright yellow spots for sucrose and sucrose *O*-methyl ethers which fluoresced strongly under an ultraviolet lamp. The R_f values for these compounds are given in Table II. The methylation procedure was repeated five times essentially as described above and the course of the reaction was followed by the chromatographic method as shown in Table II. After the second methylation the partially methylated sirup dissolved completely in methyl iodide, and acetone was then omitted from the reaction mixture. The final product was a colorless glass (1.55 g.) which did not crystallize during 6 months' standing; $[\alpha]_D^{17}$ +57.7° (c = 3.72 in chloroform). Analysis: Calc. for tri-*O*-methyl-penta-*O*-acetyl sucrose, $C_{25}H_{38}O_{16}$: OCH_3, 15.7%; acetyl, 36.2%.
Found: OCH_3, 15.5, 15.8%; acetyl, 36.2, 36.0%.

Tri-O-methyl Sucrose

A solution of the methylated penta-*O*-acetyl sucrose (1.30 g.) in 90% aqueous methanol was run onto a column of Dowex I strongly basic ion exchange resin (20×1.8 cm. diam.). After standing 24 hours the column was washed with 600 ml. of the same solvent, and the eluate was evaporated to a colorless viscous sirup (835 mg., 99%). The sirup failed to crystallize after being left for several months and a paper chromatogram showed it to consist of *ca.* 75% tri-*O*-methyl, 25% di-*O*-methyl, and 1% mono-*O*-methyl sucrose. About 650 mg. of the sirup was chromatographed on a cellulose column (30×2.6 cm. diam.) using butanol–water as developer. The di-*O*-methyl sucrose fractions on evaporation yielded 193 mg. of a colorless glass and the tri-*O*-methyl sucrose fractions yielded 472 mg. of a colorless viscous sirup which had $[\alpha]_D^{24}$ +67.6° (c = 1.74 in water). Analysis: Calc. for tri-*O*-methyl sucrose, $C_{15}H_{28}O_{11}$: OCH_3, 24.2%. Found: OCH_3, 24.9, 24.3%.

Periodate Oxidation of the Tri-O-methyl Sucrose

A sample of the chromatographically pure tri-*O*-methyl sucrose (19.2 mg.) was dissolved in 10 ml. of 0.02 *M* sodium metaperiodate solution at 25° C. and the course of the reaction was followed by titration of aliquots of the solution for periodate ion consumed and for acid formed. Found: at 3 hours, 1.7 moles periodate consumed, 0.025 moles acid formed; at 6 hours, 1.8 moles and 0.025 moles; at 24 hours, 1.8 moles and 0.025 moles. Sucrose under the same conditions gave the following results: at 1 hour, 2.3 moles periodate consumed and 0.26 moles of formic acid formed; at 3 hours, 2.7 and 0.35 moles; at 6 hours, 2.9 and 0.47 moles; at 24 hours, 3.1 and 0.61 moles. Fleury and Courtois (8) reported a consumption of 3.0 moles of periodate and production of 0.70 moles of formic acid for sucrose after 24 hours.

Acid Hydrolysis of the Tri-O-methyl Sucrose

Tri-*O*-methyl sucrose (358 mg.) was hydrolyzed in 10 ml. of 1% acetic acid at reflux temperature during 5 hours. The hydrolyzate was filtered through Celite and evaporated under reduced pressure to a colorless sirup (342 mg.). A paper chromatogram of a sample of the sirup was run on the same sheet with authentic specimens of 2-, 3-, 4-, and 6-*O*-methyl-D-glucose under the conditions described for the chromatography of partially

methylated sucrose derivatives. The hydrolyzate showed a brown-yellow, U.V.-fluorescent spot, R_f 0.29, which agreed in color and R_f value with that from 4-*O*-methyl-D-glucose. 2-*O*-Methyl- and 6-*O*-methyl-D-glucose gave brown spots which did not fluoresce under U.V. light. A bright yellow, U.V.-fluorescent spot, R_f 0.57 (R_{TG} 0.69), was the only other present on the chromatogram of the hydrolyzate and was tentatively assigned to 1,6-di-*O*-methyl-D-fructofuranose; 3,4-di-*O*-methyl-D-fructose has been reported to have a considerably lower R_f value (0.51 (R_{TG} 0.61)) as have di-*O*-methyl glucose derivatives, under these conditions (14). The hydrolyzate was chromatographed on the cellulose column and the appropriate fractions gave on evaporation 161 mg. of the di-*O*-methyl hexose and 148 mg. of the mono-*O*-methyl hexose.

The mono-*O*-methyl hexose was a colorless viscous sirup, $[\alpha]_D^{24}$ +61.2° (c = 1.43 in water), which did not crystallize after nucleation with 2-, 3-, or 6-*O*-methyl glucose. Analysis: Calc. for mono-*O*-methyl hexose, $C_7H_{14}O_6$: OCH_3, 16.0%. Found: OCH_3, 15.5, 15.9%. A phenylosazone was prepared in 40% yield which crystallized from aqueous acetone as fine yellow needles, m.p. 156–158° C. The melting point was not depressed on admixture with an authentic sample of 4-*O*-methyl-D-glucose phenylosazone (5).

The di-*O*-methyl hexose was a colorless liquid, $[\alpha]_D^{24}$ +17.4° (equilibrium value) (c = 1.84 in water). Analysis: Calc. for $C_8H_{16}O_6$: OCH_3, 29.8%. Found: OCH_3, 29.8, 29.3%. Twenty-two milligrams of the liquid was treated with 20 ml. of 0.02 *M* sodium metaperiodate solution at 25° C. and the oxidation solution was analyzed at intervals for the amounts of periodate consumed and of acid and formaldehyde produced. Found: at 4 hours, 3.1 moles periodate consumed, 1.26 moles of acid formed; at 24 hours, 3.2 and 1.58 moles and no formaldehyde; at 58 hours, 3.2 and 1.71 moles.

ACKNOWLEDGMENT

The authors wish to thank the Sugar Research Foundation, Inc., for a grant-in-aid.

REFERENCES

1. BACHMANN, W. S. Org. Syntheses, **23**, 100 (1943).
2. BARRY, C. P. and HONEYMAN, J. *In* Advances in carbohydrate chemistry. Vol. 7. *Edited by* C. S. Hudson, M. L. Wolfrom, and S. M. Cantor. Academic Press, Inc., New York. 1952.
3. BEEVERS, C. A., MCDONALD, T. R. R., ROBERTSON, J. H., and STERN, F. Acta Cryst. **5**, 689 (1952).
4. BEILSTEIN, F. K. Handbuch der Organischen Chemie. 4th ed. Vol. XXXI. J. Springer, Berlin. 1938.
5. BOURNE, E. J. and PEAT, S. *In* Advances in carbohydrate chemistry. Vol. 5. *Edited by* C. S. Hudson and S. M. Cantor. Academic Press, Inc., New York. 1950.
6. BREDERECK, H., HAGELLOCH, G., and HAMBSCH, E. Chem. Ber. **87**, 35 (1954).
7. DEWAR, J. and FORT, G. J. Chem. Soc. 496 (1944).
8. FLEURY, P. and COURTOIS, J. Bull. soc. chim. France, **10**, 245 (1943); Compt. rend. **214**, 366 (1942).
9. HASS, H. B. and LAMBORN, O. H. Ind. Eng. Chem. **47**, 1392 (1955).
10. HELFERICH, B. *In* Advances in carbohydrate chemistry. Vol. 3. *Edited by* W. W. Pigman and M. L. Wolfrom. Academic Press, Inc., New York. 1948.
11. HELFERICH, B. and DEHE, H. Ber. **58B**, 1605 (1925).
12. HELFERICH, B. and SIEBER, H. Ber. **59B**, 600 (1926).
13. HELFERICH, B. and SPEICHER, W. Ann. **579**, 106 (1953).
14. HIRST, E. L. and JONES, J. K. N. Discussions Faraday Soc. **7**, 268 (1949).
15. HOCKETT, R. C. and ZIEF, M. J. Am. Chem. Soc. **72**, 1839 (1950).
16. HOFFMAN, E. J. and HAWSE, V. P. J. Am. Chem. Soc. **41**, 235 (1919).
17. HOUGH, L., JONES, J. K. N., and WADMAN, W. H. J. Chem. Soc. 1702 (1950).
18. HURD, C. D. and GORDON, K. M. J. Am. Chem. Soc. **63**, 2657 (1941).
19. JOSEPHSON, K. Ann. **472**, 230 (1929).
20. KUHN, R., RUDY, H., and WEYGAND, F. Ber. **69**, 1543 (1936).
21. LEMIEUX, R. U. and HUBER, G. J. Am. Chem. Soc. **78**, 4117 (1956).
22. LEVI, I. and PURVES, C. B. *In* Advances in carbohydrate chemistry. Vol. 4. *Edited by* W. W. Pigman and M. L. Wolfrom. Academic Press, Inc., New York. 1949.

23. LINSTEAD, R. P., RUTENBURG, A., DAUBEN, W. G., and EVANS, W. L. J. Am. Chem. Soc. **62**, 3260 (1940).
24. MICHEEL, F. Ber. **65**, 262 (1932).
25. MOELWYN-HUGHES, E. A. Trans. Faraday Soc. **25**, 503 (1929).
26. NESS, R. K. and FLETCHER, H. G., Jr. J. Am. Chem. Soc. **74**, 5344 (1952).
27. NICHOLS, P. L. and YANOVSKY, E. Sugar, **42**, No. 9, 28 (1947).
28. PERCIVAL, E. G. V. J. Chem. Soc. 648 (1935).
29. REYNOLDS, D. D. and EVANS, W. L. Org. Syntheses, **22**, 56 (1942).
30. SHARP, V. E. and STACEY, M. J. Chem. Soc. 285 (1951).
31. SUGIHARA, J. M. *In* Advances in carbohydrate chemistry. Vol. 8. *Edited by* C. S. Hudson and M. L. Wolfrom. Academic Press, Inc., New York. 1953.
32. TAUFEL, K. and REISS, R. Z. anal. Chem. **134**, 252 (1951).
33. VERKADE, P. E., COHEN, W. D., and VROEGE, A. K. Rec. trav. chim. **59**, 1123 (1940).
34. WOLFROM, M. L. and SHAFIZADEH, F. J. Org. Chem. **21**, 88 (1956).

THE PAPILIONACEOUS ALKALOIDS

XXIII. THE STRUCTURE OF BAPTIFOLINE[1]

M. MARTIN-SMITH[2] AND LÉO MARION

ABSTRACT

Baptifoline ($C_{15}H_{20}O_2N_2$) has been found on spectroscopic evidence to contain a hydroxyl group and an α-pyridone ring. On catalytic hydrogenation it gives rise to tetrahydrobaptifoline, which has been identified as *l*-hydroxylupanine. Baptifoline is, therefore, *l*-13-hydroxyanagyrine.

Baptifoline ($C_{15}H_{20}O_2N_2$), also designated as alkaloid P3, is a base occurring in *Baptisia perfoliata* (L.) R. Br. (9) and *Baptisia minor* Lehm. (10). It is a crystalline, monoacidic alkaloid, $[\alpha]_D$ −147.7°, forming easily crystallizable salts (10).

It contains a free hydroxyl group detected by a strong band at 3260 cm.$^{-1}$ in its infrared absorption spectrum, and at 3340 cm.$^{-1}$ in that of its perchlorate. There is strong spectroscopic evidence for the presence in the base of an α-pyridone ring. The infrared spectrum of the base shows an absorption band at 1650 cm.$^{-1}$ and one at 1555 cm.$^{-1}$ with a shoulder at 1567 cm.$^{-1}$, while that of its perchlorate shows three bands at 1652, 1576, and 1552 cm.$^{-1}$. The frequencies of these three bands are almost identical with those observed in each of the spectra of cytisine, N-methylcytisine, rhombifoline, anagyrine, and thermopsine (3, 4), the only other members of the series in which the lactam group is part of an α-pyridone ring.

In the series of the C_{15} lupine alkaloids all those containing an α-pyridone ring such as anagyrine ($[\alpha]_D$ = −165.3°), thermopsine ($[\alpha]_D$ = −159.6°), and rhombifoline ($[\alpha]_D$ = −232.4°) have numerically high optical rotations whereas those containing an α-piperidone ring, such as lupanine ($[\alpha]_D$ = +61.4°), hydroxylupanine ($[\alpha]_D$ = +64.2°), and α-isolupanine ($[\alpha]_D$ = +65.9°), have optical rotations that are numerically relatively low. Hence the high optical rotation of baptifoline ($[\alpha]_D$ = −147.7°) supplies contributory evidence of the presence in the base of an α-pyridone ring.

It was therefore decided, owing to the small amount of material available, that the most promising line of attack in attempting to elucidate the structure of baptifoline would be to hydrogenate the double bonds and endeavor to relate the product to the known hydroxylupine alkaloids containing an α-piperidone ring, such as hydroxylupanine (2) and lupilaxine (12).

Accordingly, baptifoline was reduced catalytically under the conditions employed for the conversion of thermopsine to α-isolupanine (3). The reaction was rapid and at the end of 20 minutes the uptake of 2 moles of hydrogen was complete. Such catalytic reduction of the α-pyridone ring in the C_{15} lupine alkaloids is known to be stereospecific and to cause the hydrogen entering at C-6 to assume a *cis* position with respect to the methylene bridge (11). Hence the resulting tetrahydrobaptifoline could only be either an hydroxy-α-isolupanine or an hydroxylupanine, depending upon whether baptifoline was a thermopsine or an anagyrine derivative, i.e., whether the hydrogen at C-11 was *cis* or *trans* relative to the methylene bridge (cf. Ref. 11).

[1]*Manuscript received September 20, 1956.*
Contribution from the Division of Pure Chemistry, National Research Council, Ottawa, Canada.
Issued as N.R.C. No. 4164.
[2]*National Research Council of Canada Postdoctorate Fellow.*

Since it was not possible to obtain the hydrogenated product in crystalline form, it was converted to its crystalline hydrochloride. The behavior of the hydrochloride on heating was identical with that of a specimen of hydroxylupanine hydrochloride.[3] Loss of solvent was apparent at *ca.* 100° and a change of phase occurred at 180–230°. The prisms resulting from this change then melted at 272–273°, whereas the final melting point of hydroxylupanine hydrochloride was 274–276°. A search of the literature revealed that a wide range of melting points has been reported for the hydrochloride of hydroxylupanine, i.e., 273° (2), 275° (6), 283° (1), 288–289° (5), and 296–298° (7).

The infrared spectra of the hydrochlorides in chloroform solution (because of low solubility) were of little value; in nujol mulls they were weak and although they appeared identical were not too satisfactory. The samples were therefore sublimed (220–230° at 10^{-3} mm.) and the infrared spectra of the hydrochlorides taken by the potassium chloride disk method. These were undisputedly identical. Consequently, tetrahydrobaptifoline is either *d*-or *l*-hydroxylupanine and, therefore, must contain a hydrogen at C-6 which is *cis* and a hydrogen at C-11 which is *trans* relative to the methylene bridge.

As an additional confirmation, tetrahydrobaptifoline liberated from its salt was chromatographed on paper using butanol saturated with water and glacial acetic acid as the solvent phase, and developed with Munier–Dragendorff reagent (13). Its R_F value (0.40) was identical with that of hydroxylupanine chromatographed under the same conditions.

The optical rotations of tetrahydrobaptifoline hydrochloride and of hydroxylupanine hydrochloride were measured in water solutions. Because the quantity of material available was so small, the error involved in the determination was rather large. The literature records $[\alpha]_D = +45.2°$ for hydroxylupanine hydrochloride (1) and we found $[\alpha]_D^{23} = +55°$, whereas the rotation of tetrahydrobaptifoline was $[\alpha]_D^{23} = -72°$. There is no doubt, therefore, that whereas the naturally occurring hydroxylupanine is known to be dextrorotatory, tetrahydrobaptifoline is levorotatory and, hence, must be *l*-hydroxylupanine.

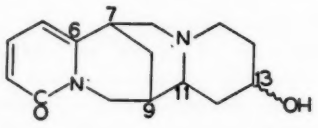

It has been established by Galinovsky, Pöhm, and Riedl (8) that hydroxylupanine is 13-hydroxylupanine and, therefore, because of the established relationship between anagyrine and lupanine (11), it can be concluded that baptifoline is *l*-13-hydroxyanagyrine, represented by the above formula.

EXPERIMENTAL

The infrared absorption spectra were taken with a Perkin–Elmer double beam spectrometer, model 21B, using a sodium chloride prism. Unless otherwise stated they were taken on nujol mulls.

Tetrahydrobaptifoline

Baptifoline (50 mg.) dissolved in glacial acetic acid (7 ml.) was hydrogenated at room temperature and atmospheric pressure in the presence of Adams' catalyst (30 mg.). At

[3]*Prepared from a specimen of hydroxylupanine given by Professor V. Deulofeu, whose courtesy is acknowledged.*

the end of 20 minutes the compound had adsorbed 2 moles of hydrogen. The solution was filtered, the catalyst washed several times with acetic acid, and the combined filtrate and washings evaporated to dryness under diminished pressure. The residual colorless oil was soluble in acetone, methanol, chloroform, and ethanol, but could not be induced to crystallize. Addition of ether to the various solutions caused oiling out.

The product was converted to the hydrochloride by adding one drop of hydrochloric acid to a methanolic solution of the base and diluting the solution with acetone. The crystalline salt was recrystallized twice from methanol–acetone from which it separated as colorless plates. On being heated the salt lost solvent at *ca.* 100°, showed a change of phase at 180–230°, and melted at 272–273°. $[\alpha]_D^{23} = -72° \pm 10°$ (*c*, 0.179 in water).

Authentic hydroxylupanine hydrochloride when heated showed the same behavior, and the final melting point was 274–276°. $[\alpha]_D^{23} = +55°$ (*c*, 0.19 in water).

Tetrahydrobaptifoline hydrochloride was sublimed (220–230° at 10^{-3} mm.) and the infrared spectrum taken by the potassium chloride disk method. The spectrum was superimposable on that of hydroxylupanine hydrochloride taken under the same conditions.

Both tetrahydrobaptifoline liberated from its hydrochloride and hydroxylupanine were spotted on paper and butanol saturated with water (10 ml.) and glacial acetic acid (0.5 ml.) used as the solvent phase. The chromatogram was developed with Munier–Dragendorff reagent (13). For both the R_F was 0.40.

ACKNOWLEDGMENT

We are indebted to Mr. R. Lauzon of these laboratories for taking the infrared absorption spectra.

REFERENCES

1. BECKEL, A. Arch. Pharm. **250**, 691 (1912).
2. BERGH, G. Arch. Pharm. **242**, 416 (1904).
3. COCKBURN, W. F. and MARION, L. Can. J. Chem. **29**, 13 (1951).
4. COCKBURN, W. F. and MARION, L. Can. J. Chem. **30**, 92 (1952).
5. COUCH, J. F. J. Am. Chem. Soc. **61**, 1523 (1939).
6. DEULOFEU, V. and GATTI, A. J. Org. Chem. **10**, 179 (1945).
7. GALINOVSKY, F. and PÖHM, M. Monatsh. **80**, 864 (1949).
8. GALINOVSKY, F., PÖHM, M., and RIEDL, K. Monatsh. **81**, 77 (1950).
9. MARION, L. and TURCOTTE, F. J. Am. Chem. Soc. **70**, 3253 (1948).
10. MARION, L. and COCKBURN, W. F. J. Am. Chem. Soc. **70**, 3472 (1948).
11. MARION, L. and LEONARD, N. J. Can. J. Chem. **29**, 355 (1951).
12. MARION, L., LEONARD, N. J., and MOORE, B. P. Can. J. Chem. **31**, 181 (1953).
13. MUNIER, Z. Bull. soc. chim. biol. **35**, 1225 (1953).

TRIARYLMETHANE COMPOUNDS AS REDOX INDICATORS IN THE SCHOENEMANN REACTION

I. MECHANISM OF THE SCHOENEMANN REACTION[1]

G. A. GRANT, R. BLANCHFIELD, AND D. MORISON SMITH

ABSTRACT

A method is outlined for the detection of anticholinesterase agents similar to sarin (isopropyl methylphosphonofluoridate) in aqueous solution at concentrations as low as 0.1 p.p.m. in 10 ml. of solution by the use of the Schoenemann reaction. A new series of indicators, 4,4′-(2-thenylidene)bis[N,N-dimethylaniline] variously substituted in the thiophene ring, was used in the investigation. The dependence of color formation on pH, chloride ion concentration, and other factors led to an explanation of the mechanism of the reaction involved. Chloride ion is necessary for the reaction and, in the absence of the indicator, free chlorine can be detected in acid solution. Presumably, then, during acidification perphosphonate ion reacts with chloride ion to give hypochlorous acid, which oxidizes the mono ion of the leuco compound to a dye.

Ions such as cyanide ion, with a lower oxidation–reduction potential than the leuco compounds, interfere with the test. Oxidation of the leuco compound by hypochlorous acid is bypassed in the method described for the detection of sarin in the presence of hypochlorous acid.

INTRODUCTION

In the search for a sensitive method for the detection, in aqueous solution, of anticholinesterase agents known as nerve gases, a number of reactions were explored. The Schoenemann reaction, which showed the most promise, has been described by Wilson, Gehauf, and Rueggeberg (8) and by Epstein and Bauer (1). It involves the formation of a perphosphonate ion by the interaction of hydrogen peroxide with phosphonofluoridate ester in basic solution as given in equation 1.

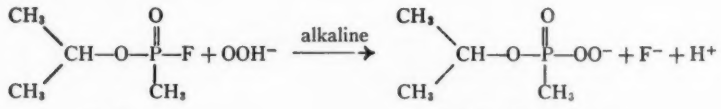

Sarin — Perphosphonate ion [1]

The perphosphonate ion is capable of producing colored oxidation products from certain organic compounds. In this respect *o*-dianisidine has been extensively investigated as an indicator by Epstein and Bauer (1) and by Thomas and Grant (2). By extraction of the orange oxidized form with organic solvents, as little as 0.1 p.p.m. of agent can be detected without interference from a number of substances which are colored in aqueous solution. It would be preferable to avoid the use of organic solvents and to have a purple or blue indicator of equal or better sensitivity. Certain leuco triarylmethane compounds, for example 4,4′-(2-thenylidene)bis[N,N-dimethylaniline], were found to give blue colors on oxidation in the Schoenemann reaction. A number of these leuco compounds, variously substituted in the thiophene ring, were synthesized and tested (7). The syntheses and properties of the leuco compounds, the results of the tests, and the spectra of the dyes will be described in detail in later papers in this series.

[1]*Manuscript received September 24, 1956.*
Contribution from Defence Research Board, Defence Research Chemical Laboratories, Ottawa, Ontario. Issued as D.R.C.L. Report 135A.

It was previously assumed that the perphosphonate ion oxidizes the reduced indicator to the colored compound in acid solution. Preliminary investigation has, however, shown that this is not the correct reaction mechanism when the triarylmethanes are employed as the redox indicators. Indeed, because of the results of the present investigation in which the principal factors involved in the Schoenemann reaction are studied, an alternative reaction mechanism must be postulated to account for the oxidation of the leuco triarylmethane compounds.

EXPERIMENTAL AND RESULTS

Testing Procedure

A procedure was adopted for the determination of the variables affecting color formation. One milliliter of a 4% aqueous solution of sodium pyrophosphate peroxide ($Na_2P_2O_7.2H_2O_2$) was added to 10 ml. of an aqueous solution of sarin (isopropyl methylphosphonofluoridate) whose concentration (0 to 10 p.p.m.) had been accurately determined by the Schoenemann reaction using *o*-dianisidine as the redox indicator, the calibration data for this indicator having previously been obtained with solutions of sarin made up by weight (3). The solutions of sarin and sodium pyrophosphate peroxide were mixed and (optimum within 30 seconds) 1 ml. of a 0.1% solution of the redox indicator in dilute hydrochloric acid (1:16) was added. The optimum concentration of hydrochloric acid was found to be a 1/16 *N* solution, which gave a final chloride ion concentration of approximately 6.5×10^{-2} gram-ions/liter. The same procedure was followed in making the blank solution except that 10 ml. of distilled water was used instead of the sarin solution. Optical density readings of the sarin solution against the blank were taken at the wavelength of the absorption maximum (*ca.* 625 mμ) using a Beckman Model DU spectrophotometer and 2 cm. Corex Cells. The optimum time for this measurement was found to be 7 minutes after the addition of the leuco compound.

Redox Measurements

Attempts were made to determine polarographically the oxidation–reduction potential for the leuco compounds in solutions of optimum pH and chloride ion concentration, using the method of Julian and Ruby (4). The rate of change of voltage was 160 mv./minute instead of the recommended 20 to 40 mv./minute because of the limitations of the Leeds and Northrup Electrochemograph, Type E. Consequently the results were inaccurate and indicated only that the redox potential for transformation of leuco compound to dye was from −0.9 to −1.0 volts while the potential at which destructive oxidation occurred was between −1.0 and −1.1 volts.

Previously, attempts had been made to determine the oxidation potential using a redox titration according to the method of Meyer and Treadwell (6). The buffers of pH 1.7 which were tried were Clark and Lubs potassium chloride – hydrochloric acid, Sorensen citrate buffer, and a solution of 0.1 *N* potassium bisulphate and 0.1 *M* potassium sulphate. Oxidizing agents tried were 0.1 *N* potassium dichromate and 0.1 *N* and 0.001 *N* ceric sulphate. For agitation, either nitrogen bubbling or magnetic stirring was used. From these measurements it was impossible to obtain accurate data, for destructive oxidation occurred near the oxidation potential.

Factors Affecting Color Development

In studying these factors use was made of only a few representative triarylmethane leuco dyes, namely 4,4′-(2-thenylidene)bis[N,N-dimethylaniline] (I(*a*)); 4,4′-(5-methyl-

2-thenylidene)bis[N,N-dimethylaniline] (I(*b*)); 4,4′-(4,5-dimethyl-2-thenylidene)bis-[N,N-dimethylaniline] (I(*c*)); 4,4′-(5-ethyl-4-methyl-2-thenylidene)bis[N,N-dimethylaniline] (I(*d*)).

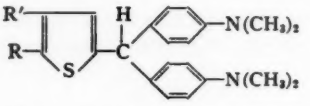

I(*a*), R = R′ = H.
I(*b*), R = CH_3, R′ = H.
I(*c*), R = R′ = CH_3.
I(*d*), R = C_2H_5, R′ = CH_3

Unless otherwise stated, compound I(*c*) was used.

Duration of Time after Initial Color Formation

The solutions were mixed as described and placed in the spectrophotometer. Density measurements were made at the absorption maximum at various times. Compounds I(*a*), I(*b*), I(*c*), and I(*d*) were used and the results are plotted in Fig. 1. These curves

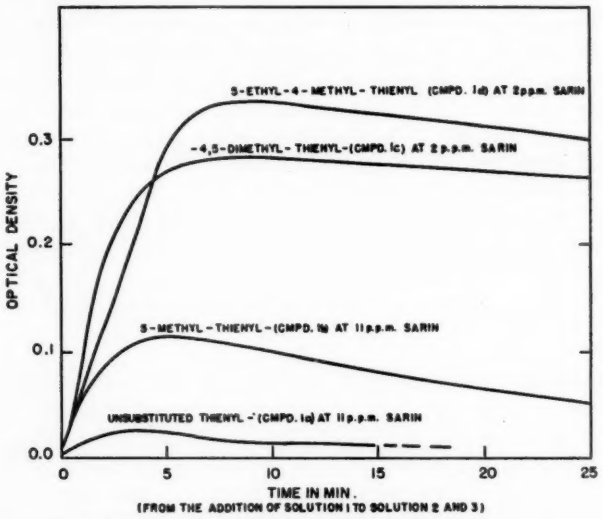

FIG. 1. Effect of time on color development.

indicate that the color develops to maximum intensity in less than 10 minutes and then fades slowly. For practical purposes a standard reaction time of 7 minutes was chosen.

Duration of Time before Introduction of Indicator Solution

The solutions of sarin and sodium pyrophosphate peroxide were mixed and various intervals of time were allowed to elapse before introduction of the solution of redox indicator. The color intensity was then measured as usual. Table I gives the figures for

TABLE I

EFFECT OF TIME DELAY IN ADDING ACIDIFIED INDICATOR SOLUTION TO PERPHOSPHONATE ION SOLUTION

Delay time (min.)	0.02	0.05	0.10	0.15	0.25	1.00	2.00	5.0	10.00
Optical density at 610 mμ	0.60	0.64	0.63	0.71	0.74	0.73	0.75	0.70	0.69

optical density at the absorption maximum in this experiment. From these data, which are indicative of the stability of the perphosphonate ion, 30 seconds was selected as the optimum interval before the addition of the indicator solution.

Acidity of the Solution in Which the Color Developed

Solutions of sarin and sodium pyrophosphate peroxide were mixed as usual. To this mixture was added leuco compound I(*a*) dissolved in a solution containing a constant concentration of sodium chloride (the optimum, 6.5×10^{-2} gram-ions/liter) and different concentrations of sulphuric acid, which controlled the pH values of the medium in which the color developed.

The effect of pH on the color developed in the Schoenemann reaction at constant chloride ion concentration is given in Fig. 2. The results indicate an optimum acidity of around pH 1.6.

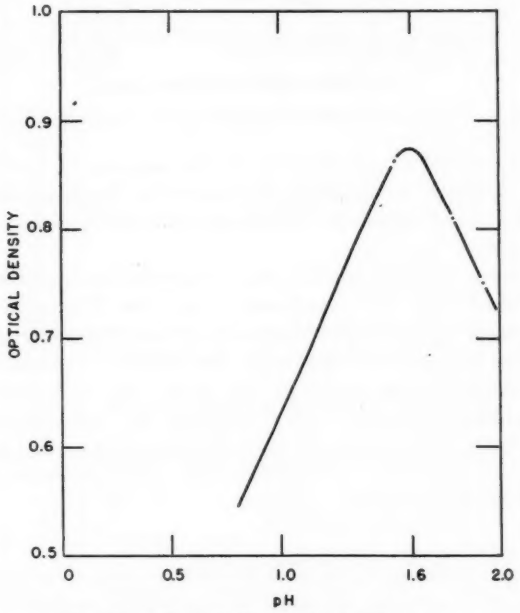

FIG. 2. Effect of pH on color development.

Concentration of Chloride Ion

To the solutions of sarin and sodium pyrophosphate peroxide, mixed as before, was added a solution of the leuco compound, prepared in solutions of 1:50 sulphuric acid containing different concentrations of chloride ion as sodium chloride.

From the results obtained on varying the concentration of chloride ion at constant pH 1.69 (Fig. 3) a concentration between 5×10^{-2} and 1 gram-ion/liter would seem to be optimum. In an attempt to determine the part played by chloride ion in the mechanism of the color formation, a solution of about 100 p.p.m. of sarin containing 3% sodium chloride was used instead of the usual 5 p.p.m. sarin solution. When the test was performed as previously outlined, but withholding the leuco compound, strong

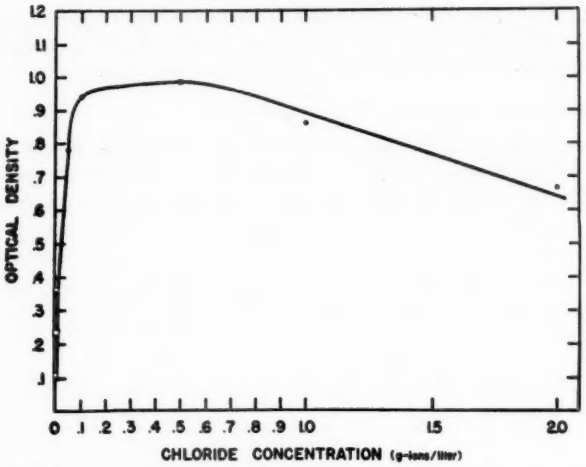

FIG. 3. Effect of chloride ion concentration on color development.

chlorine odor was apparent. Chemical proof of the presence of free chlorine was established by the color obtained on drawing the vapors in the flask through a filter paper moistened with a 0.1% *o*-dianisidine dihydrochloride solution which acted as a redox indicator for the chlorine.

The effect of chloride ion was studied when *o*-dianisidine was used as the indicator. *o*-Dianisidine dihydrochloride was converted to the free base with sodium carbonate, carefully washed free of chloride, and dissolved in absolute ethyl alcohol. The alcohol solution was brought to a boil and sulphuric acid added. The white sulphate salt was filtered and recrystallized from water in the dark. The Schoenemann reaction was carried out as previously described (1), employing the *o*-dianisidine dihydrochloride. The time of formation and intensity of the color formed was the same for the hydrochloride and sulphate. Therefore, it is evident that chloride ion is not essential when *o*-dianisidine is used as the indicator.

Chlorine

A positive test was obtained when a solution of 6 p.p.m. of aqueous chlorine was used instead of the sarin solution, presumably because of oxidation of the leuco compound by hypochlorous acid in the acid medium. When, however, a time interval of 3 minutes was allowed to elapse between the addition of the oxidizing solution and the solution of leuco compound, no color was formed, probably because the alkaline peroxide had sufficient time to oxidize the hypochlorite. Thus the perphosphonate ion as well as hypochlorite will oxidize the *o*-dianisidine but only hypochlorite will oxidize the triarylmethane compounds.

Cyanide Ion

The standard test was carried out, using a sarin solution containing 200 p.p.m. of potassium cyanide. No color was produced in the test.

Other Anticholinesterase Agents

"Tabun", which is a phosphonocyanide ester rather than a phosphonofluoride ester, was used in aqueous solution instead of sarin. The standard test was applied. No color

was obtained unless the tabun was freshly distilled and the aqueous solution just made up, whereupon a faint color appeared.

Acid–Base Titration of the Leuco Compound

Compound I(*a*) was dissolved in 1 *N* hydrochloric acid to give a 0.05 *M* solution. An aliquot of this solution was titrated with 1 *N* sodium hydroxide, using a Coleman model 3A pH Electrometer with a glass electrode.

The results for the acid–base titration are given in Fig. 4. These indicate an end

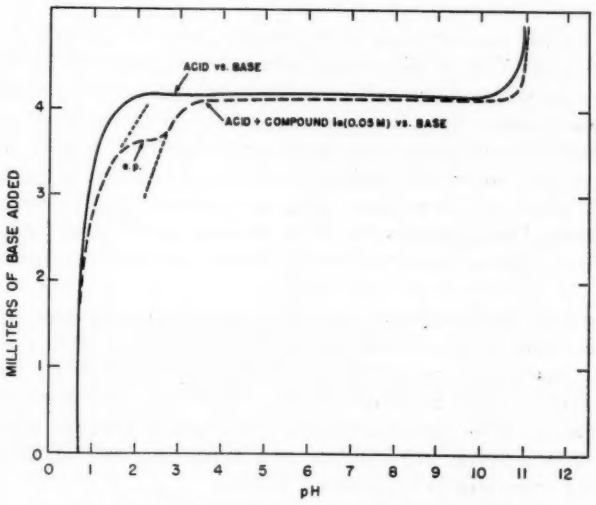

FIG. 4. pH of formation of mono ion of compounds.

point of pH 2.2 for the formation of the mono ion of the compound according to equation 2.

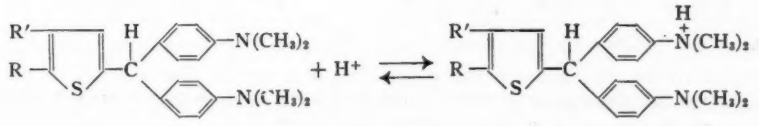

[2]

DISCUSSION

A number of facts pertaining to the Schoenemann reaction are of interest in elucidating the mechanism of reaction. The presence of chloride ion is essential to color development in the Schoenemann reaction when the triarylmethane compounds are used as indicators but it is not essential when *o*-dianisidine is used. Free chlorine is formed under the conditions of this reaction when the indicator is not present, presumably by interaction of the essential chloride ion and perphosphonate ion.

The Schoenemann reaction medium is initially alkaline (pH 9 to 10.5) and then acidified to pH 1.6 to 2.2. Therefore, a study of the oxidation–reduction reactions of free halogen in acidic and basic media may reveal some information to explain chloride ion dependence and mechanism of the reaction. All couples are written according to the convention used by Latimer (5).

The reaction between perphosphonate ion and chloride ion in basic solution may be considered as a combination of two couples.

[3]

and

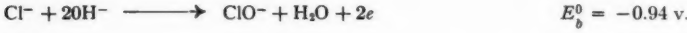

[4]

These are both equally dependent on hydroxyl ion concentration so that for the reaction to occur the potential (3) must be considerably more negative than −0.94 v. However, in alkaline peroxide solution hypochlorite ion appeared to be oxidized to chlorite or chlorate. This was evident from the fact that, when a solution of chlorine was used in place of sarin, oxidation of leuco compound took place only if acid indicator solution was added immediately after the alkaline peroxide solution, but if the hypochlorite and alkaline peroxide were allowed to react for 3 to 4 minutes prior to addition of indicator no dye was formed. This indicates the OCl^- is being oxidized to ClO_2^- and ClO_3^- ions, which have lower oxidation potential than OCl^- and are therefore unable to oxidize the indicator.

Further, when sarin was present along with hypochlorite and some time was allowed to elapse between addition of peroxide and indicator, dye formation was evident almost on a quantitative basis, which would indicate that perphosphonate ion formed in alkaline solution is not reacting with hypochlorite ion and is still available to oxidize chloride ion upon acidification. It is thus evident that the reaction between perphosphonate ion and chloride ion to produce free chlorine and hypochlorous acid must occur in acid solution, probably according to equations 5 and 6.

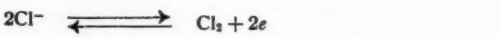

[5]

[6]

In acid solution the chlorine or hypochlorous acid appearing in accordance with equation 7 acts as an oxidizing agent on leuco compound in solution.

[7]

The equilibrium at pH 1.8 is such that the mole fraction of chlorine is 0.7 and that of hypochlorous acid is 0.3 (3). The perphosphonate ion alone cannot oxidize the leuco compound because it decomposes too readily in acid solution (1). Probably as the solution becomes more acid during mixing, the perphosphonate ion reacts with the large excess of chloride ion more rapidly than with the small amount of leuco compound, which is appreciably soluble only below pH 2.2. The HOCl formed is not removed by excess peroxide because in acid solution equation 8 applies to peroxide and the potential here is not adequate for reaction.

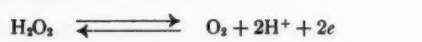

[8]

For the same reason the dye is not affected by acid peroxide although in alkaline solution it is oxidatively destroyed by peroxide.

The mechanism can then be summarized as follows. Perphosphonate is first produced (equation 1). Then, as the alkaline and acid solutions are mixed and the pH goes from 10.5 to 1.6, reaction proceeds as in equation 9.

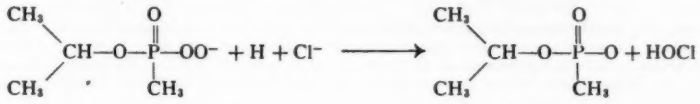

[9]

At optimum chloride ion concentration and pH the dye is produced (equation 10).

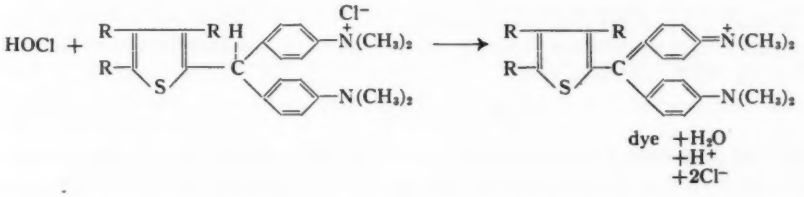

[10]

On the basis of the above mechanism an explanation of chloride ion dependence and failure of the reaction with tabun can be attempted.

The increase in dye formation with an increase of chloride concentration up to 5×10^{-1} gram-ions/liter can be considered as indicative of an increase in hypochlorous acid concentration as the result of an increase in collision frequency between perphosphonate and chloride ions and a decrease in collision frequency between perphosphonate ions. Assuming a 100% yield of perphosphonate ion the ratio of chloride ion to perphosphonate ion with 10^{-3} gram-ions/liter of chloride ion and 5 p.p.m. of sarin is approximately 1 to 30 while with 1 gram-ion/liter it is approximately 1 to 30,000. The decrease in dye yield with chloride ion concentration greater than 1 gram-ion/liter may be the result of a decrease in available hypochlorite. From equation 7 it is evident that an increase of chloride ion increases the proportion of chlorine to hypochlorite in solution. As the experiments were conducted in an open system with vigorous stirring, chlorine would escape and result in a decrease in available hypochlorous acid and generated dye.

Cyanide ion was shown to prevent dye formation. It is possible that perphosphonate ion in alkaline solution is reduced by the CN^- ion.

Therefore, the hydrolysis of tabun to give cyanide ion explains the negative results obtained with it in the Schoenemann reaction when these indicators are used.

REFERENCES

1. Epstein, J. and Bauer, V. E. Paper presented at A.C.S. Pittsburgh Conference of Analytical Chemistry and Applied Spectroscopy, Feb. 27, 1956.
2. Grant, G. A. and Thomas, H. Unpublished results.
3. Holst, G. Chem. Revs. **54**, 169 (1954).
4. Julian, D. B. and Ruby, W. R. J. Am. Chem. Soc. **72**, 4719 (1950).
5. Latimer, W. M. Oxidation potentials. 2nd ed. Prentice-Hall, Inc., New York. 1952.
6. Meyer, H. W. and Treadwell, W. D. Helv. Chim. Acta, **35**, 1444 (1952).
7. Smith, D. M., Blanchfield, R., Thompson, J. F., and Grant, G. A. Paper in preparation.
8. Wilson, G. B., Gehauf, B., and Rueggeberg, W. H. C. Paper presented at A.C.S. Pittsburgh Conference of Analytical Chemistry and Applied Spectroscopy, Feb. 27, 1956.

STRESSES AND STRAINS IN ADSORBENT–ADSORBATE SYSTEMS. II[1]

E. A. FLOOD

ABSTRACT

It has been shown previously that when adsorbates act as single component complexes, i.e. behave as single substances in complex force fields, volumetric mean adsorbate and mean adsorbent stress intensities can be calculated from adsorption isotherm data. When potentials of surface regions in the micropore system of a porous adsorbent are statistically independent of pore structure, linear mean stress intensities of the solid are related to volumetric means through an equation containing a structure factor which is independent of the nature and pressure of the adsorbed gas.

In this paper we present adsorption extension data for an active carbon rod when exposed to helium, hydrogen, nitrogen, argon, krypton, and water at pressures up to 1600 p.s.i. The data suggest that the potentials of the capillary regions are not independent of structure. An empirical correlation factor is introduced and the resulting semiempirical equation describes the data probably within the experimental error.

The results suggest that in cases of moderately strong adsorption, adsorption potentials of thick-walled capillary regions are higher than those of thin-walled regions.

INTRODUCTION

Length changes of porous solid adsorbents resulting from adsorption of vapors have been studied by a number of investigators: Meehan (9), Bangham (2, 3), McBain (8), McIntosh (1, 7), Wiig (13), Yates (14), etc., the work of Bangham and co-workers in Egypt and that of McIntosh and co-workers in this country being especially notable.

It has been customary to correlate these dimensional changes with the changes in the more or less fictious solid surface tensions or with the so-called "spreading pressures", the changes in surface tensions or spreading pressures being based on the Gibbs "adsorption isotherm", i.e. on the Gibbs model interface. The Gibbs model interface is a very convenient mathematical fiction for the treatment of cases where interfacial volumes are small compared with the whole system under consideration. However, such two-dimensional model interfaces are entirely unsuitable for the treatment of systems where the interfacial volumes are relatively large and where the behavior of the system depends largely on the distribution of densities, stress intensities, viscosities, etc. of materials within the surface regions. Since we have been mainly concerned with flow rates of adsorbed materials we have found it convenient to describe the adsorbate as a volume of a single component subjected to a complex force field, i.e., as a single component complex (5).

When vapors are adsorbed by relatively rigid porous adsorbents and the adsorbates behave as single component complexes, volumetric mean stress intensities of adsorbates and adsorbents can be calculated from relevant adsorption isotherm data, provided that the relevant isotherms correspond to paths of thermodynamic reversibility (5, 6).

We have shown that these volumetric mean stress intensities are given by the following equations:

$$[1] \qquad \overline{p_a}^v = \int_0^P \rho_a/\rho \cdot dP = \alpha P,$$

$$[2] \qquad \overline{p_c}^v = [1+\phi-\phi\alpha]P,$$

[1]*Manuscript received May 24, 1956.*
Contribution from the Division of Pure Chemistry, National Research Council, Ottawa.
Issued as N.R.C. No. 4163.

where $\overline{p_a}^v$ = volumetric mean stress intensity of adsorbate within the porous adsorbent,
ρ_a = volumetric mean density of adsorbate within adsorbent,
P = pressure of adsorbate fluid outside of porous adsorbent, i.e., the equilibrium pressure,
ρ = density of adsorbable fluid outside of adsorbent, i.e., the uniform density of the liquid or gas in equilibrium with adsorbate,
$\overline{p_e}^v$ = volumetric mean elastic or reversible stress intensity of the porous solid ($\overline{p_e}^v = 0$ when $P = 0$),
ϕ = void volume/solid volume = v_a/v_e (v_a+v_e = total volume of the porous body),
α = $\overline{p_a}^v/P$ = mean value of ρ_a/ρ averaged over the pressure interval $0 \rightarrow P$. Thus α is readily obtained from the adsorption isotherm.

The above relations are based on the equation $\Delta\overline{F_e}^v = v_e\,\Delta\overline{p_e}^v$ where $\Delta\overline{F_e}^v$ is the volumetric mean change in Gibbs free energy (or thermodynamic potential) resulting from isothermal changes in reversible or elastic states of stress which do not change the volume materially. For many purposes this is practically identical with assuming that $\Delta\overline{F_e}^v$ is proportional to the change in "solid surface tension" or "spreading pressure".

It is important to note, however, that porous active adsorbents are not normally thermodynamically uniform bodies, and hence that $\delta\Delta F_e$ for the various solid elements of the assembly are not uniform throughout the body. Hence $\Delta\overline{F_e}^v$ and $\Delta\overline{p_e}^v$ may be made up from widely differing elements; thus while $\Delta\overline{F_e}^v$ and $\Delta\overline{p_e}^v$ may be strongly negative for a given adsorption reaction, in some regions $\delta\Delta F_e$ may be positive.

The changes in length of an assembly of solid elements of different sizes and shapes will be dependent not only on $\Delta\overline{p_e}^v$ but on the actual distribution of the stress intensities and their correlation with the structure and elastic properties of the elements of the assembly. It is mathematically quite possible for $\Delta\overline{p_e}^v$ to be zero while the whole porous assembly either increases or decreases its dimensions. The general problem of correlating the net strains of a complex assembly with the changes in the internal force structure will be very involved indeed. Anything like a complete mathematical description would involve a very complex tensor or similar analysis and would require a microscopically detailed knowledge of the whole adsorption reaction (12). However, by reference to ideal systems the influence of the various physical and statistical factors on adsorption extension behavior can be illustrated very simply. Thus consider a linear array of elements of an isotropic solid of lengths l_i where each of the equal elementary lengths may be subjected to particular stress intensity component changes, δp_{ei}, resolved along the l direction. We may write for the change in length of each element:

$$\delta l_i = A_i \cdot l_i \cdot \delta p_{ei} + B_i' \cdot l_i \cdot \delta p_{ei}^2 + C_i' \cdot l_i \cdot \delta p_{ei}^3 \ldots$$

and if A_i, B_i, C_i are constant we can write:

$$[3] \qquad \frac{\delta L}{L} = \frac{\sum \delta l_i}{\sum l_i} = A \cdot \overline{\delta p_e}^L + B' \cdot \overline{\delta p_e}^2 + C' \cdot \overline{\delta p_e}^3 \ldots$$

where A, B', C' etc. are constants characteristic of the solid material and $\overline{\delta p_e}^L \cdot \overline{\delta p_e}^2$, etc. are linear average quantities.[2]

[2] *If A_i, B_i, C_i etc. and δp_{ei} are statistically independent, but not constant, Equation [3] becomes $\delta L/L = \bar{A}^L \cdot \overline{\delta p_e}^L$; if not statistically independent, Equation [3] becomes $\delta L/L = K \cdot \bar{A}^L \cdot \overline{\delta p_e}^L$ where $K \gtrless 1$. If A_i and δp_{ei} are both increasing functions of l, $K > 1$.*

Equation [3] may be written:

$$\delta L/L = A\cdot\overline{\delta p_e}^{L}+B''\cdot B'(\overline{\delta p_e}^{L})^2+C''\cdot C'(\overline{\delta p_e}^{L})^3\ldots$$

where B'', C'' are dependent on the distribution of stress intensities and thus are not necessarily properties of the adsorbent alone. For solids which obey Hooke's Law approximately, B', C' etc. are small compared with A. Hence the approximate equation,

[4] $$\delta L/L = A(1+B\,\overline{\delta p_e}^{L})\,\overline{\delta p_e}^{L}$$

where A and B are regarded as properties of the adsorbent only, should be reasonably valid for small changes in length of such assemblies. Since thermodynamic considerations enable us to correlate volumetric mean stress intensities with adsorption data, the problem resolves itself into the correlation of the linear mean stress intensities with the corresponding volumetric means and hence with corresponding adsorption isotherms. This correlation should if at all possible lead to formulae containing only measurable variables and constants characteristic of the adsorbent and adsorbate, respectively. In systems where "the forces resulting from adsorption", "the solid areas" etc. may be regarded as statistical variables, we shall show that the linear mean stress intensity changes can be correlated with the adsorption data by means of an equation of the form

$$\overline{p_e}^{L} = [1+\phi\cdot K_s\cdot K_p-\phi\cdot K_s\cdot K_p\cdot\alpha]P,$$

where $\overline{p_e}^{L}$ is the linear mean stress intensity change of the solid, K_s is a constant factor ($\geqslant 1$) dependent only upon the structure and elastic properties of the solid, and K_p is a factor dependent upon the nature and equilibrium pressure of the adsorbed fluid. When the effective surface force field is independent of the solid structure (i.e. of pore sizes, elastic properties etc.) K_p will be unity. Again, where $\Delta\overline{p_e}^{v}$ is a uniform change in hydrostatic pressure, K_p will be unity for the corresponding change in $\overline{p_e}^{L}$. However, in general K_p will be pressure dependent and may be greater or less than unity.

Accordingly, if the underlying assumptions are valid the adsorption extension of porous adsorbents should be given to a close approximation by

[5] $$\begin{cases}\delta L/L = A(1+B\overline{p_e}^{L})\overline{p_e}^{L},\\ \overline{p_e}^{L} = [1+\phi\cdot K_s\cdot K_p-\phi\cdot K_s\cdot K_p\cdot\alpha]P.\end{cases}$$

We have shown previously (6) that Equation [5], with $K_p = 1$ and $B = 0$, can be used to describe a number of experimental results fairly well. Further, that in the case of activated carbon, A corresponds closely with the linear compressibility of graphite and that plausible model pore systems can be constructed which are consistent with the observed values of K_s, ϕ, and the mechanical properties of the carbon generally.[3]

In what follows we present some simple illustrations of the statistical relations upon which Equation [5] is based, together with some additional experimental data. The new data indicate that K_p cannot be taken as unity, and hence, that in the general case we cannot regard the adsorption potential of the capillary or surface regions as statistically independent of the solid structure.

[3]*It will be noted that when $\delta L/L$ is not measured by $\overline{\delta p_e}^{v}$, i.e., where $K_s\cdot K_p \neq 1$ and $\overline{\delta p_e}^{v} \neq \overline{\delta p_e}^{L}$, it implies that there is a distortion in the sense that while the assembly as a whole may retain its shape, either particles of the assembly change their shape or their change in volume per unit volume is different, i.e., small particles swell more than large particles, or vice versa, and thus $\delta v_s \neq \delta v_e$.*

THEORETICAL ILLUSTRATIONS

Let a porous solid of length L be divided into thin sections perpendicular to L and of thickness l_i. Let A_i be the area of the ith section, a_i the area of the fluid-filled holes, and c_i the area of the solid. Thus $A_i = a_i + c_i$. Let F_i be the total external force acting normally on A_i and in equilibrium with the forces F_{ai} and F_{ci} exerted by the fluid and solid respectively. Let $P_i = F_i/A_i$, $p_{ai} = F_{ai}/a_i$, and $p_{ci} = F_{ci}/c_i$ be the corresponding mean stress intensities parallel to L. Then, balancing forces,

$$A_i P_i = a_i \cdot p_{ai} + c_i \cdot p_{ci}$$

and summing over all sections,

$$\sum P_i \cdot A_i \cdot l_i = \sum p_{ai} \cdot a_i \cdot l_i + \sum p_{ci} \cdot c_i \cdot l_i.$$

Supposing P and A constant (independent of l) we have

$$vP = v_a \cdot \overline{p_a}^{V} + v_c \cdot \overline{p_c}^{V}$$

and

$$\overline{p_c}^{V} = P + (P - \overline{p_a}^{V}) \cdot v_a/v_c = [1 + \phi - \phi\alpha]P$$

where $\phi = v_a/v_c$, $v = v_a + v_c$, and $\overline{p}^{V}$ and $\overline{\ }^{V}$ are volumetric average stress intensities of the fluid and solid respectively. Also $v_a = \bar{a}^{L} \cdot L$, where $\bar{a}^{L}$ is the linear average area of the holes averaged along the length L. Similarly $v_c = \bar{c}^{L} \cdot L$ and $A = \bar{a}^{L} + \bar{c}^{L}$. If A is large compared with the average area of single holes in the ith section, a_i and c_i will be virtually constant. Accordingly the area A is taken so as to be comparable with the average area of single holes in each section. Thus a_i and c_i may be regarded as functions of the stochastic variable l_i.

If the porous solid were immersed in a fluid of pressure P with which it did not interact at all, the stress intensity of the solid would be simply the hydrostatic pressure P. But if surface forces are involved we can describe the action of these forces in terms of the adsorbate pressure and write $p_{ci} = P + (P - p_{ai}) \cdot a_i/c_i$ where p_{ci} is the change in the solid stress intensity component parallel to L due to immersion in the fluid of hydrostatic pressure P. Hence,

$$\overline{p_c}^{L} = \frac{\sum p_{ci} \cdot l_i}{\sum l_i} = P + \frac{\sum (P - p_{ai}) \cdot a_i/c_i \cdot l_i}{\sum l_i}.$$

If p_{ai} and c_i are constant, then

$$\overline{p_c}^{L} = P + (P - \overline{p_a}^{V}) \cdot \bar{a}^{L}/\bar{c}^{L} = P + (P - \overline{p_a}^{V}) \cdot v_a/v_c = \overline{p_c}^{V}.$$

If c_i varies with l_i while p_{ai} is constant, we can write

[6] $$\overline{p_c}^{L} = P + (P - \overline{p_a}^{V}) \cdot K_s \cdot \bar{a}^{L}/\bar{c}^{L} = [1 + \phi \cdot K_s - \phi \cdot K_s \cdot \alpha]P$$

where K_s is a numerical factor which is necessarily greater than unity and whose value depends only on the variation of the solid cross sectional area c_i with l_i. Thus K_s is a constant descriptive of the solid structure but independent of the nature and equilibrium pressure of the fluid.

Equation [6] may be written $\overline{p_c}^{L} = [c_1 - c_2\alpha]P$, where only α is dependent on P and

upon the nature of the fluid. In this case the adsorption extension would be given by an equation of the form[4]

$$\delta L/L = A(c_1 - c_2\alpha)P + AB(c_1 - c_2\alpha)^2 P^2.$$

By comparison with observed values of $\delta L/L$ for various observed values of α and P with different gases ($\delta L/L$, α, and P are capable of wide variation and are readily measured) the constants A, B, C_1, and C_2 could be found. It will be noted that v_a must be known in order to obtain α from isotherm data. If the value of v_a used in calculating α were too large it would introduce a constant factor which would appear in the value of c_2. This would be the case where v_a is based on "helium density" determinations of the active carbon, since even at room temperature helium is appreciably adsorbed (11). However, since the error in this case would be small, it would be possible to evaluate the constants approximately, and then from helium extension behavior using the approximate values of the other constants to estimate the helium adsorption, correct v_a, and redetermine the constants.

However, this procedure depends upon the assumption that c_1 and c_2 are independent of the nature of the fluid, i.e. that c_1 and c_2 are independent of α and of P. Thus it depends on the assumption that the adsorbate pressure is statistically independent of the solid structure.[5]

For the more general case, Equation [6] can be written:

$$[7] \qquad \begin{aligned} \overline{p_c}^L &= P + (P - \overline{p_a}^v) \cdot K_p \cdot K_s \cdot \bar{a}^L/\bar{c}^L \\ &= [1 + \phi \cdot K_s \cdot K_p - \phi \cdot K_s \cdot K_p \cdot \alpha]P \end{aligned}$$

where K_p is dependent on the relation of $p_{a\,i}$ to a_i or to c_i. While K_s is necessarily greater than unity, K_p may be greater or less than unity and may be negative as well as positive. Thus K_p will be greater than unity where the adsorbate pressures or volumetric mean potentials are larger in the regions where the fluid areas are larger and the solid areas, c_i, smaller. Conversely, K_p will be less than unity when the adsorbate pressures are larger in the smaller holes with the thicker walls. In this latter case we should expect K_p to vary with the equilibrium pressure of the adsorbate, when the adsorbate is not an ideal gas. Thus when the mean potential of the volume of the smaller holes is greater than that of the larger holes, the density and hence the pressure will increase with increasing equilibrium pressure relatively more rapidly in the smaller holes. This will continue until the adsorbate density in both the smaller and larger holes becomes high and the com-

[4]*When $B \to 0$ and $\alpha \gg 1$, this is equivalent to stating that the elongation is proportional to the change in spreading pressure.*

[5]*It must be emphasized that when K_p differs from unity this is not to be regarded as arising primarily from lack of uniformity of adsorbate pressures but rather from a correlation between the lack of uniformity of adsorbate pressure and the lack of uniformity of structure. Such a correlation has important physical implications. If adsorbate pressures, no matter how highly variable, no matter how lacking in uniformity, are statistically independent of structure, K_p will be unity.*

The influence of the various physical factors can be illustrated in terms of change in solid surface free energies. Thus instead of writing $p_{ci} = P + (P - p_{ai}) \cdot a_i/c_i$, we can write $p_{ci} = P + \gamma_i\lambda_i/c_i$, where γ_i is the change in solid surface tension perpendicular to c_i, λ_i the length of the common perimeter of solid and void areas etc. This treatment is somewhat more complex than presented above since we now have possible correlations between the three quantities, γ_i, λ_i, and c_i. It is felt that the placing of the emphasis on adsorbate stresses which can be correlated directly with adsorption data is perhaps a more direct approach than is involved in the change of surface tension treatment. Further, it is felt that in such fine grained porous bodies the field exerted by the solid is not confined to the solid surface but extends appreciably into the micropore volume. It will be noted that when K_p is assumed unity in the treatment above, it is equivalent to assuming that the change in solid surface tension is statistically independent of structure, i.e., of λ and c.

pressibility low. At this stage further increase in equilibrium pressure will increase the pressures more nearly equally in the larger and smaller pores. In this case K_p will be initially considerably less than unity but will increase with increasing equilibrium pressure and eventually approach unity. In the case of pores of molecular dimensions, efficient close packing may be hindered so that the density in larger pores can exceed that in the very small holes. In this case K_p might eventually exceed unity by small factors. It is important to note that when the quantity adsorbed remains constant as the equilibrium pressure is changed, it implies that the adsorbate is everywhere virtually incompressible and of practically the same density. Under these conditions changes in equilibrium pressures are accompanied by a nearly uniform change in hydrostatic pressure of the adsorbate. K_p is necessarily unity for uniform changes in adsorbate pressures.

Thus fairly reliable estimates of K_s can be obtained from observed contractions on desorption from saturation with water, when the desorption isotherm branch is nearly horizontal over the region concerned.

We have assumed that the elastic constants A, B etc. of the solid are the same everywhere regardless of variations in thickness of the material. If these constants are not independent of structure, the effect of such correlations on the length changes will be to introduce a factor which is somewhat similar to K_s. Thus values of K_s estimated from adsorption-extension where K_p can be taken as unity will be a product of both of these factors.

EXPERIMENTAL RESULTS

Adsorption-extension data have been obtained for an activated carbon rod (Rod 3) when subjected to hydrostatic pressures of helium, hydrogen, nitrogen, argon, and krypton. The data appear in Figs. 1 and 2. Since the adsorption extension of Rod 3 in nitrogen is almost the same as that reported previously for Rod 1 (a similar rod from the same batch) it may be supposed that the adsorption-extensions of Rods 1 and 3 with other gases will be essentially similar. Accordingly, the adsorption-extension of Rod 1 in water vapor and liquid water is plotted together with the new data. (Because of the pressure scale used the adsorption-extension in water vapor appears as a vertical rise. The remainder of the H_2O curve shows the contraction as the liquid water pressure increases.)

In Fig. 1 the solid lines, with the exception of the H_2O extension, were calculated from

$$\delta L/L = -0.8\times10^{-7}(1-2/3\cdot10^{-5}\cdot\overline{p_c}^{L})\overline{p_c}^{L}$$

where $\overline{p_c}^{L} = [4.5-3.5\alpha]P$. Thus the product $\phi\cdot K_s\cdot K_p$ is assumed equal to 3.5 and independent of pressure and the nature of the gas. This formula yields an extension for H_2O at saturation which is much too low. The calculated curve for H_2O is that reported previously and is based on $\delta L/L = -1.1\times10^{-7}\cdot\overline{p_c}^{L}$ where $\overline{p_c}^{L} = [5.8-4.8\alpha]P\rightarrow-4.8\alpha P$ (α is very large, $\approx$40,000).

An examination of the data shows that Equation [6] cannot be made to fit them.

The data for krypton especially indicate a K_p which is an increasing function of P. While, in the case of these particular carbon rods, the water desorption isotherms near saturation are not horizontal, the variation in adsorbate density is comparatively small, and accordingly the expansion behavior of the rods near saturation should correspond

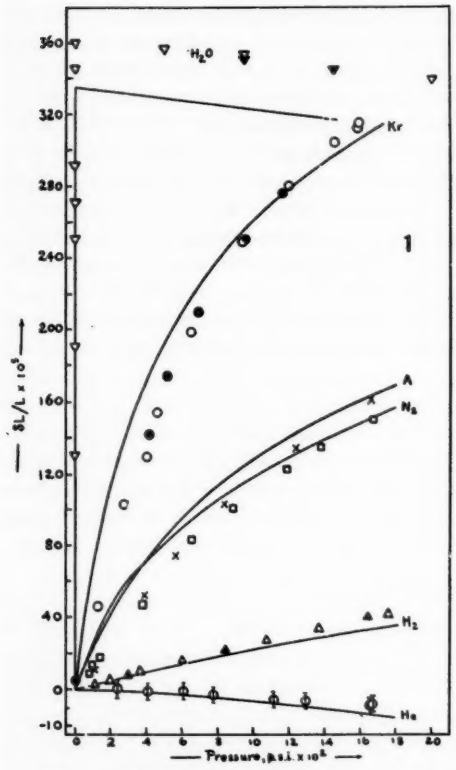

FIG. 1. Elongation as a function of fluid pressure, 25° C. Solid lines (except H_2O) calculated from $\delta L/L = -0.8\times10^{-7}(1-2/3\cdot10^{-5}\cdot\bar{p}_e^{L})\bar{p}_e^{L}$, $\bar{p}_e^{L} = (4.5-3.5\alpha)P$. Observed points, Rod 3: ○, ●, krypton, adsorption, desorption); ×, argon; □, nitrogen; △, hydrogen; Φ, helium; Rod 1: ▽, H_2O.

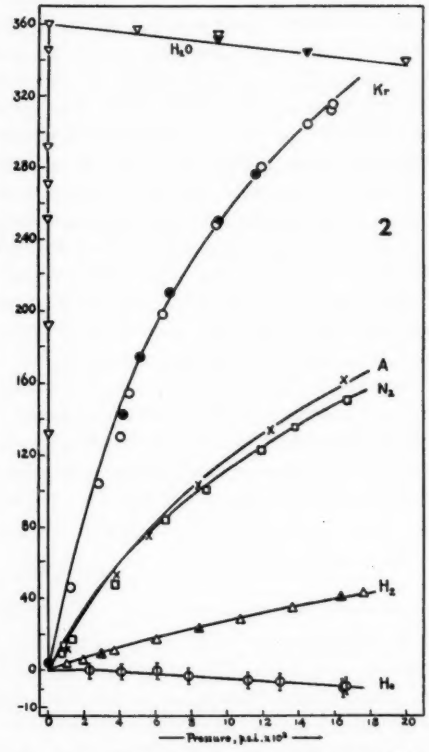

FIG. 2. Elongation as a function of fluid pressure, 25° C. Solid lines calculated from $\delta L/L = -0.88\times10^{-7}(1-1/2.10^{-5}\cdot\bar{p}_e^{L})\bar{p}_e^{L}$, $\bar{p}_e^{L} = [1+5K_p-5K_p\alpha]P$. Observed points, Rod 3: ○, ●, krypton (adsorption, desorption); ×, argon; □, nitrogen; △, hydrogen; Φ, helium; Rod 1: ▽, H_2O.

fairly closely to Equation [6] with $K_p = 1$ and thus afford a measure of K_s. It was found that both the water and helium adsorption-extension could be fitted very closely by means of the equation

$$\delta L/L = -0.88\times10^{-7}(1-1/2\cdot10^{-5}\cdot\overline{p_e}^{L})\overline{p_e}^{L}$$

where $\overline{p_e}^{L} = [6-5\alpha]P$. This is equivalent to putting $K_p = 1$ and $\phi\cdot K_s = 5$.

As we have shown, selective adsorption yields a K_p factor greater or less than unity according as the adsorption is relatively greater in the larger or smaller pores. For non-condensable gases, the former case leads to a K_p which is a decreasing function of P, the latter to an increasing function of P.

In carbons with mean pore diameters considerably greater than the diameters of the adsorbate molecules, one might expect selective adsorption of large gas molecules in the smaller pores. In such cases the adsorption should be fairly large, i.e., α should be

fairly large. If α is very large the fluid in both large and small pores should reach high densities at relatively low equilibrium pressures and thus K_p tend toward unity at relatively low equilibrium pressures. Evidently the value of α itself should afford some measure of these selective trends. Accordingly, we put $K_p = 1-D\alpha^{\frac{1}{2}}$ and found suitable values for D by trial. While this formula has no theoretical basis and cannot be correct for large values of α, all of the data[6] can be described practically within the experimental error by its use. The solid lines in Fig. 2 are plotted from

$$\delta L/L = -0.88\times10^{-7}(1-1/2\cdot10^{-5}\cdot\overline{p_c}^{L})\overline{p_c}^{L}$$

and

$$\overline{p_c}^{L} = [1+\phi\cdot K_s\cdot K_p-\phi\cdot K_s\cdot K_p\cdot\alpha]P$$

where $\phi = 1.304$; $K_s = 3.834$; $K_p = 1-D\alpha^{\frac{1}{2}}$; and $D = 0$ for H_2O and helium, 0.116 for krypton, 0.168 for A and N_2, and 0.172 for H_2.

It may be pointed out that both the compressibility and the variation of compressibility with pressure in the formula correspond quite closely to those of graphite under a pressure of about 10^4 lb. per sq. in. (4). Further, that the departure of K_p from unity is greatest in the case of krypton as might be expected. Thus all of the data are described practically quantitatively using only one arbitrary constant whose values vary in a physically plausible manner. It will be noted that the length changes vary from -5 (-20 for the liquid water from saturation to 2000 lb./in.) to $+360$ with a probable error of measurement of less than ±2, while the variations in values of P and α in the equation cover ranges from 0 to 2000 lb./in. and 0 to 40,000 respectively.

APPENDIX I—EXPERIMENTAL DETAILS

1. Materials

Activated Carbon Rods

Except where noted, all experiments were carried out with carbon rod No. 3. This carbon rod is essentially similar to Rod 1 whose properties have been reported previously (6). Like Rod 1 it was selected from a batch of long, straight zinc chloride activated rods especially prepared for us by courtesy of the National Carbon Company.

Rod 3 is 109.7 mm. in length and has a mean diameter of 1.79 mm. Thus the geometric or total volume is 0.276 cc. The carbon volume as measured by helium displacement and corrected for helium adsorption is 0.434 cc. per cc. and the void volume 0.566 cc. per cc. Assuming the mercury density to be the same as Rod 1, this yields a carbon density of 1.75. (If not corrected for helium adsorption, the helium density is 1.95.)

In selecting Rod 3 from the batch some care was taken to obtain a rod giving a similar nitrogen extension to Rod 1 and for which equilibrium was rapidly attained on either increase or decrease of the equilibrium pressure. In the case of one rod, it was noticed that even 1 or 2 hours after expansion from higher pressures there was a small slow evolution of gas. When this rod was heated for 6 to 8 hours at 600° C. the equilibrium was obtained quite rapidly. Rod 3 was heated during 4 to 5 hours at 500° C. alternately in a high vacuum and in a pure dry helium stream. On cooling to room temperature in helium it was exposed to saturated water vapor and finally to air. Helium extension measurements were made both before and after exposure to hydrogen and krypton. A few nitrogen-extension and adsorption points were taken at the end of the experiments. These points fell on the curves obtained at the beginning of the series. Accordingly, it

[6] *Excepting water vapor at low relative pressures (cf. Appendix II).*

seems unlikely that changes in surface complexes or chemisorbed material can have influenced our results appreciably.

Gases

The helium, hydrogen, nitrogen, argon, and krypton were supplied by the Dominion Oxygen Company, and were specified as not less than 99.99% pure. The krypton was spectroscopically pure. Except in the case of krypton the gases were passed through a bed of activated charcoal suitably cooled (liquid nitrogen in the case of He and H_2, solid CO_2 in the case of N_2 and A). The krypton was used as supplied.

2. Experimental Procedures and Methods

The procedures used throughout were essentially similar to those reported previously (6). The main modifications were as follows: The whole apparatus was enclosed in a thermostatic air bath, the temperature of which was kept constant at 24.8° C. within ±0.1° C. The room containing the apparatus was also thermostatically controlled and maintained at 27° C. to usually within ±2° C.

Pressures in the range 14 to 500 p.s.i. were measured by means of a piston gauge. Higher pressures were measured by means of a Bourdon-type gauge calibrated by the Metrology Section of the National Research Council. Pressures from 1 atm. to 1 cm. Hg were measured by means of a mercury manometer constructed of precision bore 20 mm. glass tubing together with a reasonably high grade cathetometer. Mercury pressure readings were corrected for temperature, the value of g etc. Manometric pressure readings of the order of ½ atm. were reproducible within considerably better than 0.01%. With the piston gauge, differences of the order of one part in 10^4 could be readily detected (the accuracy of the piston gauge was limited by the accuracy of determining the barometric pressure, oil "head" of leads etc.).[7] These pressures are considered to be correct within ±0.2% or better. The Bourdon gauge dial readings are considered correct within about ±½ a scale division, i.e., within ±5 p.s.i. or ±1% in the neighborhood of 500 p.s.i., and within ±0.3% at 1500 p.s.i. Thus in the range of pressure 600–1200 p.s.i. the data are considered to be somewhat less reliable than in either the higher or lower (piston gauge) range. Length changes were measured essentially as described previously. In place of the travelling microscope used previously, two rigidly fixed parallel microscopes with micrometer eyepieces were used. The scale was 10 times larger than that used previously and reproducibility of individual length change measurements was usually within $\pm 2 \times 10^{-4}$ mm. The larger values of $\delta L/L$ reported are considered to be correct within ±1%, the maximum helium contraction within ±30%.

Measurements of ρ_a/ρ at various pressures were based upon the following equation:

$$v_x = v - v_c + v_a(a-1)$$

where v is the volume of a container and v_x is the apparent volume of the container. v_c is the carbon volume, v_a the void volume, and $a = \rho_a/\rho$ = the mean density of gas within v_a divided by ρ, the density of the gas in the tube. Two different procedures were used. At low pressures ($5–10^{-2}$ mm.) gas from a second known volume (about equal to v_x) was expanded into an evacuated charcoal filled container, the empty volume of which was only a little larger than $v_a + v_c$. This procedure is not capable of great accuracy

[7]*There is also an appreciable correction due to the different "capillary depressions" of the mercury in the U-tube in contact with oil on one side and gas on the other.*

because of the difficulty of measuring low gas pressures of the small volumes (0.5–10.0 cc.). However, when a is appreciably greater than unity, approximate limiting values of a can be obtained.[8] At high pressures, gas was expanded out from the high pressure capillary of volume v_x into a large volume (about $10^2 \times v_x$) where the pressure could be accurately measured. If v_0 represents the volume after expansion (corrected for the change in a, i.e., if v_L = the large volume, $v_0 = v_L + v - v_c + v_a(a' - 1)$, where a' is the value of a at the low pressure after expansion). If $(p_0v_0)'$ is the pv value after expansion from the tube containing the charcoal at the high pressure P_1 and (p_0v_0) is the pv value after expansion from the empty tube at P_1, then a is given by:

$$a = \frac{v_a + v_c}{v_a} + \frac{v}{v_a}\left\{\frac{(p_0v_0)'(P_1 - (p_0v_0)/P_1}{(p_0v_0)/P_1}\right\}$$

Thus by plotting $(p_0v_0)'/P$ and $(p_0v_0)/P$ against P we can obtain a or ρ_a/ρ without having to correct for deviations from the gas laws except at the low pressures p_0, where the corrections are small and well known. v_c was first determined by helium displacement at higher pressures. Fig. 3 shows the apparent volumes of the high pressure capillary and leads as obtained from helium expansion data with and without the carbon rod.[9] The volumes are calculated using Schneider's virial coefficient for helium (10). Assuming no adsorption at 1700 lb. v_c was taken as 0.105 and $v_a = 0.276 - 0.105 = 0.171$. Then a or ρ_a/ρ was plotted as a function of P and $\int_0^P \rho_a/\rho \cdot dP = \alpha P$ calculated for all of the gases.

Since Halsey (11) has shown that the energy of interaction of helium and activated carbon is quite considerable it is to be expected that helium adsorption at 1700 p.s.i. at room temperature would be appreciable. That the helium is adsorbed is suggested by the decreasing values of v_c. Helium adsorption is also indicated by the low compressibility of the carbon in helium (Figs. 1 and 2).

In order to estimate helium adsorption, we have assumed that the ratio of the surface potentials for krypton and helium for our carbon rod is similar to that reported by Steele and Halsey (11). Taking 4000 cal. as the mean potential per mole for krypton together with Van der Waal's constants for krypton, we have calculated, using (*a*) a Leonard-Jones 6–12 potential and (*b*) a square potential, the surface area and mean distance between surfaces that are necessary to be consistent with the known micropore volume and krypton adsorption data for our carbon using both a platelet and cubic model pore system. Surface areas of the order of 500 sq. m./g. with distance apart 10 Å for the platelet model and about 700 sq. m./g. and 20 Å side length for the cubic model are thus obtained. For the same models and a surface potential for helium of 700 cal. per mole of gas adsorbed the calculated value of ρ_a/ρ for helium at 1700 p.s.i. varies from about 1.09 to 1.15 depending on the model and form of potential function. Accordingly, the value of ρ_a/ρ for helium at 1700 p.s.i. was taken as 1.1 and all the values of ρ_a/ρ for the other gases multiplied by 1.1. In Figs. 4 and 5 values of ρ_a/ρ (after multiplying by 1.1) are plotted as functions of P.

[8] *In general, the rise in "a" from equilibrium pressure of 1 mm. to 10^{-2} mm. is comparatively small. Accordingly the Jura type error in the areas $\int_0^P v\,dP$ or $\int_0^P \rho a/\rho \cdot dP$ are not significant unless "a" rises to quite unreasonable values at pressures below 10^{-2} mm.*

[9] *The discontinuity between 600 and 800 p.s.i. is considered to be due to discrepancy in gauge calibrations. The Bourdon gauge is considered to give pressure readings which are too low at the lower end of the scale. The graph indicates some distortion of v which was allowed for in calculation of a.*

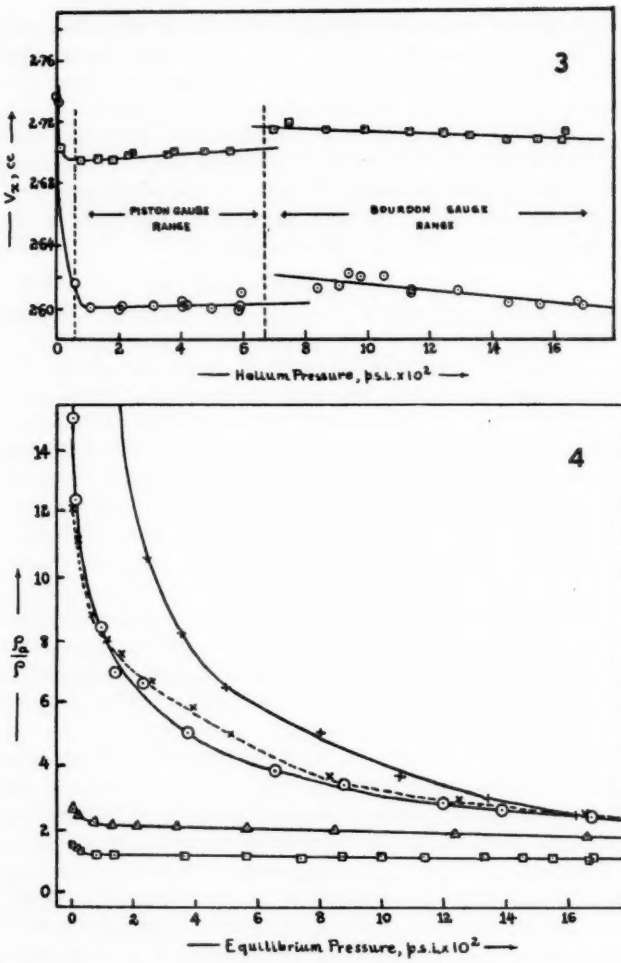

FIG. 3. Apparent volume of capillary as a function of helium pressure, 25° C. ○, empty volumes; □, with carbon Rod 3 present.

FIG. 4. Ratios of densities of gas within carbon void volume to corresponding equilibrium gas densities. □, helium; △, hydrogen; ○, nitrogen; ×, argon; +, krypton.

APPENDIX II

While mathematically K_p can be either much greater than unity or much less than unity, even negative, physical considerations suggest that at higher fluid adsorbate densities K_p should approach unity, both because, in general, reactions of fluids with highly localized fields tend toward more uniform residual fields as well as because of the relative incompressibilities of adsorbates approaching liquid densities.

As reported previously, at low relative pressures of H_2O vapor, these rods show contractions in length and radius as the equilibrium pressure increases from zero. Along

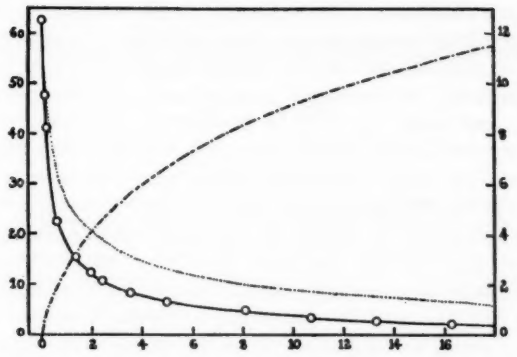

FIG. 5. ρ_a/ρ, α, and $\overline{p_a}^v$ as functions of krypton equilibrium pressure, 25° C. Left-hand ordinate, ρ_a/ρ and $1/P\int_0^P \rho_a/\rho \cdot dP$ or α. Right-hand ordinate, p.s.i. $\times 10^2$. Abscissa, equilibrium pressure p.s.i. $\times 10^2$. Solid line, curve drawn through observed values of ρ_a/ρ. Dotted line, $1/P \times$ area under solid line, i.e. α or $1/P \int_0^P \rho_a/\rho \cdot dP$. Broken line, volumetric mean pressure of adsorbed krypton.

these paths $\Delta\overline{p_a}^v$ must be positive if no thermodynamically irreversible processes occur. (The contractions we are referring to here must not be confused with those very marked contractions observed on H_2O desorption by McIntosh and others which are due to hysteresis effects. Negative values of $\Delta\overline{p_a}^v$ are to be expected on decreasing equilibrium pressure paths in cases of marked hysteresis.) While it might appear at first sight that $\Delta\overline{p_e}^v$ cannot be negative while $\Delta\overline{p_e}^L$ is strongly positive, it is apparent that if the sum $\sum(P-p_{a_i})\cdot a_i/c_i\cdot l_i$ includes both positive and negative values of $P-p_{a_i}$, when positive $P-p_{a_i}$ is associated with very small c_i, the positive values may be so much more strongly weighted that the sum is positive while the corresponding sum $\sum(P-p_{a_i})\cdot a_i\cdot l_i$ is negative.[10]

At higher relative pressures and higher adsorbate densities, we might expect the elastic behavior of the assembly to depend largely on its gross mechanical structure, i.e., on its pore sizes and shapes as measured by K_s, K_p being nearly unity.

Although by inverse coupling a mechanical system can be constructed which will decrease in over-all dimensions when each individual member of the system increases its length, such an arrangement seems quite impossible in the case of a more or less random assembly of interconnected solid particles. Accordingly if contractions occur along thermodynamically reversible paths of increasing equilibrium pressure, they must be associated with positive $\delta\Delta F_e$ in some regions of the solid.

At low surface coverages the elastic behavior of such assemblies should depend relatively more on the detailed structure of the surface fields and relatively less on the over-all mechanical or pore structure. In the case of surface fields whose equipotential contours have sharp maxima and minima, where the maxima are separated by distances of molecular dimensions, adsorption may reduce the field energy in the region of the maxima while increasing the energy in the region of the minima. This could result from such "co-operative effects" as attractive forces of adsorbate molecules or in the case of rod-like molecules, from "bridging" effects, where the distances between sites (maxima) are somewhat greater than the bond distances between the atoms or groups held by the

[10] *Such considerations cannot lead to large positive values of $\Delta\overline{p_e}^L$ for small constant P. When P is not constant from section to section $\Delta\overline{p_e}^L$ can be large and positive for small $\overline{P}^L$ while $\Delta\overline{p_e}^v$ is negative.*

sites. In either of these two cases, if the supporting solid is relatively weak in the regions of the minima, the resulting contractions in these regions can easily outweigh the expansions of the regions of the maxima and K_p become negative. These two mechanisms can be partially distinguished. At coverages approaching zero the attractive co-operative effects must vanish, and hence K_p must be positive at very low pressures and become negative as the co-operative effects come into play. On the other hand, bridging effects do not necessarily vanish as the adsorbate density approaches zero. Thus where K_p is negative from zero equilibrium pressures it may be taken as evidence of bridging effects. As we have seen, in both cases K_p should become positive at higher adsorbate densities.

While in a previous paper it was suggested that the initial contraction observed with H_2O vapor may have been due to irreversible condensation phenomena, this contraction may well have been due to one of the above mechanisms. It seems improbable that the small contractions observed by McIntosh (7) with butane, ethyl chloride, and dimethyl ether at low relative pressures can all have been due to irreversible condensations.

ACKNOWLEDGMENT

The author is indebted to Dr. J. A. Morrison for valuable suggestions and criticisms of a draft form of this paper.

The author is also indebted to Dr. R. D. Heyding and to Dr. P. H. Stirling for their help in constructing the apparatus.

REFERENCES

1. Amberg, C. H. and McIntosh, R. Can. J. Chem. **30**, 1012 (1952).
2. Bangham, D. H. and Fakhoury, N. Proc. Roy. Soc. A, **130**, 81 (1930).
3. Bangham, D. H. and Maggs, F. A. P. Proceedings of Conference on the Ultrafine Structure of Coal and Cokes, June 24, 25, 1943. The British Coal Utilization Research Association. (Distributing Agents, H. K. Lewis and Co. Ltd., London.)
4. Basset, J. Compt. rend. **213**, 829 (1941).
5. Flood, E. A. Can. J. Chem. **33**, 979 (1955).
6. Flood, E. A. and Heyding, R. D. Can. J. Chem. **32**, 660 (1954).
7. Haines, R. S. and McIntosh, R. J. Chem. Phys. **15**, 28 (1947).
8. McBain, J. W., Porter, J. L., and Session, R. F. J. Am. Chem. Soc. **55**, 2294 (1953).
9. Meehan, F. T. Proc. Roy. Soc. A, **115**, 199 (1927).
10. Schneider, W. G. and Duffie, J. A. H. J. Chem. Phys. **17**, 751 (1949).
11. Steele, W. A. and Halsey, G. D. J. Chem. Phys. **22**, 979 (1954).
12. Truesdell, C. J. Rational Mech. and Anal. **1**, 125 (1952).
13. Wiig, E. O. and Juhola, A. J. J. Am. Chem. Soc. **71**, 561 (1949).
14. Yates, D. J. C. Proc. Roy. Soc. A, **224**, 526 (1954).

SYNTHESIS OF 3,5-DI-*O*-METHYL-D-GLUCOSE[1]

C. T. BISHOP

ABSTRACT

3,5-Di-*O*-methyl-D-glucose has been synthesized by methylation of 1,2-*O*-*iso*propylidene-6-*O*-trityl-D-glucofuranose and removal of the blocking groups by acid hydrolysis. The di-*O*-methyl glucose furnished a crystalline osazone without loss of a methoxyl group and yielded a monobasic and dibasic acid when oxidized by bromine and nitric acid respectively. Both acids formed gamma lactones and crystalline amides by which the parent compound is characterized. The foregoing reactions proved the structure of 3,5-di-*O*-methyl-D-glucose predicted by its method of synthesis.

INTRODUCTION

In a review of the methyl ethers of glucose published in 1950, Bourne and Peat (1) reported that 3,5-di-*O*-methyl-D-glucose was the only dimethyl ether of the cyclic forms of D-glucose that had not been prepared. The present publication describes a short synthesis of 3,5-di-*O*-methyl-D-glucose and proof of its structure.

While the work reported here was in progress, Huffman *et al.* (3) reported a synthesis of 3,5-di-*O*-methyl-D-glucose using the same blocking groups but a slightly different sequence of reactions. These authors characterized the 3,5-di-*O*-methyl-D-glucose as the crystalline 3,5-di-*O*-methyl-D-gluconamide and the structure of the parent sugar was proved by oxidation with periodate to yield the known 2,4-di-*O*-methyl-D-arabinose. In the present report the sequence of reactions in the synthesis furnished a new compound of D-glucose, 1,2-*O*-*iso*propylidene-6-*O*-trityl-D-glucofuranose, and 3,5-di-*O*-methyl-D-glucose was further characterized as the new crystalline diamide of 3,5-di-*O*-methyl-D-glucaric acid. The physical constants previously reported (3) for the sirupy 3,5-di-*O*-methyl-D-glucose and the crystalline 3,5-di-*O*-methyl-D-gluconamide were confirmed in the present work and an independent proof of structure of the 3,5-di-*O*-methyl-D-glucose was obtained. The work reported here is therefore complementary to that of Huffman *et al.* (3) and parallels it only in the preparation of 3,5-di-*O*-methyl-D-gluconamide.

The synthesis was achieved by the following series of reactions: D-glucose→1,2;5,6-di-*O*-*iso*propylidene-D-glucofuranose → 1,2-*O*-*iso*propylidene-D-glucofuranose → 1,2-*O*-*iso*propylidene-6-*O*-trityl-D-glucofuranose → 1,2-*O*-*iso*propylidene-3,5-di-*O*-methyl-6-*O*-trityl-D-glucose → 3,5-di-*O*-methyl-D-glucose. The structure of the 3,5-di-*O*-methyl-D-glucose was proved by the following facts: the compound formed an osazone without loss of a methoxyl group showing that a free hydroxyl group was present at C_2. Oxidation of the di-*O*-methyl glucose with bromine afforded a gamma lactone, recognized by its slow rate of hydrolysis, which proved that a free hydroxyl group was located at C_4. Nitric acid oxidation of the di-*O*-methyl glucose yielded a glucaric acid without loss of any methoxyl group, thus showing that hydroxyl groups were located at C_1 and at C_6. It was clear, therefore, from the above evidence that the two methyl groups in the di-*O*-methyl glucose occupied positions 3 and 5, a result to be expected from the mode of synthesis.

[1]*Manuscript received October 4, 1956.*
Contribution from the Division of Applied Biology, National Research Council, Ottawa, Canada. Presented in part before the Organic Chemistry Section at the 38th Annual Conference of the Chemical Institute of Canada, Quebec, Que., May 30 – June 1, 1955.
Issued as N.R.C. No. 4165.

EXPERIMENTAL

Paper strip chromatograms were run in butanol: ethanol: water—5: 1: 4, and sugars were located on the paper by aniline oxalate spray reagent (2). Evaporations were carried out at 40° C. or less and all melting points are corrected. Specific rotations are equilibrium values unless otherwise stated.

*1,2-O-Isopropylidene-6-O-trityl-*D*-glucofuranose* (*I*)

To 1,2-*O-iso*propylidene-D-glucofuranose (m.p. 158–159.5° C., $[\alpha]_D^{24} = -12°$, 12.8 g.) in dry pyridine (120 ml.) was added triphenylchloromethane (15.66 g.) and the solution was allowed to stand at room temperature for 24 hours. Water was then added until a permanent turbidity formed and after 2 hours the mixture was poured into a large excess (1 liter) of ice water. The product separated as a white gum which was washed three times with water by decantation and was then dissolved in chloroform. To remove pyridine the chloroform solution was washed with cold 3% aqueous acetic acid till the washings were acid (test paper) and then with water till the washings were neutral. The washed chloroform solution was dried over anhydrous sodium sulphate and then evaporated to yield 1,2-*O-iso*propylidene-6-*O*-trityl-D-glucofuranose (I) as a puffy, aerated glass (25.4 g., 98%) having $[\alpha]_D^{24} = -21° \pm 1°$ ($c = 2.6\%$ in methanol), $= -3° \pm 2°$ ($c = 2.1\%$ in chloroform). Analysis: Calc. for $C_{28}H_{30}O_6$: C, 72.7%; H, 6.54%; trityl, 52.6%. Found: C, 72.56%; H, 6.27%; trityl, 52.4%.

*1,2-O-Isopropylidene-3,5-di-O-methyl-6-O-trityl-*D*-glucofuranose* (*II*)

(*a*) Compound I (25 g.) was refluxed in methyl iodide (250 ml.) and silver oxide (25 g.) was added in eight equal portions at half-hour intervals (6). The mixture was refluxed overnight and filtered, and the silver salts were washed with chloroform. The partially methylated product was recovered by evaporation of the combined filtrate and washings. A total of four such methylations yielded a product (22 g.) having a constant methoxyl content of 10% as compared to the theoretical value of 12.65% for II.

(*b*) In a separate experiment a portion (200 mg.) of the product methylated by Purdie's reagents was hydrolyzed as described below for the preparation of III. Examination of the hydrolyzate by paper strip chromatography showed that it contained a di-*O*-methyl and a mono-*O*-methyl ether of glucose. The mono-*O*-methyl derivative crystallized from a methanol solution of the mixture and its physical constants, m.p. 162–163.5° C. and $[\alpha]_D^{25} = +60° \pm 2°$ ($c = 2\%$ in water), were in good agreement with those reported (4) for 3-*O*-methyl-D-glucose. No other mono-*O*-methyl isomer could be detected and the di-*O*-methyl-D-glucose was chromatographically identical with 3,5-di-*O*-methyl-D-glucose. It was therefore apparent that the hydroxyl group at C_5 was resistant to methylation, an observation also made by Huffman *et al.* (3).

To a solution of the partially methylated product (21.8 g.) in tetrahydrofuran (170 ml.), sodium hydroxide pellets (23 g.) were added. The mixture was stirred vigorously during the dropwise addition of dimethyl sulphate (50 ml.). Stirring was continued for a further 20 hours after which sufficient water was added to dissolve all solids and the solution was warmed at 55° C. for 1½ hours. Tetrahydrofuran was evaporated and the residual aqueous mixture was extracted five times with one-half its volume of fresh portions of chloroform. The chloroform extract was dried over anhydrous sodium sulphate and evaporated to yield 21.0 g. (78%) of 1,2-*O-iso*propylidene-3,5-di-*O*-methyl-6-*O*-trityl-D-glucofuranose. Samples for analyses were dried to constant weight at 60° C. and 0.02 mm. over magnesium perchlorate. The product, thus dried, showed no hydroxyl absorption band at

3400–3500 cm.$^{-1}$ in its infrared spectrum and had $[\alpha]_D^{27} = -30° \pm 2°$ ($c = 1.4\%$ in ethanol). Analysis: Calc. for $C_{30}H_{34}O_6$: C, 73.4%; H, 6.98%; OCH_3, 12.65%; trityl, 49.6%. Found: C, 71.79%; H, 6.66%; OCH_3, 12.5%; trityl, 49.1%.

3,5-Di-O-methyl-D-glucose (III)

Compound II (21 g.) was dissolved in ethanol (140 ml.) and 12% aqueous hydrochloric acid was added until a slight permanent turbidity developed (60 ml.). This solution was then refluxed on a boiling water bath for 5 hours. Ethanol was removed by evaporation and the triphenylcarbinol which precipitated was filtered and washed thoroughly with hot water. The clear aqueous solution was neutralized by Amberlite IR-4B resin and evaporated to yield a golden yellow sirup, 7.2 g., 77% yield or 59% based on 1,2-*O*-*iso*-propylidene-D-glucofuranose. Examination of this product by paper chromatography showed that it contained traces of a mono-*O*-methyl-D-glucose. A portion (5.5 g.) of the sirup was therefore chromatographed on Celite (5), this procedure yielding chromatographically pure 3,5-di-*O*-methyl-D-glucose (III) as a straw colored sirup. A sample was distilled for analysis, b.p. (bath temperature) 165–170° C. at 0.04 mm., and showed $[\alpha]_D^{26} = -20° \pm 2°$ ($c = 1.1\%$ in water).
Analysis: Calc. for $C_8H_{16}O_6$: C, 46.15%; H, 7.75%; OCH_3, 29.8%. Found: C, 46.96%; H, 7.99%; OCH_3, 29.9%.

Osazone Formation

When the 3,5-di-*O*-methyl-D-glucose (63 mg.) was heated with phenyl hydrazine hydrochloride (400 mg.) and sodium acetate (400 mg.) in water (3 ml.) in a boiling water bath for 2 hours, the corresponding osazone was obtained, m.p. 64–65° decomp., $[\alpha]_D^{25} = -83°$ in ethanol ($c = 1.5\%$), after recrystallization from aqueous ethanol.
Analysis: Calc. for $C_{20}H_{26}O_4N_4$: C, 62.16%; H, 6.78%; N, 14.50%; OCH_3, 16.06%. Found: C, 62.15%; H, 6.55%; N, 13.90%; OCH_3, 16.0%.
The 3,5-di-*O*-methyl-D-glucose phenylosazone was extremely unstable, the carbon content decreasing to values of 61.07%, 60.96% after the sample had been exposed to air for successive 2 hour periods.

3,5-Di-O-methyl-D-glucono-γ-lactone

A solution of 3,5-di-*O*-methyl-D-glucose (100 mg.) in water (2 ml.) was oxidized by bromine (0.3 ml.) in the presence of barium carbonate (30 mg.). The oxidation was allowed to proceed in the dark at room temperature for 24 hours. The mixture was acidified with *N* hydrochloric acid and bromine was removed by aeration. The clear, colorless, aqueous solution was then extracted continuously with chloroform for 36 hours. Evaporation of the chloroform extract yielded sirupy 3,5-di-*O*-methyl-D-gluconic acid which was heated at 95° C. and 0.02 mm. for 2 hours to yield 3,5-di-*O*-methyl-D-glucono-γ-lactone (51 mg.).
Analysis: Calc. for $C_8H_{14}O_6$: OCH_3, 30.1%. Found: OCH_3, 29.2%. $[\alpha]_D^{25} = +14° \rightarrow +6°$ in four days ($c = 1\%$).

3,5-Di-O-methyl-D-gluconamide

3,5-Di-*O*-methyl-D-gluconic acid was converted to its methyl ester by refluxing with 2% methanolic hydrogen chloride for 18 hours. Reaction of the ester with methanolic ammonia at 5° C. and evaporation of the solvent yielded 3,5-di-*O*-methyl-D-gluconamide, m.p. 148–150° C., $[\alpha]_D^{26} = +23° \pm 2°$ ($c = 1.5\%$ in methanol); reported (3) m.p. 150–152° C., $[\alpha]_D^{23} = +29°$ ($c = 0.7\%$ in methanol).

3,5-Di-O-methyl-D-glucosaccharo-1,4-lactone

A sample (53 mg.) of 3,5-di-*O*-methyl-D-glucose was heated for 1 hour in nitric acid (sp. gr. 1.2, 2.5 ml.) on a boiling water bath. The solution was then evaporated under diminished pressure at 35° C. and nitric acid was removed from the residue by repeated addition and evaporation of water. The residual yellow sirup was then dried to constant weight (46 mg.) over solid potassium hydroxide at 0.02 mm. This product gave the correct analysis for a monolactone of a di-*O*-methyl glucosaccharic acid and showed the slow hydrolysis in water, measured by change in rotation, characteristic of furanolactones; $[\alpha]_D^{25} = +5° \rightarrow -3°$ in four days ($c = 2.2\%$ in water).

Analysis: Calc. for $C_8H_{12}O_7$ (monolactone): OCH_3, 28.2%. Calc. for $C_8H_{10}O_6$ (dilactone): OCH_3, 30.85%. Found: OCH_3, 28.5%.

3,5-Di-O-methyl-D-glucosaccharodiamide

3,5-Di-*O*-methyl-D-glucosaccharo-1,4-lactone (150 mg.) was shaken with an excess of ethereal diazomethane until gas evolution ceased. The ether and excess diazomethane were removed by evaporation under diminished pressure at 30° C. and the residue was taken up in methanolic ammonia (6 ml.). After being stored at 5° C. for 2 days the solution was evaporated slowly in a partially evacuated desiccator to yield crystalline 3,5-di-*O*-methyl-D-glucosaccharodiamide (100 mg.), which was recrystallized from ethanol to a constant m.p. of 164–165° C.; $[\alpha]_D^{26} = +19\pm2°$ ($c = 1.7\%$ in methanol). This compound gave a positive Weerman test (7) for α-hydroxy amides.

Analysis: Calc. for $C_8H_{16}O_6N_2$: C, 40.67%; H, 6.83%; N, 11.86%; OCH_3, 26.3%. Found: C, 39.92%; H, 6.57%; N, 11.38%; OCH_3, 25.6%.

ACKNOWLEDGMENTS

The author would like to thank F. Rollin for carrying out the infrared analyses reported here.

REFERENCES

1. Bourne, E. J. and Peat, S. Advances in Carbohydrate Chem. **5**, 145 (1950).
2. Horrocks, R. H. and Manning, G. B. Lancet, **256**, 1042 (1949).
3. Huffman, G. W., Lewis, B. A., Smith, F., and Spriestersbach, D. R. J. Am. Chem. Soc. **77**, 4346 (1955).
4. Irvine, J. C. and Hogg, T. P. J. Chem. Soc. 1386 (1914).
5. Lemieux, R. U., Bishop, C. T., and Pelletier, G. A. Can. J. Chem. **34**, 1365 (1956).
6. Purdie, T. and Irvine, J. C. J. Chem. Soc. 1021 (1903).
7. Weerman, R. A. Rec. trav. chim. **37**, 16 (1917).

THE ANALYSIS OF NUCLEAR MAGNETIC RESONANCE SPECTRA

I. SYSTEMS OF TWO AND THREE NUCLEI[1]

H. J. BERNSTEIN, J. A. POPLE,[2] AND W. G. SCHNEIDER

ABSTRACT

This paper is concerned with the general problem of the interpretation and analysis of nuclear magnetic resonance spectra of systems in which chemical shift and spin-coupling constants are of the same order of magnitude. Only nuclei of spin 1/2 are considered. Detailed methods are developed for:

(*a*) Two chemically non-equivalent nuclei of the same species (written AB),

(*b*) Three nuclei of the same species, two of which are equivalent (written AB_2),

(*c*) Three nuclei (ABX), two of which are of the same species (AB) and the third (X) is either a different species or has a resonance signal well separated from A and B.

Proton resonance spectra of S-guaiazulene, 2,6-lutidine, and 2,3-lutidine are reported and used as examples of the methods of analysis.

1. INTRODUCTION

The broad features of the nuclear magnetic resonance spectra of fluids can be explained in terms of transitions of non-interacting nuclei between the Zeeman levels split by an external magnetic field. Nuclei of the same species which are chemically non-equivalent may resonate at different applied fields on account of different electronic screening effects. This type of displacement is usually called a chemical shift. Under higher resolution, the absorption bands are observed to possess further fine structure which can be attributed to the indirect interaction of nuclear moments via the electrons (4, 6, 9, 10). If there are nuclei of two different species present, or if the chemical shift between non-equivalent nuclei of the same species is large, this fine structure is often of a fairly simple multiplet form and can be interpreted in terms of rules based on a simple interaction Hamiltonian and first-order perturbation theory (5). If several coupling constants are involved, however, the multiplet structure becomes more complicated. Hahn and Maxwell (6) have analyzed spectra for several types of groupings of nuclei and McConnell, McLean, and Reilly (8) have given a general method of dealing with spin multiplets and have discussed 1,1-difluoroethylene as an example.

The resonance spectra become more complex again in substances where there are non-equivalent nuclei of the same species whose relative chemical shifts are of the same order of magnitude as the splittings due to spin coupling. If the chemical shifts are still moderately large, higher order perturbation methods can be used with some effect (1, 2) but, eventually, individual multiplets become merged in a general mixed group of lines which may have few features of regularity. One is then faced with the problem of interpreting such a band system, assigning each line to a definite transition, and finally extracting numerical values for the chemical shift and spin-coupling constants. The present series of papers will be concerned with the details of such analyses. Spectra will be classified according to the number and arrangement of nuclei in various nuclear groupings. A complete understanding and fingerprinting of characteristic bands of simple groups is an essential step towards the interpretation of the spectra of more complex molecules.

[1]*Manuscript received September 13, 1956.*
Contribution from the Division of Pure Chemistry, National Research Council, Ottawa, Canada.
Issued as N.R.C. No. 4166.

[2]*Visiting Research Associate, Summer, 1956. Permanent address: Department of Theoretical Chemistry, University of Cambridge, England.*

Some theoretical work on spectra of this type has already been published by Hahn and Maxwell (7) and by Bannerjee, Das, and Saha (3). We shall consider a wider range of groupings, illustrating some cases by reporting measurements on appropriate examples and giving detailed assignments and analyses. To make the presentation complete we shall give a review of the basic quantum-mechanical formulation and include the analysis of some groups which have already been treated by slightly different methods in the references quoted above.

2. CLASSIFICATION OF NUCLEAR GROUPS

It is convenient to introduce a notation for typical groups of nuclei which may appear in molecules and which will possess characteristic NMR spectra. We shall use the symbols $A, B, \ldots$ for non-equivalent nuclei of the same species whose relative chemical shifts are of the same order of magnitude as the spin couplings between them. $X, Y, \ldots$ will be used for another such set whose signals are not close to those of the set $A, B, \ldots$. The nuclei in the set $X, Y, \ldots$ may or may not be of the same species as those in the set $A, B, \ldots$. The only feature that is important in the theory is that the chemical shift between the groups $A, B, \ldots$ and $X, Y, \ldots$ is large compared with any of the spin couplings. Equivalent nuclei will be described by the same symbol. Thus 1,1-difluoroethylene (I) is an example of A_2X_2, for the carbon nuclei have no moments and may be

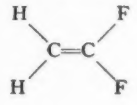

I

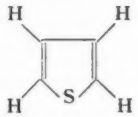

II

ignored. The protons in thiophene (II), on the other hand, would be described as an A_2B_2 group, for the chemical shift between the α and β hydrogens is observed to be relatively small.

In later sections of this paper, we shall give a detailed analysis of the NMR spectra characteristic of groups of two and three nuclei AB, AB_2, and ABX, all having spin $\frac{1}{2}$.

3. QUANTUM-MECHANICAL CALCULATION OF ENERGY LEVELS AND TRANSITION INTENSITIES

The basic quantum-mechanical method of finding the energies and transition intensities corresponding to the stationary states of the nuclear spin system has been described by several authors (4, 5, 6, 8, 9, 10) and we shall only summarize those features which are necessary for further development. McConnell, McLean, and Reilly (8) have given a full treatment and have developed the theory in a way which makes maximum use of molecular symmetry. We shall follow their notation to some extent.

The Hamiltonian consists of two parts,

$$\mathcal{H} = \mathcal{H}^{(0)} + \mathcal{H}^{(1)}. \qquad [3.1]$$

$\mathcal{H}^{(0)}$ corresponds to the interaction of the nuclear magnetic moments with the external field. It is given by

$$\mathcal{H}^{(0)} = \sum_i \eta_i H_i I_z(i), \qquad [3.2]$$

where $2\pi\eta_i$ is the gyromagnetic ratio of nucleus i, H_i the magnetic field at this nucleus, and $I_z(i)$ the spin angular momentum component in the z-direction (in units of $h/2\pi$).

For nuclei of spin $\frac{1}{2}$, $I_z(i)$ can take values $+\frac{1}{2}$ or $-\frac{1}{2}$. The sign convention is such that the external field is in the *negative* z-direction so that nuclei with positive spins have high energies. The magnetic field H_i will vary from one nucleus to another because of different electronic screening.

The other part of the Hamiltonian corresponds to the spin coupling and can be written

$$\mathcal{H}^{(1)} = \sum_{i<j} J_{ij}\, \mathbf{I}(i) \cdot \mathbf{I}(j), \tag{3.3}$$

where $\mathbf{I}(i)$ is the vector spin angular momentum (in units of $h/2\pi$). J_{ij} is the coupling constant between nuclei i and j and will have the dimensions of energy.

In the present paper we shall deal only with groups of nuclei of spin $\frac{1}{2}$ so that $I_z = \pm\frac{1}{2}$ and there will only be two wave functions α and β for each nucleus. For a system of p such nuclei, there will be 2^p possible energy states. All the wave functions can be written as linear combinations of 2^p basic product functions such as

$$\psi_n = \alpha(1)\, \beta(2)\, \alpha(3) \ldots \beta(p). \tag{3.4}$$

This product will usually be shortened to $\alpha\beta\alpha \ldots \beta$. If the nuclei were actually independent, these products would themselves be stationary state wave functions. The interaction Hamiltonian [3.3], however, causes mixing and the correct stationary state functions are those linear combinations of these products which diagonalize the matrix of the Hamiltonian [3.1]. The corresponding energies are solutions of the secular equation

$$|\mathcal{H}_{mn} - E\, \delta_{mn}| = 0 \tag{3.5}$$

where $\delta_{mn} = 1$ if $m = n$, and is zero otherwise.

McConnell, McLean, and Reilly (8) have indicated how it may be simpler to work with a different set of basic functions which belong to irreducible representations of the symmetry group. Thus, for two equivalent nuclei, one would replace the basic set $\alpha\alpha$, $\alpha\beta$, $\beta\alpha$, $\beta\beta$ by

$$\alpha\alpha,\ (\alpha\beta+\beta\alpha)/\sqrt{2},\ \ (\alpha\beta-\beta\alpha)/\sqrt{2},\ \beta\beta. \tag{3.6}$$

The third of these is antisymmetric with respect to interchange of the nuclei, all others being symmetric. Other examples of the use of symmetrized basic functions will be encountered later.

The secular equation [3.5] factorizes into equations of lower degree in E if we make use of the following *mixing rules:*

(1) There is no mixing between states of different total spin F_z where

$$F_z = \sum_i I_z(i). \tag{3.7}$$

(2) There is no mixing between states of different symmetry.

We therefore classify the basic functions by symmetry and total spin. It is then only necessary to diagonalize the submatrix $\mathcal{H}_{mn}$ of those elements which have common symmetry and spin. The set of functions [3.6], for example, all differ from one another either in spin or symmetry. There is, therefore, no mixing and these are the correct stationary state wave functions for the symmetrical two-nuclear system A_2.

There are simple rules for evaluating the matrix elements $\mathcal{H}_{mn}$ between single products

ψ_m and ψ_n of the type [3.4] (McConnell, McLean, and Reilly (8)). We repeat these for completeness. First

$$[3.8] \qquad (\psi_m|\mathscr{H}^{(0)}|\psi_m) = \tfrac{1}{2}\sum_i \eta_i H_i S_i$$

where $S_i = +1$ if nucleus i has α-spin in ψ_m and $S_i = -1$ if it has β-spin. The matrix element $(\psi_m|\mathscr{H}^{(0)}|\psi_n)$ $(m \neq n)$ vanishes.

The matrix elements of $\mathscr{H}^{(1)}$ are given by

$$[3.9] \qquad (\psi_m|\mathscr{H}^{(1)}|\psi_m) = \tfrac{1}{4}\sum_{i<j} J_{ij} T_{ij}$$

where $T_{ij} = +1$ or -1 according as spins i and j are parallel or antiparallel in ψ_m. Thus, for example,

$$[3.10] \qquad (\alpha\beta\alpha|\mathscr{H}^{(1)}|\alpha\beta\alpha) = \tfrac{1}{4}(-J_{12}+J_{13}-J_{23}).$$

Finally

$$[3.11] \qquad (\psi_m|\mathscr{H}^{(1)}|\psi_n) = \tfrac{1}{2} U J_{ij} \qquad (m \neq n)$$

where $U = 1$ if ψ_m only differs from ψ_n by an interchange of spins i and j and is zero otherwise. For example

$$[3.12] \qquad \begin{aligned} (\alpha\beta\alpha\beta|\mathscr{H}^{(1)}|\beta\alpha\alpha\beta) &= \tfrac{1}{2}J_{12}, \\ (\alpha\beta\alpha\beta|\mathscr{H}^{(1)}|\beta\alpha\beta\alpha) &= 0. \end{aligned}$$

If the basic set consists of some linear combinations of products, corresponding matrix elements are easily evaluated by expansion.

Having obtained a set of energy levels and corresponding wave functions, selection rules for transitions are required. McConnell *et al.* (8) derive the following two selection rules:

(1) In any allowed transition, the change of total spin

$$[3.13] \qquad \Delta F = \pm 1.$$

(2) All allowed transitions must be between two states of the same symmetry.

The intensity of the transition between two states p and q is proportional to the square of the transition moment

$$[3.14] \qquad (\phi_p|M_x|\phi_q)$$

where ϕ_p, ϕ_q are the stationary state wave functions and M_x is the x-component of the magnetic moment operator

$$[3.15] \qquad M_x = \sum_i \eta_i I_x(i).$$

The matrix element [3.14] can be expanded in terms of matrix elements of single products $(\psi_p|M_x|\psi_q)$. This is zero unless ψ_p and ψ_q differ only in the spin of one nucleus i, in which case it is equal to $\eta_i/2$.

4. TWO NUCLEI *AB*

The simplest system in which the effects of chemical shift and spin coupling are intermingled consists of two non-equivalent nuclei of the same species isolated from the

effects of any other nuclear moments. If the applied field is H_0, the local fields at nuclei A and B can be written

$$[4.1] \qquad \begin{aligned} H_A &= H_0(1-\sigma_A) \\ H_B &= H_0(1-\sigma_B) \end{aligned}$$

where σ_A and σ_B are non-dimensional screening constants. The relative chemical shift can be measured by the difference $\sigma_B-\sigma_A$, which may, of course, take either sign.

The basic functions and the diagonal matrix elements are (if the spin-coupling constant is J):

	n	ψ_n AB	F_z	$\mathscr{H}_{nn}$
	1	$\alpha\alpha$	1	$\eta H_0(1-\frac{1}{2}\sigma_A-\frac{1}{2}\sigma_B)+\frac{1}{4}J$
[4.2]	2	$\alpha\beta$	0	$\eta H_0(-\frac{1}{2}\sigma_A+\frac{1}{2}\sigma_B)-\frac{1}{4}J$
	3	$\beta\alpha$	0	$\eta H_0(\frac{1}{2}\sigma_A-\frac{1}{2}\sigma_B)-\frac{1}{4}J$
	4	$\beta\beta$	-1	$\eta H_0(-1+\frac{1}{2}\sigma_A+\frac{1}{2}\sigma_B)+\frac{1}{4}J$

The only non-vanishing off-diagonal element is

$$[4.3] \qquad \mathscr{H}_{23} = \tfrac{1}{2}J.$$

The only mixing that will occur, therefore, is between ψ_2 and ψ_3. If we define a positive quantity C and an angle θ by

$$[4.4] \qquad \begin{aligned} C\cos 2\theta &= \tfrac{1}{2}\eta H_0(\sigma_B-\sigma_A), \\ C\sin 2\theta &= \tfrac{1}{2}J \end{aligned}$$

the stationary state wave functions ϕ_n and energies E_n are given by:

	n	ϕ_n	E_n
	1	$\alpha\alpha$	$\eta H_0(1-\frac{1}{2}\sigma_A-\frac{1}{2}\sigma_B)+\frac{1}{4}J$
[4.5]	2	$\cos\theta(\alpha\beta)+\sin\theta(\beta\alpha)$	$-\frac{1}{4}J+C$
	3	$-\sin\theta(\alpha\beta)+\cos\theta(\beta\alpha)$	$-\frac{1}{4}J-C$
	4	$\beta\beta$	$\eta H_0(-1+\frac{1}{2}\sigma_A+\frac{1}{2}\sigma_B)+\frac{1}{4}J$

The allowed transitions with corresponding energies (relative to the mean $\frac{1}{2}\eta H_0(2-\sigma_A-\sigma_B)$) and relative intensities are given in Table I.

TABLE I

TRANSITION ENERGIES AND INTENSITIES FOR AB

Transition	Energy	Relative intensity
$3\rightarrow 1$	$\frac{1}{2}J+C$	$1-\sin 2\theta$
$4\rightarrow 2$	$-\frac{1}{2}J+C$	$1+\sin 2\theta$
$2\rightarrow 1$	$\frac{1}{2}J-C$	$1+\sin 2\theta$
$4\rightarrow 3$	$-\frac{1}{2}J-C$	$1-\sin 2\theta$

The general appearance of this spectrum depends only on the ratio $|J/\eta H_0(\sigma_B-\sigma_A)|$. If we suppose that the signs are such that $\sigma_B > \sigma_A$ and $J > 0$, so that B is more screened than A, the spectrum is as illustrated in Fig. 1. As we start from small J, the spectrum changes from two doublets into a symmetrical group of four lines, the inner pair being

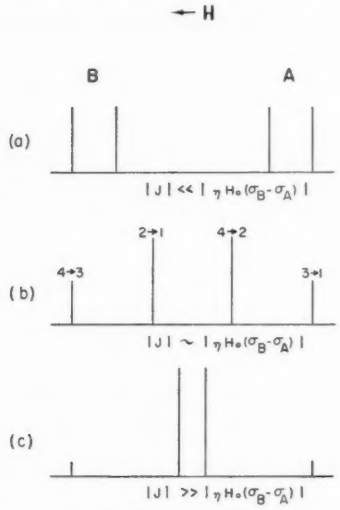

FIG. 1. Typical spectra for two nuclei AB.

stronger than the outer. Eventually the two central lines degenerate into a single one and the outer ones become forbidden, so that only a single signal is observed for A_2. In the intermediate stage we may still describe the right-hand pair qualitatively as predominantly A-lines, although the actual transition is a mixed one in which there is some change of spin of the B-nucleus.

If either or both of $(\sigma_B-\sigma_A)$ and J changes sign, it is easily seen from [4.4] and Table I that the appearance of the spectrum remains identical, although the detailed assignment shown in Fig. 1 may change. Thus, from an AB spectrum, it is not possible to determine which of the two nuclei is more screened, nor is it possible to obtain the sign of the coupling constant J.

The numerical analysis of such a spectrum is straightforward. The separation between either the right-hand pair or the left-hand pair is equal to $|J|$. The total separation of the extreme lines is $|J|+2C$, which gives C and consequently $|\sigma_B-\sigma_A|$ using [4.4].

Spectrum of S-Guaiazulene

As an example of a spectrum in which two-nuclei systems AB occur we consider the ring protons of S-guaiazulene.

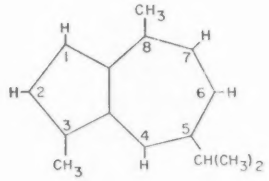

There are two sets of AB nuclei; the two hydrogens on the 1 and 2 positions of the five-membered ring, and the two hydrogens on the 6 and 7 positions of the seven-membered ring.

The spectrum of the sample contained in a 5 mm. spinning tube was measured with a Varian V–4300 NMR spectrometer, equipped with field stabilizer, at a fixed frequency of 40 Mc./sec. The more prominent signals in this spectrum (as well as in the other spectra presented in this paper) were cycled by the side-band technique to an accuracy of $\pm\frac{1}{2}$ c./sec. and the remaining signal separations were obtained by interpolation on the recorder chart. Where necessary a capillary containing cyclohexane was introduced in the spinning sample to provide a reference signal for the cycling procedure. The error in the frequency measurements gives rise to an inherent error of about 4–5% in the final values of the chemical shift and in the spin–spin coupling constants derived from the spectrum. The error in the measured intensities (areas) of the individual signals is considerably larger being of the order of 10% for strong, well-resolved signals.

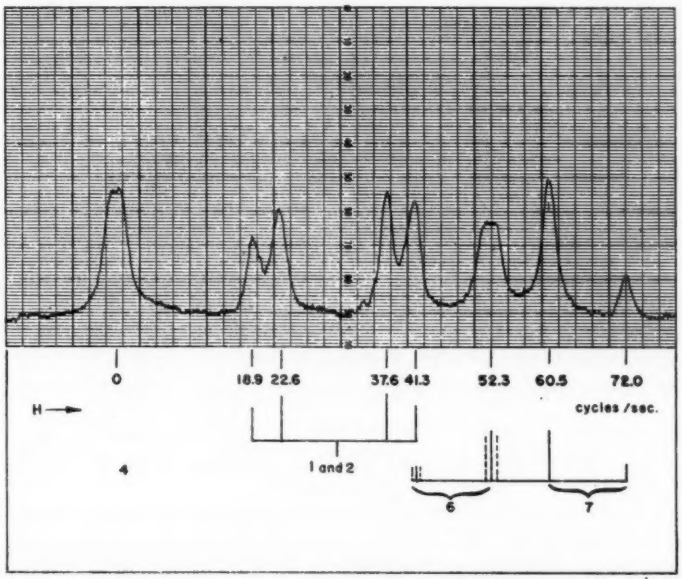

FIG. 2. Spectrum of the ring protons of S-guaiazulene at 40 Mc./sec.

The spectrum of the ring protons of S-guaiazulene is shown in Fig. 2. The separation of the signals is indicated in c./sec. in the direction of increasing magnetic field. Neglecting the small doubling in the signals at 0 and 52.3 c./sec., the spectrum can be broken down into a single line (0 c./sec., arising from proton 4) and two quartets of the AB type overlapping at 41.3 c./sec. The quartet (18.9, 22.6, 37.6, 41.3) approximates Fig. 1(*a*) and the other (41.3, 52.3, 60.5, 72.0) is similar to Fig. 1(*b*). The doubling of the signals at 0 and 52.3 c./sec. can be explained by introducing a coupling constant between protons 4 and 6. This might reasonably be expected to be larger than the coupling between 4 and 7, 1, or 2. On this hypothesis, therefore, the signals at 41.3 and 52.3 are assigned to proton 6, the doubling at 41.3 being unobserved because of the overlap. Consequently the other signals of this quartet (60.5, 72.0) originate from proton 7.* It is not possible, however, to distinguish between the signals of protons 1 and 2.

**The possibility of spin coupling between protons 4 and 6, and the tertiary hydrogen of the isopropyl group cannot be excluded. This would not alter the above assignment.*

Application of the above formulae (Table I) leads to the analysis given in Table II. The value $J_{46} = 1.3$ c./sec. is obtained from the doubling of the signals at 0 and 52.3 c./sec. (see under case ABX below).

TABLE II

ENERGIES AND RELATIVE INTENSITIES IN THE SPECTRUM OF S-GUAIAZULENE

Transition*	Origin	Energy (c./sec.)	Relative intensity†	
			Calc.	Obs.
	4	0	2.00	2.2
3 → 1	1 and 2	18.9	0.80	0.7
4 → 2	"	22.6	1.20	1.2
2 → 1	"	37.6	1.20	1.1
4 → 3	"	41.3	0.80	1.2
3 → 1	6	41.3	0.42	
4 → 2	6	52.3	1.58	1.7
2 → 1	7	60.5	1.58	1.6
4 → 3	7	72.0	0.42	0.3

$J_{12} = 3.7$ c./sec. $\quad \eta H_0|\sigma_1 - \sigma_2| = 18.3$ c./sec.
$J_{67} = 11.5$ c./sec. $\quad \eta H_0(\sigma_7 - \sigma_6) = 16.0$ c./sec.
$J_{46} = 1.3$ c./sec.

In the actual experimental arrangement, the applied field is varied to obtain resonance at a fixed frequency. Therefore, the higher energy transitions are observed at lower applied fields.
†*Intensities are normalized to give total ring proton intensity of 10.*

5. THREE NUCLEI AB_2

If we have a system of three nuclei, two of which are equivalent, there are two different spin-coupling constants J and J'. This arrangement has a symmetry of reflection in

the plane bisecting the BB line. As explained in Section 3, it is then convenient to replace the basic set of product functions $\alpha\alpha\alpha$, $\alpha\alpha\beta$, $\alpha\beta\alpha$, ... by a set all of which are either symmetric or antisymmetric under such a reflection. We have already seen that for two equivalent nuclei, such a set is $\alpha\alpha$, $(\alpha\beta+\beta\alpha)/\sqrt{2}$, $(\alpha\beta-\beta\alpha)/\sqrt{2}$, $\beta\beta$. Combining these with either α or β for nucleus A, we get the basic set listed in Table III. The symbols s and a are used to denote symmetric and antisymmetric states, respectively, and the value of the total spin F_z is appended as a suffix. Screening constants are again defined by

$$H_A = H_0(1-\sigma_A), \qquad H_B = H_0(1-\sigma_B) \qquad [5.1]$$

and we then obtain diagonal elements of $\mathcal{H}$ as given in the table. The only off-diagonal matrix elements are between $1s_{\frac{1}{2}}$ and $2s_{\frac{1}{2}}$ and between $1s_{-\frac{1}{2}}$ and $2s_{-\frac{1}{2}}$. These are both equal to $J/\sqrt{2}$.

The functions $s_{3/2}$, $a_{\frac{1}{2}}$, $a_{-\frac{1}{2}}$, and $s_{-3/2}$ do not mix and are therefore themselves stationary state wave functions. To find the symmetric stationary state functions for spins $\pm\frac{1}{2}$,

TABLE III

BASIC FUNCTIONS AND DIAGONAL MATRIX ELEMENTS FOR AB_2

Function	ABB	Diagonal matrix element
$s_{3/2}$	$\alpha\alpha\alpha$	$\frac{1}{2}\eta H_0(3-\sigma_A-2\sigma_B)+\frac{1}{4}(2J+J')$
$1s_{1/2}$	$\alpha(\alpha\beta+\beta\alpha)/\sqrt{2}$	$\frac{1}{2}\eta H_0(1-\sigma_A)+\frac{1}{4}J'$
$2s_{1/2}$	$\beta\alpha\alpha$	$\frac{1}{2}\eta H_0(1+\sigma_A-2\sigma_B)+\frac{1}{4}(-2J+J')$
$a_{1/2}$	$\alpha(\alpha\beta-\beta\alpha)/\sqrt{2}$	$\frac{1}{2}\eta H_0(1-\sigma_A)-\frac{3}{4}J'$
$a_{-1/2}$	$\beta(\alpha\beta-\beta\alpha)/\sqrt{2}$	$\frac{1}{2}\eta H_0(-1+\sigma_A)-\frac{3}{4}J'$
$1s_{-1/2}$	$\alpha\beta\beta$	$\frac{1}{2}\eta H_0(-1-\sigma_A+2\sigma_B)+\frac{1}{4}(-2J+J')$
$2s_{-1/2}$	$\beta(\alpha\beta+\beta\alpha)/\sqrt{2}$	$\frac{1}{2}\eta H_0(-1+\sigma_A)+\frac{1}{4}J'$
$s_{-3/2}$	$\beta\beta\beta$	$\frac{1}{2}\eta H_0(-3-\sigma_A-2\sigma_B)+\frac{1}{4}(2J+J')$

we have to solve 2×2 secular equations. We define positive quantities C_+, C_- and angles θ_+, θ_- by

$$
\begin{aligned}
C_+ \cos 2\theta_+ &= \eta H_0(\sigma_B-\sigma_A)+\tfrac{1}{4}J,\\
C_+ \sin 2\theta_+ &= J/\sqrt{2},\\
C_- \cos 2\theta_- &= \eta H_0(\sigma_B-\sigma_A)-\tfrac{1}{4}J,\\
C_- \sin 2\theta_- &= J/\sqrt{2}.
\end{aligned}
\qquad [5.2]
$$

Corresponding wave functions and energies are:

[5.3]

State	Wave function	Energy
$1's_{\frac{1}{2}}$	$\cos\theta_+\alpha(\alpha\beta+\beta\alpha)/\sqrt{2}+\sin\theta_+\beta\alpha\alpha$	$\frac{1}{2}\eta H_0(1-\sigma_B)+\frac{1}{4}(J'-J)+C_+$
$2's_{\frac{1}{2}}$	$-\sin\theta_+\alpha(\alpha\beta+\beta\alpha)/\sqrt{2}+\cos\theta_+\beta\alpha\alpha$	$\frac{1}{2}\eta H_0(1-\sigma_B)+\frac{1}{4}(J'-J)-C_+$
$1's_{-\frac{1}{2}}$	$\cos\theta_-\alpha\beta\beta+\sin\theta_-\beta(\alpha\beta+\beta\alpha)/\sqrt{2}$	$\frac{1}{2}\eta H_0(-1+\sigma_B)+\frac{1}{4}(J'-J)+C_-$
$2's_{-\frac{1}{2}}$	$-\sin\theta_-\alpha\beta\beta+\cos\theta_-\beta(\alpha\beta+\beta\alpha)/\sqrt{2}$	$\frac{1}{2}\eta H_0(-1+\sigma_B)+\frac{1}{4}(J'-J)-C_-$

The observable transition energies together with relative intensities are given in Table IV. Each transition may be labelled according to its behavior in the limit when the spin coupling constants J and J' tend to zero. The labelling given in the table is appropriate for the case $\sigma_B > \sigma_A$, that is the B nuclei are more shielded than the A. In this case $\theta_+, \theta_- \to 0$ as $J, J' \to 0$. Thus, for example, the transition $2's_{\frac{1}{2}} \to s_{3/2}$ becomes $\beta\alpha\alpha \to \alpha\alpha\alpha$ and is, therefore, labelled an A transition, since in this limit only the A-spin is changed. The transition $1's_{-\frac{1}{2}} \to 2's_{\frac{1}{2}}$, on the other hand, becomes $\alpha\beta\beta \to \beta\alpha\alpha$ and cannot be described as A or B. In the limit it will correspond to the simultaneous change of spin of all three nuclei and may be referred to as a *combination line*. It is actually forbidden in the limit, but should appear with non-zero intensity in the general intermediate case. However, the same band also becomes forbidden in the other limit of zero chemical shift so that its intensity is always low.

If $\sigma_B < \sigma_A$, that is if the single nucleus is more highly screened, $\theta_+, \theta_- \to \frac{1}{2}\pi$ as $J, J' \to 0$, so that some relabelling is necessary in Table IV.

All the transition energies and intensities are independent of the B–B coupling constant J', so that the structure of the spectrum, apart from a scaling factor, is a function only of the non-dimensional ratio $J/\eta H_0(\sigma_B-\sigma_A)$. The pattern of lines for a series of values of this ratio is illustrated in Fig. 3 for $\sigma_B > \sigma_A$ and $J > 0$.

TABLE IV

ENERGIES AND INTENSITIES FOR AB_2

Transition	Origin*	Energy	Relative intensity
1. $2's_{1/2} \rightarrow s_{3/2}$	A	$\frac{1}{2}\eta H_0(2-\sigma_A-\sigma_B)+\frac{1}{4}J+C_+$	$[\sqrt{2}\sin\theta_+-\cos\theta_+]^2$
2. $2's_{-1/2} \rightarrow 1's_{1/2}$	A	$\eta H_0(1-\sigma_B)+C_++C_-$	$[\sqrt{2}\sin(\theta_+-\theta_-)+\cos\theta_+\cos\theta_-]^2$
3. $a_{-1/2} \rightarrow a_{1/2}$	A	$\eta H_0(1-\sigma_A)$	1
4. $s_{-3/2} \rightarrow 1's_{-1/2}$	A	$\frac{1}{2}\eta H_0(2-\sigma_A-\sigma_B)-\frac{1}{4}J+C_-$	$[\sqrt{2}\sin\theta_--\cos\theta_-]^2$
5. $1's_{-1/2} \rightarrow 1's_{1/2}$	B	$\eta H_0(1-\sigma_B)+C_+-C_-$	$[\sqrt{2}\cos(\theta_+-\theta_-)+\cos\theta_+\sin\theta_-]^2$
6. $1's_{1/2} \rightarrow s_{3/2}$	B	$\frac{1}{2}\eta H_0(2-\sigma_A-\sigma_B)+\frac{1}{4}J-C_+$	$[\sqrt{2}\cos\theta_++\sin\theta_+]^2$
7. $2's_{-1/2} \rightarrow 2's_{1/2}$	B	$\eta H_0(1-\sigma_B)-C_++C_-$	$[\sqrt{2}\cos(\theta_+-\theta_-)-\sin\theta_+\cos\theta_-]^2$
8. $s_{-3/2} \rightarrow 2's_{-1/2}$	B	$\frac{1}{2}\eta H_0(2-\sigma_A-\sigma_B)-\frac{1}{4}J-C_-$	$[\sqrt{2}\cos\theta_--\sin\theta_-]^2$
9. $1's_{-1/2} \rightarrow 2's_{1/2}$	Comb.	$\eta H_0(1-\sigma_B)-C_+-C_-$	$[\sqrt{2}\sin(\theta_+-\theta_-)+\sin\theta_+\sin\theta_-]^2$

*Based on $\sigma_B > \sigma_A$.

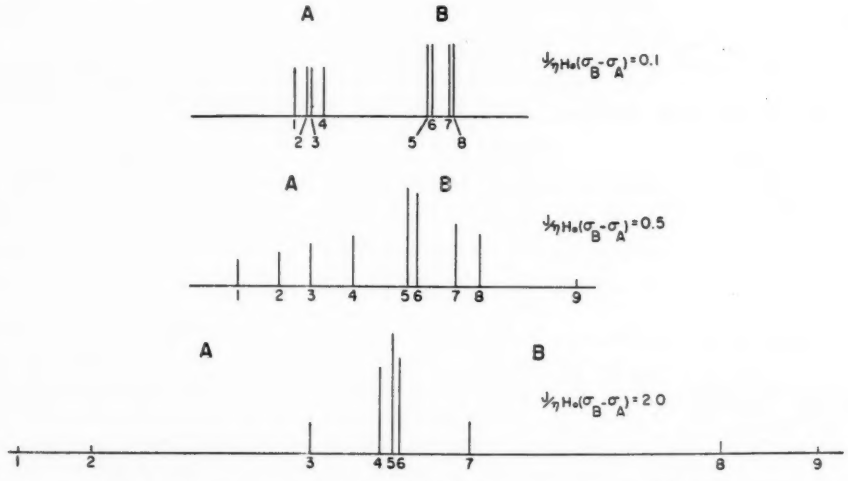

FIG. 3. Typical spectra of three nuclei AB_2 (numbering as in Table IV).

If $\sigma_B > \sigma_A$ and $J < 0$, the appearance of the spectrum is identical although the assignment in terms of the numbering in Table IV needs revising. If $\sigma_B < \sigma_A$, the patterns have to be reversed. From such a spectrum, therefore, it is possible to determine $\sigma_B - \sigma_A$ including sign, but only the magnitude of J.

The following features, which are of use in the practical analysis of a spectrum, may be noted from Table IV:

(*a*) Line 3 immediately gives the position of pure chemical shift for the A-nucleus, unmodified by spin coupling.

(*b*) The corresponding position for the B nuclei is the mean of the transitions 5 and 7.

Numerical values of the transition energies of Table IV (lines 1–9) are given for a range of values of this ratio in Table V. All energies are measured relative to the undisplaced A-line (line 3) and the scale is adjusted so that the chemical shift is one unit.

In practice, there may be difficulties in resolving lines which are close together, and values of the chemical shift and J are better obtained by adjusting the ratio $J/\eta H_0(\sigma_B-\sigma_A)$ using Table V until the best fit of the pattern is obtained.

TABLE V

ENERGIES OF TRANSITIONS RELATIVE TO UNDISPLACED A-LINE

J / $\eta H_0(\sigma_B-\sigma_A)$	Energy								
	A 1	A 2	A 3	A 4	B 5	B 6	B 7	B 8	Comb. 9
0	0	0	0	0	−1	−1	−1	−1	−2
0.1	+0.105	+0.010	0	−0.095	−0.950	−0.955	−1.050	−1.055	−2.010
0.2	+0.218	+0.040	0	−0.178	−0.904	−0.918	−1.096	−1.122	−2.040
0.3	+0.338	+0.088	0	−0.250	−0.862	−0.888	−1.138	−1.200	−2.088
0.4	+0.463	+0.153	0	−0.310	−0.826	−0.863	−1.174	−1.290	−2.153
0.5	+0.593	+0.233	0	−0.360	−0.797	−0.843	−1.203	−1.390	−2.233
0.6	+0.726	+0.326	0	−0.400	−0.774	−0.826	−1.226	−1.500	−2.326
0.7	+0.862	+0.429	0	−0.433	−0.755	−0.812	−1.245	−1.617	−2.429
0.8	+1.000	+0.540	0	−0.460	−0.740	−0.800	−1.260	−1.740	−2.540
0.9	+1.140	+0.658	0	−0.482	−0.729	−0.790	−1.271	−1.868	−2.658
1.0	+1.281	+0.781	0	−0.500	−0.719	−0.781	−1.281	−2.000	−2.781
1.2	+1.566	+1.038	0	−0.528	−0.706	−0.766	−1.294	−2.272	−3.038
1.4	+1.855	+1.306	0	−0.549	−0.696	−0.755	−1.304	−2.551	−3.306
1.6	+2.146	+1.581	0	−0.564	−0.690	−0.746	−1.310	−2.836	−3.581
1.8	+2.438	+1.862	0	−0.576	−0.685	−0.738	−1.315	−3.124	−3.862
2.0	+2.732	+2.146	0	−0.586	−0.682	−0.732	−1.318	−3.414	−4.146

Spectrum of 2,6-Lutidine

As an example of the application of these formulae we have measured and analyzed the spectrum of the ring protons on 2,6-lutidine. In this molecule these protons are expected to have a simple spectrum since the complicating effects of coupling with the

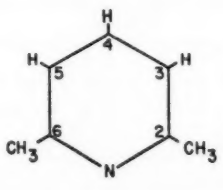

methyl protons and the nitrogen nucleus are relatively small because of extra separation.

The spectrum of 2,6-lutidine is reproduced in Fig. 4 and is easily fitted into the scheme of Fig. 3. The best over-all fit of pattern is obtained with the ratio $J/\eta H_0(\sigma_B-\sigma_A)$ equal to 0.375. Adjustment of the scale then gives:

[5.4] Chemical shift $\eta H_0(\sigma_B-\sigma_A) = 21.9$ c./sec.

$J = 8.2$ c./sec.

The spectrum of 2,6-lutidine at lower resolution has been analyzed previously by Baker (2). Values of 16 and 6 c./sec. were found for the chemical shift and spin–spin coupling

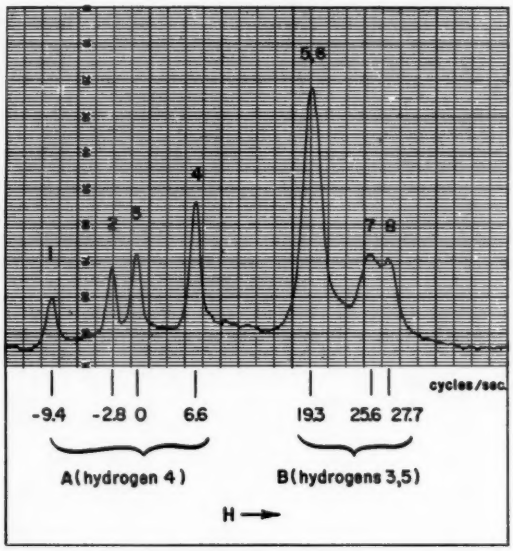

FIG. 4. Ring proton spectrum of 2,6-lutidine at 40 Mc./sec. (numbering as in Table IV).

constant respectively. The calculated energies and intensities using the parameters from [5.4] are compared with observed values in Table VI. Lines 5 and 6 are unresolved in this spectrum; this is consistent with the small calculated separation. The combination signal was not observed, presumably because of its very low intensity.

TABLE VI

COMPARISON OF CALCULATED AND OBSERVED SPECTRUM FOR 2,6-LUTIDINE

Line	Energy (c./sec. relative to line 3)		Relative intensity	
	Calc.	Obs.	Calc.	Obs.
1	−9.4	−9.4	0.68	0.45
2	−3.0	−2.8	0.90	0.75
3	0	0	1.00	0.9
4	6.5	6.6	1.42	1.6
5	18.3	19.3	2.42	5.0
6	19.0		2.32	
7	25.5	25.6	1.68	3.3
8	27.7	27.7	1.58	
9	46.7	—	0.002	—

6. THREE NUCLEI *ABX*

We now consider the case of two nuclei, A, B, where the relative chemical shift is of the same order of magnitude as the spin-coupling constants, coupled to a third nucleus X which may either be of a different species or of the same species with its signal well separated from the AB region. We will deal with the latter case, although the notation

is easily modified to apply to the former. There will be three coupling constants, as follows:

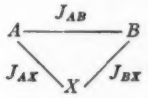

If the external field is H_0, the fields at the three nuclei will be written

$$\begin{aligned} H_A &= H_0(1-\sigma_A), \\ H_B &= H_0(1-\sigma_B), \\ H_X &= H_0(1-\sigma_X). \end{aligned} \tag{6.1}$$

In this case we may, without loss of generality, suppose that $\sigma_B > \sigma_A$.

The most convenient set of basic functions, since there is no symmetry, are single products of the type $\alpha\beta\alpha$. These functions and the corresponding diagonal matrix elements are:

	ABX	Diagonal matrix element
1.	$\alpha\alpha\alpha$	$\frac{1}{2}\eta H_0(3-\sigma_A-\sigma_B-\sigma_X)+\frac{1}{4}(J_{AB}+J_{AX}+J_{BX})$
2.	$\alpha\alpha\beta$	$\frac{1}{2}\eta H_0(1-\sigma_A-\sigma_B+\sigma_X)+\frac{1}{4}(J_{AB}-J_{AX}-J_{BX})$
3.	$\alpha\beta\alpha$	$\frac{1}{2}\eta H_0(1-\sigma_A+\sigma_B-\sigma_X)+\frac{1}{4}(-J_{AB}+J_{AX}-J_{BX})$
4.	$\beta\alpha\alpha$	$\frac{1}{2}\eta H_0(1+\sigma_A-\sigma_B-\sigma_X)+\frac{1}{4}(-J_{AB}-J_{AX}+J_{BX})$
5.	$\alpha\beta\beta$	$\frac{1}{2}\eta H_0(-1-\sigma_A+\sigma_B+\sigma_X)+\frac{1}{4}(-J_{AB}-J_{AX}+J_{BX})$
6.	$\beta\alpha\beta$	$\frac{1}{2}\eta H_0(-1+\sigma_A-\sigma_B+\sigma_X)+\frac{1}{4}(-J_{AB}+J_{AX}-J_{BX})$
7.	$\beta\beta\alpha$	$\frac{1}{2}\eta H_0(-1+\sigma_A+\sigma_B-\sigma_X)+\frac{1}{4}(J_{AB}-J_{AX}-J_{BX})$
8.	$\beta\beta\beta$	$\frac{1}{2}\eta H_0(-3+\sigma_A+\sigma_B+\sigma_X)+\frac{1}{4}(J_{AB}+J_{AX}+J_{BX})$

[6.2]

The off-diagonal matrix elements of the Hamiltonian will involve only the coupling constants, J_{AB}, J_{AX}, and J_{BX}. The non-vanishing ones are:

$$\begin{aligned} \mathscr{H}_{23} &= \tfrac{1}{2}J_{BX} & \mathscr{H}_{56} &= \tfrac{1}{2}J_{AB} \\ \mathscr{H}_{24} &= \tfrac{1}{2}J_{AX} & \mathscr{H}_{57} &= \tfrac{1}{2}J_{AX} \\ \mathscr{H}_{34} &= \tfrac{1}{2}J_{AB} & \mathscr{H}_{67} &= \tfrac{1}{2}J_{BX} \end{aligned} \tag{6.3}$$

This gives the complete matrix for the general problem of three nuclei ABC.

Now we are assuming that $\eta H_0\sigma_X$ is large compared with any of the spin-coupling constants. This means that there will be mixing between functions 3 and 4 but neither will mix appreciably with function 2 although it has the same total spin. Similarly there will be mixing only between 5 and 6. The problem is therefore reduced to the solution of 2×2 secular equations and the final energy levels can then be written in explicit analytical form. If we define

$$\begin{aligned} D_+ \cos 2\phi_+ &= \tfrac{1}{2}\eta H_0(\sigma_B-\sigma_A)+\tfrac{1}{4}(J_{AX}-J_{BX}), \\ D_+ \sin 2\phi_+ &= \tfrac{1}{2}J_{AB}, \\ D_- \cos 2\phi_- &= \tfrac{1}{2}\eta H_0(\sigma_B-\sigma_A)-\tfrac{1}{4}(J_{AX}-J_{BX}), \\ D_- \sin 2\phi_- &= \tfrac{1}{2}J_{AB}, \end{aligned} \tag{6.4}$$

the mixed wave functions and energy levels are:

[6.5]

State	Wave function	Energy
$3'$	$\cos\phi_+(\alpha\beta\alpha)+\sin\phi_+(\beta\alpha\alpha)$	$\frac{1}{2}\eta H_0(1-\sigma_X)-\frac{1}{4}J_{AB}+D_+$
$4'$	$-\sin\phi_+(\alpha\beta\alpha)+\cos\phi_+(\beta\alpha\alpha)$	$\frac{1}{2}\eta H_0(1-\sigma_X)-\frac{1}{4}J_{AB}-D_+$
$5'$	$\cos\phi_-(\alpha\beta\beta)+\sin\phi_-(\beta\alpha\beta)$	$\frac{1}{2}\eta H_0(-1+\sigma_X)-\frac{1}{4}J_{AB}+D_-$
$6'$	$-\sin\phi_-(\alpha\beta\beta)+\cos\phi_-(\beta\alpha\beta)$	$\frac{1}{2}\eta H_0(-1+\sigma_X)-\frac{1}{4}J_{AB}-D_-$

Once again we may classify the lines according to their origin in the absence of spin coupling. Of the total of 15 possible transitions, four will arise from each of the three nuclei and there will be three combination lines. Again the latter are generally weak. A complete table of transition energies and intensities is given in Table VII.

TABLE VII

ENERGIES AND INTENSITIES FOR ABX

	Transition	Origin	Energy	Relative intensity
1.	$8\rightarrow 6'$	B	$\frac{1}{2}\eta H_0(2-\sigma_A-\sigma_B)-\frac{1}{4}(2J_{AB}+J_{AX}+J_{BX})-D_-$	$(\cos\phi_--\sin\phi_-)^2$
2.	$7\rightarrow 4'$	B	$\frac{1}{2}\eta H_0(2-\sigma_A-\sigma_B)-\frac{1}{4}(2J_{AB}-J_{AX}-J_{BX})-D_+$	$(\cos\phi_++\sin\phi_+)^2$
3.	$5'\rightarrow 2$	B	$\frac{1}{2}\eta H_0(2-\sigma_A-\sigma_B)+\frac{1}{4}(2J_{AB}-J_{AX}-J_{BX})-D_-$	$(\cos\phi_-+\sin\phi_-)^2$
4.	$3'\rightarrow 1$	B	$\frac{1}{2}\eta H_0(2-\sigma_A-\sigma_B)+\frac{1}{4}(2J_{AB}+J_{AX}+J_{BX})-D_+$	$(\cos\phi_++\sin\phi_+)^2$
5.	$8\rightarrow 5'$	A	$\frac{1}{2}\eta H_0(2-\sigma_A-\sigma_B)-\frac{1}{4}(2J_{AB}+J_{AX}+J_{BX})+D_-$	$(\cos\phi_-+\sin\phi_-)^2$
6.	$7\rightarrow 3'$	A	$\frac{1}{2}\eta H_0(2-\sigma_A-\sigma_B)-\frac{1}{4}(2J_{AB}-J_{AX}-J_{BX})+D_+$	$(\cos\phi_++\sin\phi_+)^2$
7.	$6'\rightarrow 2$	A	$\frac{1}{2}\eta H_0(2-\sigma_A-\sigma_B)+\frac{1}{4}(2J_{AB}-J_{AX}-J_{BX})+D_-$	$(\cos\phi_--\sin\phi_-)^2$
8.	$4'\rightarrow 1$	A	$\frac{1}{2}\eta H_0(2-\sigma_A-\sigma_B)+\frac{1}{4}(2J_{AB}+J_{AX}+J_{BX})+D_+$	$(\cos\phi_+-\sin\phi_+)^2$
9.	$8\rightarrow 7$	X	$\eta H_0(1-\sigma_X)-\frac{1}{2}(J_{AX}+J_{BX})$	1
10.	$5'\rightarrow 3'$	X	$\eta H_0(1-\sigma_X)+D_+-D_-$	$\cos^2(\phi_+-\phi_-)$
11.	$6'\rightarrow 4'$	X	$\eta H_0(1-\sigma_X)-D_++D_-$	$\cos^2(\phi_+-\phi_-)$
12.	$2\rightarrow 1$	X	$\eta H_0(1-\sigma_X)+\frac{1}{2}(J_{AX}+J_{BX})$	1
13.	$7\rightarrow 2$	Comb.	$\eta H_0(1+\sigma_X)$	0
14.	$5'\rightarrow 4'$	Comb.	$\eta H_0(1-\sigma_X)-D_+-D_-$	$\sin^2(\phi_+-\phi_-)$
15.	$6'\rightarrow 3'$	Comb.	$\eta H_0(1-\sigma_X)+D_++D_-$	$\sin^2(\phi_+-\phi_-)$

Spectra of this type are most readily interpreted by considering the coupling constants J_{AX} and J_{BX} as perturbations. If these are both zero, the AB region of the spectrum will consist of four lines as discussed in section 4. In Table VII these four lines correspond to the pairs (1, 2), (3, 4), (5, 6), and (7, 8). If J_{AX} and J_{BX} are now introduced, the two B pairs are both split by

[6.6] $$\tfrac{1}{2}(J_{AX}+J_{BX})+(D_--D_+)$$

and the two A pairs by

[6.7] $$\tfrac{1}{2}(J_{AX}+J_{BX})-(D_--D_+).$$

If the coupling constants J_{AX} and J_{BX} are equal, the splittings will be identical ($D_+ = D_-$). If $J_{AX} < J_{BX}$ then $D_+ < D_-$ and, if the sum $J_{AX}+J_{BX}$ is positive, the B-splitting will be larger. However, if the signs of both J_{AX} and J_{BX} are reversed, there will be no change in the observed spectrum. This is illustrated schematically in Fig. 5. If the splittings are considerably larger than shown in this figure, there may be some crossing of lines. Also the A-splitting expression [6.7] may be negative, in which case the assignment in Fig. 5 would be 1, 2, 3, 4, 6, 5, 8, 7 from right to left.

Some check on the assignments in the AB region can be obtained from the structure of the X spectrum, which is closely related. There is a symmetrical quartet (Fig. 6)

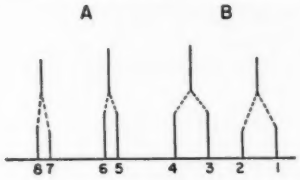

FIG. 5

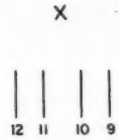

FIG. 6

FIG. 5. Relation of AB region of ABX spectrum to the pure AB spectrum.
FIG. 6. X signals in the ABX spectrum.

which is such that the 9–10 separation is equal to the A-splittings [6.7] and the 9–11 separation is equal to the B-splittings [6.6]. If [6.7] is negative, the assignment of the X spectrum would be 10, 9, 12, 11, from right to left.

Spectra with the biggest coupling between X and A can be described in a similar manner. The A-splittings would then be greater ($D_+ > D_-$) and the X signals would have to be reassigned 9, 11, 10, 12 or 11, 9, 12, 10.

Spectrum of 2,3-Lutidine

The analysis of an ABX spectrum will be illustrated by the ring protons in 2,3-lutidine.

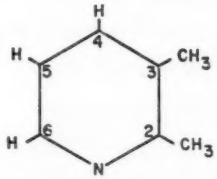

In this molecule the signals from the proton in the 6-position (H_6) are well separated from the other two (H_5 and H_4). The complete spectrum is shown in Fig. 7.

All 12 non-combination lines are clearly visible. Comparison with Fig. 5 shows that we have the coupling case $J_{BX} > J_{AX}$. Since we expect the coupling between protons attached to neighboring carbon atoms to be dominant, we assign the B signals to H_5.

The splittings of the pairs in the AB region are 4.6, 4.5, 1.5, and 1.5 c./sec. The corresponding separations in the X signal are 4.8, 4.8, 1.7, and 1.7 c./sec., in good agreement with the theory. As mentioned above, there are two possible assignments, which we will consider in turn.

Assignment 1, 2, 3, 4, 5, 6, 7, 8, 9, 10, 11, 12

From the average values of the splittings we have

$$\begin{aligned} \tfrac{1}{2}(J_{AX}+J_{BX})+(D_--D_+) &= 4.7, \\ \tfrac{1}{2}(J_{AX}+J_{BX})-(D_--D_+) &= 1.6. \end{aligned} \qquad [6.8]$$

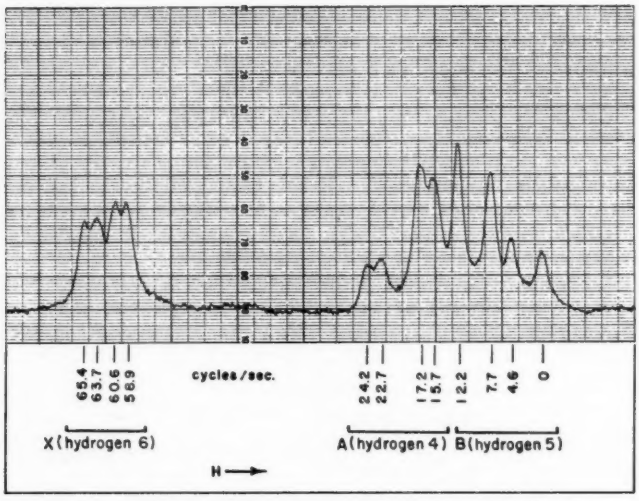

FIG. 7. Ring proton spectrum of 2,3-lutidine at 40 Mc./sec.

From Table VII we see that the coupling constant J_{AB} is equal to the separation between lines 1 and 3 (7.7 c./sec.) or between lines 5 and 7 (7.0 c./sec.). We, therefore, choose the mean value 7.35 c./sec.

The value D_+ is equal to half the separation between lines 2 and 6 or between 4 and 8 (mean value 6.15 c./sec.). Similarly D_- is half the separation between lines 1 and 5 or 3 and 7 (mean value 7.7 c./sec.). From the definitions [6.4] we deduce:

$$[6.9] \qquad \eta H_0(\sigma_B-\sigma_A) = 11.8 \text{ c./sec.}, \qquad J_{BX}-J_{AX} = 3.55 \text{ c./sec.}$$

Combining [6.9] with [6.8] we obtain values for all parameters.

Assignment 1, 2, 3, 4, 6, 5, 8, 7, 10, 9, 12, 11

Equations [6.8] have to be replaced by

$$[6.10] \qquad \begin{aligned} \tfrac{1}{2}(J_{AX}+J_{BX})+(D_--D_+) &= 4.7, \\ \tfrac{1}{2}(J_{AX}+J_{BX})-(D_--D_+) &= -1.6. \end{aligned}$$

The other steps are as before and we obtain

$$[6.11] \qquad J = 7.35 \text{ c./sec.}, \quad D_+ = 5.4 \text{ c./sec.}, \quad D_- = 8.4 \text{ c./sec.}$$

The other chemical shift parameter $\eta H_0\sigma_X$ is easily obtained by fitting the separation between any of the lines in the AB and X spectra. The sum of the transition energies for lines 2, 3, 6, and 7 is equal to $\frac{1}{2}\eta H_0(2-\sigma_A-\sigma_B)$ and when combined with $\eta H_0(\sigma_B-\sigma_A)$ gives the origin of signals A and B. The two complete sets of parameters are given in Table VIII. The observed energies and intensities are compared with those calculated from these parameters in Table IX.

The agreement between calculated and observed energies is equally good for either assignment. From the calculated intensities it appears that it should be possible, in principle, to distinguish between the two assignments. However, the observed intensities, obtained by estimating area under the incompletely resolved peaks, are not yet accurate enough for this purpose.

TABLE VIII

CHEMICAL SHIFTS AND COUPLING CONSTANTS FOR 2,3-LUTIDINE (C./SEC.)*

	First assignment	Second assignment
Chemical shift $\eta H_0(\sigma_A-\sigma_X)$ (hydrogen 6 – hydrogen 4)	43.4	43.4
Chemical shift $\eta H_0(\sigma_B-\sigma_A)$ (hydrogen 4 – hydrogen 5)	11.7	11.5
J_{56} (J_{BX})	5.0	5.2
J_{45} (J_{AB})	7.35	7.35
J_{46} (J_{AX})	1.3	−2.0

**The signs of the spin-coupling constants are undetermined. The sign of J_{AB} may be negative and the signs of J_{AX} and J_{BX} may be reversed simultaneously.*

TABLE IX

OBSERVED AND CALCULATED SPECTRA FOR 2,3-LUTIDINE

Transition (1st assignment)	Origin	Energy, c./sec.			Relative intensity		
		Calc. I	Calc. II	Obs.	Calc. I	Calc. II	Obs.
8 → 6′	*B*	0	0	0	0.52	0.56	0.82
7 → 4′	*B*	4.7	4.6	4.6	0.40	0.32	0.64
5′ → 2	*B*	7.4	7.4	7.7	1.48	1.44	1.45
3′ → 1	*B*	12.1	12.0	12.2	1.60	1.68	1.63
8′ → 5′	*A*	15.4	15.6	15.7	1.48	1.68	2.80
7 → 3′	*A*	17.0	16.8	17.2	1.60	1.44	
6′ → 2	*A*	22.7	22.8	22.7	0.52	0.32	0.94
4′ → 1	*A*	24.3	24.2	24.2	0.40	0.56	
8 → 7	*X*	59.1	59.1	58.9	1.00	0.99	2.10
5′ → 3′	*X*	60.7	60.5	60.6	1.00	0.99	
6′ → 4′	*X*	63.7	63.7	63.7	1.00	0.99	1.67
2 → 1	*X*	65.4	65.1	65.4	1.00	0.99	

REFERENCES

1. ANDERSON, W. A. Phys. Rev. **102**, 151 (1956).
2. ARNOLD, J. T. Phys. Rev. **102**, 136 (1956).
3. BANNERJEE, M. K., DAS, T. P., and SAHA, A. K. Proc. Roy. Soc. A, **226**, 490 (1954).
4. GUTOWSKY, H. S., MCCALL, D. W., and SLICHTER, C. P. Phys. Rev. **84**, 589 (1951).
5. GUTOWSKY, H. S., MCCALL, D. W., and SLICHTER, C. P. J. Chem. Phys. **21**, 279 (1953).
6. HAHN, E. L. and MAXWELL, D. E. Phys. Rev. **84**, 1246 (1951).
7. HAHN, E. L. and MAXWELL, D. E. Phys. Rev. **88**, 1070 (1952).
8. MCCONNELL, H. M., MCLEAN, A. D., and REILLY, C. A. J. Chem. Phys. **23**, 1152 (1955).
9. RAMSEY, N. F. Phys. Rev. **91**, 303 (1953).
10. RAMSEY, N. F. and PURCELL, E. M. Phys. Rev. **85**, 143 (1952).

RADIATION-INDUCED EXCHANGE OF DEUTERIUM BETWEEN HEAVY WATER AND DISSOLVED HYDROGEN[1]

J. BARDWELL[2] AND P. J. DYNE

ABSTRACT

Exchange of deuterium between deuterium oxide and molecular hydrogen is induced by gamma rays from Co^{60}. The reaction was studied by irradiating heavy water solutions saturated with hydrogen gas, and then analyzing the gas with a mass spectrometer. The reaction rate conforms to the exponential exchange law. The exchange yield is independent of dose rate and of hydrogen concentration over a moderate range. Prolonged irradiation leads to a steady state where the isotopic composition of the gas is close to that of the solution. This state differs greatly from that for thermodynamic equilibrium at room temperature.

INTRODUCTION

The exchange of hydrogen isotopes between water and molecular hydrogen provides a method for the preparation of heavy water (12, 13). The method depends upon the fact that the equilibrium constant for the exchange reaction

$$HD + H_2O \rightleftharpoons H_2 + HDO \qquad [1]$$

varies considerably with temperature, being 3.6 at 25° C. for H_2O and HDO in the liquid state* and calculated by Urey (17) to be 1.36 at 527° C. This last value has been confirmed experimentally (3, 4, 15) within the uncertainties in Urey's calculations. It is reasonable to assume that the catalyzed exchange depends upon the transitory existence of adsorbed hydrogen atoms.

When aqueous solutions are exposed to high energy radiations chemical transformations occur that are explained, in part, by the postulate of dissociation of water into H atoms and OH radicals (2). It was of interest, therefore, to discover whether the exchange of hydrogen isotopes, represented by Equation 1, could be induced by high energy radiations, for example by gamma rays from Co^{60}.

In this paper some experiments will be reported dealing with the kinetics and position of equilibrium of the exchange reaction between dissolved hydrogen gas and slightly enriched water (1% D_2O or less). The progress of the exchange was followed by collecting the dissolved gas and analyzing it for HD with a mass spectrometer.

While this investigation was in progress, Gordon and Hart published some results of an investigation of the gamma-ray induced reaction between D_2 and H_2O (8). They found that both HD and H_2 are formed, the production of H_2 being much greater than could be accounted for by exchange of HD with H_2O. They also observed that the yield is affected by pH.

EXPERIMENTAL

Apparatus

The apparatus used for preparing and irradiating solutions of hydrogen is shown in Fig. 1. A cylindrical radiation cell (volume 32 ml.) was connected by two capillaries to a

[1]*Manuscript received September 9, 1956.*
Contribution from the Chemistry and Metallurgy Division, Atomic Energy of Canada Limited, Chalk River, Ontario. Issued as A.E.C.L. No. 380.
[2]*Present address: Department of Chemistry, University of Saskatchewan, Saskatoon, Saskatchewan.*
**Obtained by a short extrapolation from the data of Cerrai et al. (4) and corrected according to the method of Kirshenbaum (Ref. 11, p. 25) for the difference in vapor pressures between* H_2O *and* HDO.

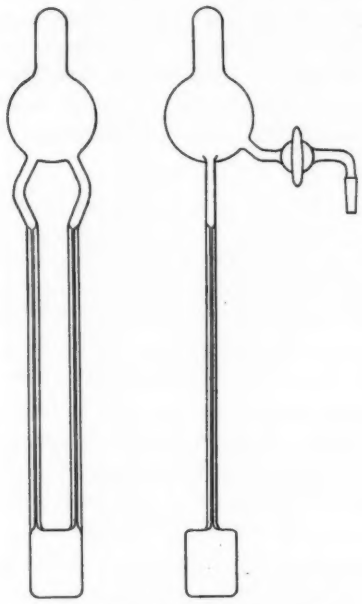

FIG. 1. The irradiation apparatus.

bulb (volume 118 ml.) to which was sealed a stopcock. During irradiation the apparatus was held upright, so that liquid completely filled in the capillaries and thus served to isolate the solution, during irradiation, from hydrogen gas contained in the bulb. The design of the apparatus was such that contact of the solution with stopcock grease was minimized.

The remainder of the apparatus consisted of a vacuum system, one part of which served for adding purified hydrogen, one for removing surplus undissolved gas after irradiation, and one for collecting dissolved gas for analysis.

Preparation of Solution for Irradiation

A solution of heavy water containing 0.749 mole % D_2O was prepared by mixing weighed quantities of pure D_2O and water that had been redistilled from potassium permanganate. Other solutions containing 0.264, 0.382, and 0.504 mole % D_2O were prepared by further dilutions with redistilled water. In all cases allowance was made for the deuterium content of ordinary water, taken as 0.015 mole % D_2O (11). Although it is convenient to express the concentrations of such solutions as mole % D_2O, it is realized that in these dilute solutions the only deuterated species present in significant quantity is HDO.

After the radiation apparatus had been thoroughly cleaned and rinsed, heavy water solution (33 ml.) was introduced. The liquid was then freed of dissolved air by repeated freezing and pumping. The temperature of the apparatus was adjusted to 25° C., and purified hydrogen admitted. The hydrogen used was purified by being passed through a hot palladium thimble (6) and a liquid nitrogen trap. When the desired partial pressure of hydrogen was reached (usually 726 mm.) the stopcock was closed and the apparatus detached from the vacuum system. A solution of hydrogen was then prepared by shaking

the apparatus vigorously for 15 minutes. That this procedure succeeded in giving a saturated solution was verified by collecting and measuring the dissolved gas, by the method described below. The amount collected was 2.5×10^{-5} moles, which corresponds to a concentration of hydrogen in the solution of 7.6×10^{-4} moles/liter. The accepted value of the solubility at 25° C. and a partial pressure of 726 mm. is 7.52×10^{-4} moles/liter (19).

Irradiation Method

The source consisted of three capsules each holding approximately 70 curies of Co^{60}. The capsules could be moved radially within a lead castle and a high intensity of radiation resulted when all three were brought in contact with the solution container. The rate of energy deposition within the radiation cell was determined by the standard ferrous ion method. The *G*-value of this dosimeter was taken as 15.5 ions oxidized per 100 ev. absorbed (10). Most of the experiments described below were done with a dose rate of 1.01×10^{22} ev./liter/hr. The temperature of the source room was 25±2° C.

Method of Collecting Dissolved Gas

Immediately after each irradiation the solution in the capillaries was frozen, by surrounding the capillaries with pulverized dry ice, and the hydrogen gas in the bulb was pumped off and discarded. During this step the irradiated solution remained intact, being protected from degassing by the ice in the capillaries. After the ice had melted, the apparatus was inverted and the irradiated solution was degassed by being heated to 50° C. The liquid was then frozen with a slurry of dry ice in acetone. The gas was collected by an apparatus consisting of a liquid nitrogen trap, for removal of water vapor, a Toepler pump modified to serve also as a McLeod gauge, and a detachable calibrated gas holder (volume about 3 ml.). The collected gas was then analyzed with a mass spectrometer, and the liquid used as a solvent for hydrogen in the next experiment. Repeated use of the liquid was permissible since its deuterium content was reduced by only one part in 10^5 in each experiment.

Deuterium Analysis

The isotopic composition of the extracted gas was determined with a Model 21–201 Consolidated Nier mass spectrometer. The instrument was calibrated by a method similar to that of Alfin-Slater, Rock, and Swislocki (1). Known mixtures of HD and H_2 were prepared from heavy water solutions by the zinc reduction method (9). Mass spectrometric analysis of the gases obtained yielded the mass 3: mass 2 ratios given in Table I. The calibration curve is shown in Fig. 2. A standard experimental procedure was followed in all the mass spectrometric analyses, and care was taken to minimize instrumental errors such as the "memory effect" (1, 11).

TABLE I

CALIBRATION OF MODEL 21-201 CONSOLIDATED NIER MASS SPECTROMETER FOR DEUTERIUM ANALYSIS

Composition of gas		Mass spectrometer reading for mass 3: mass 2 ratio $\times10^6$
Atom %D	HD/H_2 ratio $\times10^6$	
0.015	300	850
0.264	5310	6510
0.504	10180	12260
0.749	15210	18080

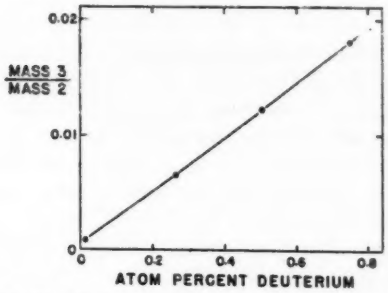

FIG. 2. Calibration of Model 21–201 Consolidated Nier mass spectrometer for deuterium analysis.

RESULTS

Exchange Equilibrium

Results showing the progress of the radiation-induced exchange reaction are shown in Fig. 3 where the deuterium content of the dissolved gas is plotted against irradiation time and dose. The values obtained on prolonged irradiation (not shown in Fig. 3) are given in Table II, together with values of the equilibrium constant for the reaction

$$H_2 + HDO \rightleftarrows HD + H_2O$$

calculated from these data. The average value of this equilibrium constant is 0.83. The equilibrium constant for the exchange written in Equation 1 is the reciprocal of this quantity, i.e. approximately 1.2. This value may be compared with the known equilibrium constants for the catalyzed exchange, viz. 3.6 at 25° C. and 1.2 at 750° C. (4, 17).

TABLE II

EXCHANGE EQUILIBRIUM FOR THE RADIATION INDUCED REACTION: $H_2 + HDO \rightleftarrows HD + H_2O$

Mole % D_2O in water	Irradiation time (hours)	Atom % deuterium in gas	$K_{eq.}$
0.382	41.4	0.306	0.80
0.749	65.0	0.643	0.86

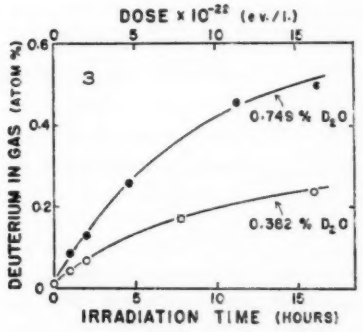

FIG 3. Progress of radiation induced exchange of deuterium between heavy water solution and dissolved hydrogen.

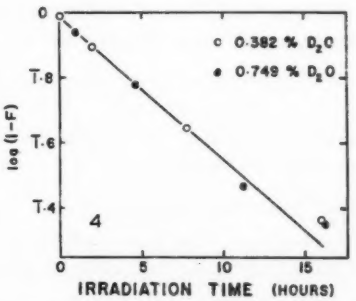

FIG 4. Graphical test of exponential exchange law. F is the fractional exchange.

Exchange Kinetics

Consideration of the kinetics of simple exchange reaction shows that the transfer of a tracer atom follows an exponential law (5, 7, 18). Conformity to this law is revealed by a linear relation between $\log(1-F)$ and time, where F is the fractional exchange; here, the fractional exchange is the ratio of the deuterium content of the gas at time t to the content when equilibrium is reached. Values of F were calculated for the data given in Fig. 3 using as equilibrium compositions the experimental compositions of the gas obtained after prolonged irradiation (Table II). In Fig. 4 $\log(1-F)$ is plotted against time of irradiation and it is seen that the results conform satisfactorily to the theoretical relationship. Furthermore the results with two concentrations of heavy water fall on the same line.

Calculation of Exchange Rate, R

In considering the effect of experimental variables, it is convenient to define the exchange rate, R, as the number of gram-atoms of hydrogen (including deuterium) exchanged per liter per hour. It may be shown (18) that R is related to the change of F by the equation:

$$Rt = -(A)(B)/[(A)+(B)] \ln(1-F) . \qquad [2]$$

(A) and (B) are the concentrations of the two compounds participating in the exchange, expressed as gram-atoms of the exchanging element per liter. Since here the water concentration, (B), is vastly greater than the molecular hydrogen concentration, Equation 2 reduces to:

$$Rt = -(A)\ln(1-F) \qquad [3]$$

or

$$R = -2.303(A)\, d \log(1-F)/dt. \qquad [4]$$

(A) is the number of gram-atoms of hydrogen, in the form of molecular hydrogen, per liter, i.e. twice the solubility of hydrogen in moles per liter. For the results plotted in Fig. 4, (A) is 1.50×10^{-3} gram-atoms per liter. When this value, together with the slope of the line in Fig. 4, is substituted in Equation 4, R is found to be 1.57×10^{-4} gram-atoms/liter/hr. with a dose rate of 1.01×10^{22} ev./liter/hr.

Calculation of Exchange Yield, G

The yield of a radiation induced reaction is expressed as the number of atoms produced by 100 ev. of absorbed energy, and is designated by G. If the dose rate is d electron volts per liter per hour and the exchange rate is R gram-atoms/liter/hr., the exchange yield is given by:

$$G = 100N_AR/d \qquad [5]$$

N_A is Avogadro's number. The results shown in Fig. 4 give a G-value of 0.94 hydrogen atoms exchanged per 100 ev.

Effect of Dose Rate on R and G

Energy deposition in the irradiated solution was reduced from 1.01×10^{22} ev./liter/hour to 0.185×10^{22} ev./liter/hr. by withdrawing each Co^{60} capsule 4.5 cm. from the solution container. Irradiations of 5.46 and of 10.92 hours were done, and the values of R and G calculated using Equations 4 and 5. The results are shown in Table III. A more than fivefold change in dose rate is seen to have very little effect on the exchange yield.

TABLE III

EFFECT OF DOSE RATE ON R AND G
Hydrogen pressure, 726 mm. Mole % D_2O in water, 0.749.

Dose rate, ev./l./hr.	Exchange rate, R, g-atom/l./hr.	Exchange yield, G, atoms per 100 ev.
1.01×10^{22}	1.57×10^{-4}	0.94
0.185×10^{22}	0.320×10^{-4}	1.04

Effect of Hydrogen Concentration

In one experiment the partial pressure of hydrogen was reduced from 726 mm. to 363 mm. and the resulting solution irradiated for 1 hour. It was assumed that the concentration of dissolved hydrogen was proportional to the partial pressure. The results are shown in Table IV. Evidently R and G are not strongly dependent on hydrogen concentration.

TABLE IV

EFFECT OF CONCENTRATION OF DISSOLVED HYDROGEN
Mole % D_2O in water, 0.749. Dose rate, 1.01×10^{22} ev./l./hr.

Partial pressure of hydrogen, mm.	Exchange rate, R, g-atom/l./hr.	Exchange yield, G, atoms per 100 ev.
363	1.65×10^{-4}	0.99
726	1.57×10^{-4}	0.94

Irradiation of Gas-free Water

A conceivable interpretation of the foregoing results was that H_2 and HD were being formed by direct decomposition of the heavy water solution. This possibility was explored in an experiment where the addition of hydrogen was omitted entirely, the liquid used being degassed by alternate freezing and pumping until the pressure of gas, non-condensable by liquid nitrogen, was 0.004 mm. The degassed liquid was then irradiated at maximum intensity for 20 hours. After the irradiation, the degassing procedure was repeated and the total amount of gas present in the apparatus measured. The quantity of gas found was barely measurable with the apparatus used, being at most 10^{-8} moles. Since approximately 2×10^{-5} moles of gas would be needed to explain the observed production of HD, it is clear that solution decomposition cannot account for the apparent exchange.

The D_2–H_2O Exchange

An attempt was made to follow the exchange by observing the alteration in the isotopic composition of the liquid instead of the gas. In one experiment natural water (0.015 mole % D_2O) was saturated with deuterium gas (99.5% D_2) at one atmosphere pressure, and the solution was irradiated at maximum intensity for 10 periods of 8 hours each. After each 8 hour period the water was resaturated with deuterium gas and again irradiated. At the end of the experiment the water was analyzed for HDO using an infrared method (14, 16). The deuterium oxide content, expressed as D_2O, was now 0.023 mole %. The increase, although definite, was too small to permit convenient quantitative study of the reaction. Furthermore, calculation of a reliable G-value is impossible because the D/H ratio of the dissolved gas is changing continuously throughout the experiment. The result does, however, show directly that water is involved in the exchange.

DISCUSSION

As the results given in this paper are of a preliminary nature, no extensive discussion of the exchange mechanism will be attempted. The observation that the *G*-value is independent of dose rate and hydrogen concentration is similar to the result obtained by Gordon and Hart for the D_2–H_2O exchange (8). When the actual magnitudes of the *G*-values of the two exchanges are compared, interesting differences appear. For the D_2–H_2O exchange Gordon and Hart reported a *G*-value of about 2.7 (8). This is about three times the values reported here for the H_2–HDO exchange. As we have been able to obtain results in other experiments consistent with those of Gordon and Hart for the D_2–H_2O system, there is no likelihood that the difference is experimental and it must be attributed to an isotope effect. This could be both in the initial process of forming radicals H or D and OH or OD from HDO and in the subsequent reactions of these species with D_2 or H_2 respectively.

The most interesting feature of the results reported above is the equilibrium state reached when irradiation is prolonged. It has been shown that here the isotopic composition of the gas approaches that of the heavy water solution, the apparent equilibrium constant for reaction [1] being 1.2. There is little doubt that the true equilibrium constant at 25° C. is 3.6 (4). This discrepancy shows that the radiation cannot be regarded as simply a catalyst for the exchange. Apparently the radiation itself dictates a final steady state, far removed from that for thermodynamic equilibrium at room temperature.

The results show clearly that there exists a "radiation steady state" which, in the absence of radiation, is metastable relative to the thermal equilibrium state. It has been pointed out that when one attempts to describe the radiation steady state by a formal equilibrium constant, the value obtained resembles that for thermal equilibrium at a high temperature (approximately 750° C.). More detailed interpretation of the radiation steady state requires consideration of the relative rates of production of H and D atoms and OH and OD radicals and knowledge of their subsequent reactions.

ACKNOWLEDGMENTS

The authors are greatly indebted to Dr. R. H. Betts for many valuable suggestions, and to R. Jones, J. H. Graham, and M. Daoust for doing the mass spectrometric analyses.

REFERENCES

1. Alfin-Slater, R. B., Rock, S. M., and Swislocki, M. Anal. Chem. **22**, 421 (1950).
2. Allen, A. O. Discussions Faraday Soc. No. **12**, 79 (1952).
3. Bonhoeffer, K. F. and Rummel, K. W. Naturwiss. **22**, 45 (1934).
4. Cerrai, E., Marchetti, C., Renzoni, R., Roseo, L., Silvestri, M., and Villani, S. Chem. Eng. Progr. Symposium Ser. **50**, 271 (1954).
5. Duffield, R. B. and Calvin, M. J. Am. Chem. Soc. **68**, 557 (1946).
6. Farkas, A. and Melville, H. W. Experimental methods in gas reactions. MacMillan & Co., Ltd., London. 1939. p. 151.
7. Friedlander, G. and Kennedy, J. W. Nuclear and radiochemistry. John Wiley & Sons, Inc., New York. 1955. p. 315.
8. Gordon, S. and Hart, E. J. J. Am. Chem. Soc. **77**, 3981. (1955).
9. Graff, J. and Rittenberg, D. Anal. Chem. **24**, 878 (1952).
10. Hochanadel, C. J. J. Phys. Chem. **56**, 587 (1952).
11. Kirshenbaum, I. Physical properties and analysis of heavy water. McGraw-Hill Book Co., Inc., New York. 1951.
12. Rae, H. K. Chemistry in Canada. **7**, 27 (1955).
13. Selak, P. J. and Frinke, J. Chem. Eng. Progr. **50**, 221 (1954).
14. Stevens, W. H. and Thurston, W. Private communication.
15. Suess, H. E. Z. Naturforsch. **4***a*. 328 (1949).
16. Thornton, V. and Condon, F. E. Anal. Chem. **22**, 690 (1950).
17. Urey, H. C. J. Chem. Soc. 562 (1947).
18. Wahl, A. C. and Bonner, N. A. Radioactivity applied to chemistry. John Wiley & Sons, Inc., New York. 1951. p. 7.
19. Winkler, L. W. Ber. **24**, 89 (1891).

MASS SPECTROMETRIC STUDY OF THE SPECIES CS, SO, AND CCl_2 PRODUCED IN PRIMARY HETEROGENEOUS REACTIONS[1]

L. P. BLANCHARD[2] AND P. LE GOFF

ABSTRACT

In a flow system and at very low pressures, the reactions of CS_2, H_2S, SO_2, and CCl_4, on pure and carburized tungsten ribbons, were studied at 1300–2000° K.

In the decomposition of CS_2, on *pure* tungsten, CS and S_2 are found—in that of H_2S, H_2 and S_2—in that of SO_2, O_2 and SO or S_2, according to the temperature—CCl_4 gives CCl_2, Cl_2, and Cl. H_2, S_2, and Cl_2 molecules are probably formed by recombination on the walls of atoms produced on the ribbon. With *carburized* tungsten the formation of S_2 and O_2 is replaced by that of CS and CO. On the contrary, no decarburization occurs with chlorine.

Ionization potentials of the different species are measured and the deduced bond dissociation energies are discussed.

INTRODUCTION

The details of the experimental technique used in this work have been described elsewhere (4). The substance which is to be decomposed is made to flow through a reaction chamber in which a tungsten ribbon has been mounted. The vapor, at a pressure of 10^{-5} mm. Hg, is pumped through the chamber at the rate of 5 liters per second. When the ribbon is heated to a temperature T, the steady state concentration of X changes from $[X]_0$ to $[X]_T$. It can be shown that the collision efficiency b leading to the decomposition of the gas is governed by the following equation: $b = (1-u)/v_m u$ where u is the ratio $[X]_T/[X]_0$, or that fraction of X which has not reacted, and v_m is a constant depending on the geometry of the reacting surface—in this case $v_m = 2.5$. Analyses of reactants and products are carried out by means of a mass spectrometer, the ionization chamber of which forms an integral part of the reaction vessel.

The ratio u is readily obtained from variations in the intensity of the parent-peak of X provided, of course, that no product from the reaction contributes to the intensity of this same peak. For all peaks in the spectrum of X, a ratio v of the intensity of each peak when the ribbon is hot to that when it is cold can be determined. The difference $(v-u)$ is proportional to the concentration of reaction products which contribute to the intensity of the peak under consideration. When products with mass peaks other than those observed in the spectrum of X are formed, a unit w proportional to the concentration of the product is obtained by taking the ratio of the intensity of each peak to that of the parent-peak X_0.

As described in preceding articles (5, 6), results of investigations on the decomposition of hydrocarbon vapors on tungsten surfaces have brought to light the formation of a carbon (or tungsten–carbide) layer at the surface of the ribbon. Furthermore, the rate of diffusion of carbon in tungsten was found to play a fundamental role in the mechanisms of reactions, particularly so in the formation of methyl radicals (7). Results obtained on the role that this layer plays in the decomposition of substances containing sulphur or chlorine are given below.

Decomposition of CS_2

The decomposition of CS_2 on both pure and carburized tungsten ribbons was investigated from 1500° to 2100° K. The principal peak variations that were observed

[1]*Manuscript received September 13, 1956.*
Contribution from the Department of Chemistry, University of Nancy, Nancy, France.
[2]*National Research Council of Canada Postdoctorate Fellow.*

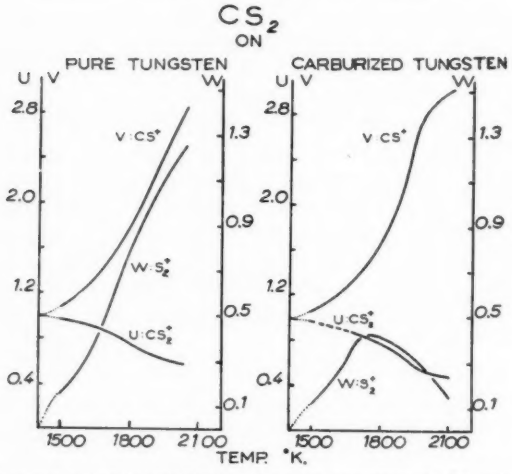

FIG. 1. Relative variations of ion intensities in the mass spectrum of CS_2 with the temperature of a pure tungsten and a carburized tungsten ribbon.

have been reproduced in Fig. 1. For the sake of clarity all experimental points have been omitted, though the error involved is of the same order of magnitude as that shown in Fig. 4 for the decomposition of CCl_4.

With increasing temperature the intensity of the parent-peak, mass 76, was found to decrease, starting from about 1400° K. This was accompanied by increases in the intensities of mass 44 (CS^+) and mass 64 (S_2^+), while that of mass 32 (S^+) remained essentially constant. From the observed peak increases, one would be led to believe that CS_2 decomposes as follows:

$$CS_2 \rightarrow CS + \tfrac{1}{2}S_2. \qquad [1]$$

Furthermore the nature of these products was confirmed by the measurement of their appearance potentials (A.P.)—mass 32 (S^+):12.5±0.4 v.; mass 44 (CS^+):11.8±0.2 v.; and mass 64 (S_2^+):10.0±0.3 v.—which were determined with the tungsten ribbon maintained at 1850° K. The A.P.'s of the last two peaks are not incompatible with the figures given by Smyth and Blewett (10) namely:

10.6±0.3 v. for CS^+ from CS and 10.7±0.3 v. for S_2^+ from S_2.*

Though the presence of atomic sulphur could not be detected even from the A.P. of mass 32, given above,—the ionization potential (I.P.) of S being 10.3 volts (3)—thermodynamic calculations (12) show that the sulphur leaving the hot ribbon should be in the atomic state. A high probability of recombination (≈ 1) of S on the reactor walls would readily explain its *apparent* absence. This is supported by the fact that the usual polymers of sulphur were observed: S_2, some S_4, but no S_3 or S_5.

Dyne and Ramsay (1) found that CS radicals have a relatively long life—up to 4 minutes—which seems to have been borne out in this work by the fact that no recom-

**The above results along with the A.P. of CS^+ from CS_2, which was found to be 15.7±0.1 v., enabled the dissociation energy of the bond (SC—S) to be calculated at 90±7 kcal. per mole. It is interesting to note that though the A.P.'s of the ions CS^+ from CS and from CS_2 were both about 1 volt above the figures reported earlier (10), the difference between the two values led to a dissociation energy of he bond (SC—S) which is in good agreement with that given in this last reference.*

bination products of CS were detected. This leads to reactions for the decomposition of CS_2 which agree both with experimental results and thermodynamics:

$$CS_2 \xrightarrow{\text{ribbon}} CS + S, \qquad [II]$$

$$2S \xrightarrow{\text{walls}} S_2. \qquad [III]$$

The possibility that CS_2 decomposed directly to sulphur and carbon was discarded when no carbon monoxide was formed after the carbon disulphide was replaced by oxygen on the hot non-carburized tungsten ribbon. Trace amounts of carbon dissolved in tungsten are known to be highly reactive in the presence of oxygen (6, 8).

When the pure tungsten was replaced by a ribbon containing under 3% carbon by weight, the decomposition of CS_2 at all temperatures was found to proceed at a faster rate. The main difference, however, resided in the fact that at 1700° K. the intensity of mass 64 (S_2^+) went through a maximum. At the same time mass 44 (CS^+) increased more than in the previous case.

From 1400° to 1700° K. the decomposition of CS_2 appears to be the same as in reactions [II] and [III]; above 1700° K, when the mobility of carbon in tungsten becomes great, the surface of the ribbon is supplied with a more than ample amount of carbon, and under these conditions, decarburization of the tungsten begins to take place by the following reaction:

$$CS_2 + C_{(w)} \rightarrow 2CS. \qquad [IV]$$

From known thermodynamic properties though in general they were poorly defined (9, 12), it was possible to verify that the reactions postulated for the decomposition of CS_2 are possible under the operating conditions that were used: temperatures between 1300° K. and 2100° K. and a pressure of CS_2 equal to 2×10^{-5} mm. mercury. It should be noted however, that it is practically impossible to calculate with any degree of accuracy from this data the equilibrium constant of reaction [IV]. For example at 2000° K. it is found that the value of K lies somewhere between 3×10^{-6} and $7\times10^{+4}$. It will be seen further on that CS and CS_2 are found simultaneously in the decomposition products of H_2S and SO_2, coming from a carburized tungsten ribbon, which tends to prove that even at 2000° K. and at a pressure of 10^{-5} mm. mercury the equilibrium of reaction [IV] is not entirely displaced to the right, as is the case in the analogous reaction:

$$CO_2 + C \rightarrow 2CO. \qquad [IV\text{-}a]$$

On pure carbon surfaces, even at the highest temperature—2100° K.—no decomposition of CS_2 could be detected.

Decomposition of H_2S

In the decomposition of H_2S on pure tungsten the observed products are S_2 and H_2. Here, as in the case of CS_2, atomic sulphur is believed to come away from the hot tungsten surface and undergo a recombination process on the cooler reactor walls. As pointed out earlier (4) it is not possible to establish whether hydrogen is formed on the hot ribbon in the atomic or molecular state.

The search for HS radicals was somewhat misleading. As shown in Fig. 2, the curve for mass 33 (HS^+) lies slightly above that for mass 34 (H_2S^+). To explain this it must be remembered that the error involved in the experimental points that determined the position of these curves is almost as large as the difference existing between the two

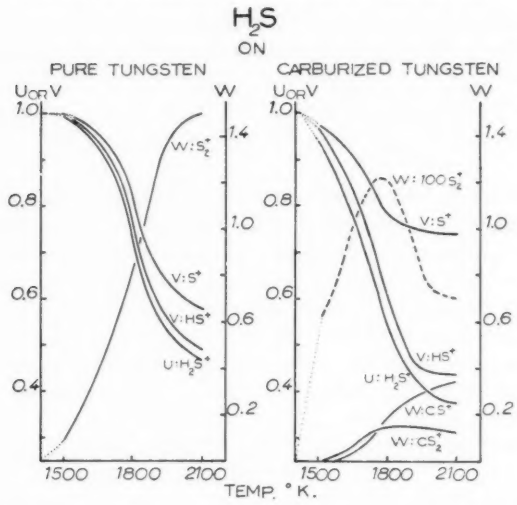

FIG. 2. Relative variations of ion intensities in the mass spectrum of H_2S with the temperature of a pure tungsten and a carburized tungsten ribbon.

curves. Furthermore a study of the appearance potential of HS^+ at different ribbon temperatures showed no variations in the observed value: 12.7 ± 0.4 volts.

On carburized tungsten the decomposition of H_2S proceeded at a faster rate at all temperatures. H_2, CS, and CS_2 were the principal products. As shown in Fig. 2 a very small concentration of S_2 was observed—the dashed line plotted at 100 times its actual height. This concentration dropped off above 1800° K. while that of CS increased sharply. This is explained by the fact that decarburization of the ribbon by sulphur becomes important only when the mobility of carbon in tungsten is sufficiently great, i.e. above 1800° K.

Again no HS radicals could be detected.

Above 1800° K. the deviation of the S^+ curve away from the H_2S^+ curve is attributed to the contributions from CS and CS_2.

The ionization potential of the CS radical was again easily measured. The figure obtained, 11.9 ± 0.3 v., agrees well with that obtained during the decomposition of CS_2. The A.P. of S_2^+ was 10.3 ± 0.2 v. in both cases, i.e., on pure tungsten and on carburized tungsten. This corresponds to the I.P. of S_2 (10).

Summarizing the decomposition of H_2S:

(*a*) *On pure tungsten*

$$H_2S \xrightarrow{\text{ribbon}} H_2 + S, \qquad [V]$$

$$\text{and } 2S \xrightarrow{\text{walls}} S_2. \qquad [III]$$

(*b*) *On carburized tungsten*

$$H_2S + C_{(w)} \rightarrow H_2 + S, \qquad [VI]$$

$$2CS \rightleftharpoons CS_2 + C. \qquad [VII]$$

(*c*) While on *pure carbon surfaces*, no decomposition could be detected even at 2100° K.

Decomposition of SO_2

The decomposition of SO_2 on pure and carburized tungsten was investigated from 1300° to 2100° K. On *pure tungsten* the appearance potential of mass 64, which was 13.0±0.3 v. at 1300° K.—this being the ionization potential of SO_2(11)—was only 10.7± 0.5 v. at 1900° K. As this corresponds to the I.P. of S_2, it was concluded that S_2, especially at the higher temperatures, is an abundant final product of the reaction. Since this substance also contributes to the intensity of mass 64, the parent-peak of SO_2, it was not possible to associate variations in intensity of this peak with the relative abundance u of SO_2 in the reaction chamber. This fact is illustrated further by the curves in Fig. 3.

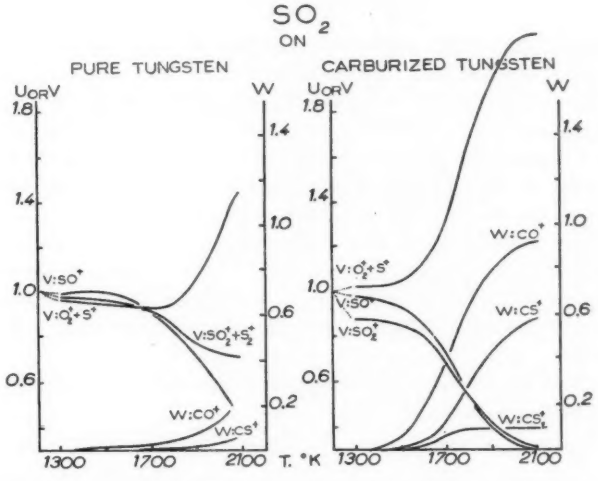

Fig. 3. Relative variations of ion intensities in the mass spectrum of SO_2 with the temperature of a pure tungsten and a carburized tungsten ribbon.

It can be seen that v of SO_2^+ does not decrease as rapidly as does v of SO^+. In fact above 1700° K., v of SO_2^+ assumes a greater value than that for v of SO^+. The true curve u for SO_2^+ lies somewhere below the v curves given in this figure.

The small but definite difference which was found between v of SO^+ and v of SO_2^+ indicated that some SO was formed, especially between 1300 and 1700° K. The appearance potential of SO^+ from SO_2, which was 16.1±0.2 v., dropped to 12.1±0.3 v. when the temperature was raised to 1700° K. This new potential is believed to be the ionization potential of the substance SO.*

The continuous increase in v of mass 32 with increasing temperature from about 1700° K. was attributed to the formation of O_2 when the appearance potential of this peak at 1900° K. was found to be 12.6±0.2 v. This figure agrees well with the I.P. of O_2, which is reported to be 12.5 v. (3) and not with that of atomic sulphur at 10.3 v. From these results it was concluded that below 1700° K. and on pure tungsten the decomposition of SO_2 proceeded as follows:

$$SO_2 \rightarrow SO + \tfrac{1}{2}O_2. \qquad \text{[VIII]}$$

**From the above potentials a dissociation energy for the bond* (OS—O) *was calculated at 92±7 kcal. per mole assuming, of course, the usual restrictions: no excess of electronic or kinetic energy.*

From the previously mentioned thermodynamic data (9, 12), it was found that at equilibrium the ratio $[SO]/[SO_2]$ should be 0.015 at 1300° K. and 1.5 at 2000° K. for a pressure of SO_2 of about 10^{-5} mm. Hg.

On the other hand, above 1700° K. one would be led to conclude that SO_2 decomposes according to reaction [IX]:

$$SO_2 \rightarrow \tfrac{1}{2}S_2 + O_2. \qquad [IX]$$

But this reaction is impossible from a thermodynamic point of view since, even at 2000° K., the ratio $[O_2]/[SO_2]$ would not surpass 0.05 at equilibrium.

Instead, reaction [X],

$$SO_2 \xrightarrow{\text{ribbon}} S + O_2, \qquad [X]$$

is postulated, since calculations show that at 2000° K. the ratio $[O_2]/[SO_2]$ should be approximately 1.6 at equilibrium. Furthermore it was shown in the decomposition of CS_2 that S_2 at these temperatures is entirely dissociated, and that the apparent absence of atomic sulphur can only be explained by a rapid recombination on the cooler walls.*,†

On carburized tungsten the reaction proceeded in general at a faster rate. The formation of O_2 and some S_2 observed on pure tungsten gave way to an abundance of CO and CS. As in the case of H_2S, the simultaneous formation of CS and CS_2 was again observed though the abundance of CS_2 was relatively small. As can be seen in Fig. 3, at the lower temperatures a greater amount of SO was formed. A measurement of the appearance potential of this peak confirmed the presence of the particle SO. Again the peak at mass 64 was perturbed by the formation of a lesser amount of S_2—identified by A.P. determination.

At temperatures as low as 1200° K., SO_2 invariably reacts with carbon on the surface of the ribbon according to reaction [XI]:

$$SO_2 + C_{(w)} \rightarrow SO + CO. \qquad [XI]$$

But as the temperature is raised to approximately 1700° K. the instability of SO becomes more important, resulting in further reactions with carbon (see reaction XII) with the subsequent equilibrium of reaction [IV].

$$SO + 2C_{(w)} \rightarrow CS + CO \qquad [XII]$$

It was calculated that at equilibrium, reaction [XII] is totally displaced to the right even at 2000° K. The particle SO in the presence of carbon is thus seen to be unstable. The big increase with temperature of peak 32 must be attributed to S^+ ions from the spectra of CS and CS_2: its appearance potential curve presents two breaks around 12.5 v. and 14 v.

Attempts to decompose SO_2 on pure carbon drew negative results even at 2100° K.

Decomposition of CCl_4

The mass spectrum of CCl_4‡ showed that the intensity of the parent-peak was too small to follow any changes occurring in the abundance of this substance, and conse-

**During the decomposition of SO_2 on pure tungsten small concentrations of CO and CS were recorded. The presence of these substances is explained by the decomposition of hydrocarbon vapors coming from the vacuum pumps. This vapor though at a pressure of 10^{-8} mm. Hg deposits between 20 and 30 atoms of carbon per molecule on the tungsten surface (6, 8), which in turn are immediately transformed to CO and CS.*

†At the temperatures used in this work, the compound WS_2 would be completely dissociated (9).

‡Mass spectrum of CCl_4 with an electron energy of 50 ev.: $CCl_4^+ < 0.1$; $CCl_3^+ = 100.0$; $CCl_2^+ = 26.8$; $CCl^+ = 32.7$; $Cl^+ = 23.8$; $Cl_2 = 2$; $Cl^- = 0.5$.

quently that recourse to some other peak was necessary. A study of the ion CCl_3^+ revealed that though the intensity of this peak decreased with increasing temperature, its appearance potential remained constant at 11.7±0.3 v.† As this figure is much higher than the I.P. of the CCl_3 radical—8.78 volts (2)—it was assumed that the concentration of CCl_3 radicals formed by the decomposition reaction of CCl_4 was insignificantly small and that the intensity of the CCl_3^+ peak at all temperatures was therefore proportional to the concentration of CCl_4 in the system.

The large increase in intensity of the CCl_2^+ peak—see Fig. 4— would indicate that CCl_2 radicals were formed in the reaction. The contribution of these radicals to the CCl^+ peak would readily explain the moderate difference that was found to exist between u and v of CCl^+.

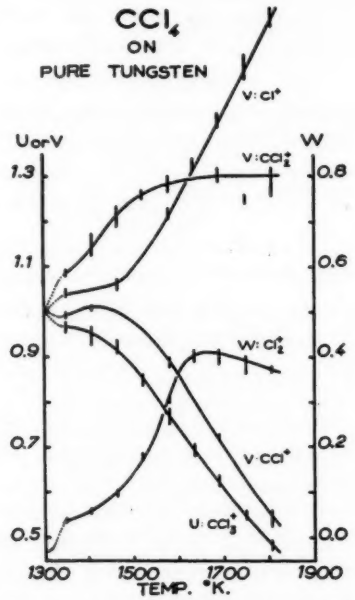

FIG. 4. Relative variations of ion intensities in the mass spectrum of CCl_4 with the temperature of a pure tungsten ribbon.

The decomposition of CCl_4 gave rise not only to CCl_2 radicals but also to chlorine, as can be seen from the increases in intensity of mass 35 and mass 70. It would appear from the curves in Fig. 4 that Cl_2 was the predominant product below 1600° K., while the abundance of Cl atoms assumed a greater importance above 1600° K. This result is supported by the fact that at 1700° K. the A.P. of mass 35 was 13.2±0.2 v., a value which agrees with the I.P. of Cl at 13.00 v. (3). However it must be noted that thermodynamic calculations show that at equilibrium chlorine should leave the ribbon entirely in the atomic state at any of the temperatures here considered.

On carburized tungsten the results were essentially the same as were obtained with pure tungsten, leading to the conclusion that chlorine or chlorinated compounds do not react rapidly—if at all—with carbon dissolved in tungsten as is the case with compounds

†*This result agrees well with two other determinations: 11.67±0.10* (2) *and 11.83±0.05 v.* (13).

containing oxygen or sulphur. This excluded in particular the following interesting reaction:

$$CCl_4 + C_{(w)} \rightarrow 2CCl_2. \qquad [XIII]$$

With the ribbon maintained at 1700° K., the I.P. of the CCl_2 radical was 13.2±0.2 v., and the A.P. of CCl^+ from CCl_2 was 16.3±0.2 v. The A.P.'s of the corresponding ions obtained from CCl_4 were respectively: 16.5±0.2 v. and 19.4±0.1 v. With these figures two different values for the dissociation energy of the (CCl_2—Cl) bond have been calculated. This situation arose from the fact that the nature of the species—Cl, Cl_2, or Cl^-—formed in the ionization–dissociation process along with the positive ions is not known. The energies involved in the formation of these substances are quite large and cannot be overlooked—the electronic affinity of chlorine being 3.8 volts and the dissociation energy of the (Cl—Cl) bond being 2.47 volts. The four possible processes involved in the formation of CCl_2^+ ions from CCl_4 are given in Table I.

TABLE I

ENERGY CHANGES INVOLVED IN THE PROCESSES THAT YIELD CCl_2^+ FROM CCl_4

No.	Ionization process	Δ_I in volts
I*a*	$e^- + CCl_4 \rightarrow CCl_2^+ + 2\,Cl + 2e$	0.0
I*b*	" $\rightarrow$ " $+Cl_2 + 2e^-$	2.47
I*c*	" $\rightarrow$ " $+Cl + Cl^- + e^-$	3.8
I*d*	" $\rightarrow$ " $+2Cl^-$	7.6

Assuming that the particles do not have any excess electronic or kinetic energy, the equation for the A.P. of CCl_2^+ from CCl_4 can be written as follows:

$$[1] \quad A(CCl_2^+, CCl_4) = I(CCl_2) + D(CCl_2—Cl) + D(CCl_3—Cl) - \Delta_I$$

where Δ_I is a term which is readily deduced from the electronic affinity of chlorine or the dissociation energy of the (Cl—Cl) bond, and assumes a different value depending on the process involved (see Table I).

The formation of CCl^+ from CCl_4 can be obtained by five different processes. These have been outlined in Table II along with the various energies Δ_{II} involved, the A.P. equation in this case being:

$$[2] \quad A(CCl^+, CCl_4) = I(CCl) + D(CCl—Cl) + D(CCl_2–Cl) + D(CCl_3—Cl) - \Delta_{II}.$$

The A.P. equation for the formation of CCl^+ from CCl_2 is as follows:

$$[3] \quad A(CCl^+, CCl_2) = I(CCl) + D(CCl—Cl) - \Delta_{III}$$

where Δ_{III} in this case depends on one of two possible processes (see Table III).

TABLE II

ENERGY CHANGES INVOLVED IN THE PROCESSES THAT YIELD CCl^+ FROM CCl_4

No.	Ionization process	Energy Δ_{II} in volts
II*a*	$e^- + CCl_4 \rightarrow CCl^+ + 3Cl + 2e^-$	0.0
II*b*	" $\rightarrow$ " $+Cl_2 + Cl + 2e^-$	2.47
II*c*	" $\rightarrow$ " $+2\,Cl + Cl^- + e^-$	3.8
II*d*	" $\rightarrow$ " $+Cl_2 + Cl^- + e^-$	6.27
II*e*	" $\rightarrow$ " $+Cl + 2Cl^-$	7.6

TABLE III

ENERGY CHANGES INVOLVED IN THE PROCESSES THAT YIELD CCl^+ FROM CCl_2

No.	Ionization process	Energy Δ_{III} in volts
III*a*	$e^- + CCl_2 \rightarrow CCl^+ + Cl + 2e^-$	0.0
III*b*	" $\rightarrow$ " $+Cl^- + e^-$	3.8

Substituting in equations [1], [2], and [3] the numerical values obtained in this work along with the dissociation energy of the bond (CCl_3—Cl) reported recently by Lossing *et al.* (2)—2.95±0.15 v.—two expressions for the dissociation energy of the (CCl_2—Cl) bond were deduced:

(*a*) $D(CCl_2—Cl) = \Delta_I + 0.35 \pm 0.4$ volts,

(*b*) $D(CCl_2—Cl) = \Delta_{II} - \Delta_{III} + 0.15 \pm 0.4$ volts.

An examination of the data given in Tables I, II, and III will show that two and only two solutions will satisfy both equations simultaneously.

First solution: $\Delta_I = \Delta_{II} = 2.47$ v. and $\Delta_{III} = 0$;
hence $D(CCl_2—Cl) = 62 \pm 7$ kcal./mole.

In this case the actual processes involved would be I*b*, II*b*, and III*a*, thus indicating that the ionization–dissociation of CCl_4 tends towards the formation of Cl or even Cl_2 when possible, and away from the formation of Cl^-.

Second solution: $\Delta_I = \Delta_{III} = 3.8$ v. and $\Delta_{II} = 7.6$ v.
hence $D(CCl_2—Cl) = 93 \pm 7$ kcal./mole.

In this case the actual processes involved would be I*c*, II*e*, and III*b*. The tendencies would be reversed, favoring the formation of Cl^-.

The authors are inclined to believe that the first solution is the more likely one. The value 93 kcal./mole for $D(CCl_2—Cl)$ is highly improbable since it is so much greater than that of $D(CCl_3—Cl) = 67.9 \pm 3$ kcal./mole (2).

In the somewhat analogous problem of the four C—H bond dissociation energies in methane, $D(CH_2—H)$ is probably about the same or not much greater than $D(CH_3—H)$.

Furthermore with an electron potential of 50 volts, the intensity of the Cl^- peak was less than 0.005 times the intensity of the CCl_3^+ peak. It could be concluded that negative ions, Cl^-, do not perturb the appearance potential measurements. Restrictions nevertheless have already been made for this type of reasoning (2).

Further results on the influence of the carbon content of tungsten on the heterogeneous reactions of these and other gaseous substances are to be published soon in the "Journal de Chimie Physique".

RÉSUMÉ

On étudie les réactions, à très basse pression et en régime dynamique, de CS_2, H_2S, SO_2 et CCl_4, sur des rubans de tungstène pur ou carburé portés à 1300°–2000° K.

Dans la décomposition de CS_2 sur tungstène *pur*, on observe les particules CS et S_2—dans celle de H_2S, on trouve H_2 et S_2—dans celle de SO_2, on trouve O_2 et SO ou S_2 suivant la température, enfin CCl_4 donne CCl_2, Cl_2 et Cl. Les molécules H_2, S_2 et Cl_2 résultent probablement de la recombinaison sur les parois d'atomes formés sur le ruban. Sur

métal *carburé*, la formation de S_2 et O_2 est remplacée par celle de CS et CO. Par contre, le chlore ne donne lieu à aucune décarburation du métal.

On mesure les potentiels d'ionisation des diverses particules formées et on discute les valeurs des énergies de dissociation de liaisons qui s'en déduisent.

ACKNOWLEDGMENTS

The assistance of Miss Ruth Valentin in obtaining many of the experimental results is gratefully acknowledged.

The work described here was carried out in the laboratories of Professor M. Letort, to whom the authors are indebted for the facilities which were placed at their disposal.

One of us (L.P.B.) is indebted to the National Research Council of Canada for a Postdoctorate Overseas Fellowship.

REFERENCES

1. DYNE, P. J. and RAMSAY, D. A. J. Chem. Phys. **20**, 1055 (1952).
2. FARMER, J. B., HENDERSON, I. H. S., LOSSING, F. P., and MARSDEN, D. G. H. J. Chem. Phys. **24**, 348 (1956).
3. GAYDON, A. G. Dissociation energies. Chapman & Hall, Ltd., London. 1947.
4. LE GOFF, P. J. chim. phys. **53**, 369 (1956).
5. LE GOFF, P. and LETORT, M. Compt. rend. **239**, 970 (1954).
6. LE GOFF, P. and LETORT, M. J. chim. phys. Communication à la 6ème Réunion de la Société de Chimie Physique (Paris—June 1956).
7. LE GOFF, P. and LETORT, M. J. chim. phys. **53**, 480 (1956).
8. LE GOFF, P. and VALENTIN, R. J. chim. phys. (to be published).
9. RICHARDON-JEFFES, F. D. J. Iron Steel Inst. (London), **171**, 167 (1952).
10. SMYTH, H. D. and BLEWETT, J. P. Phys. Rev. **46**, 276 (1934).
11. SMYTH, H. D. and MUELLER, D. W. Phys. Rev. **43**, 121 (1933).
12. ST-PIERRE, G. and CHIPMAN, J. J. Am. Chem. Soc. **76**, 4787 (1954).
13. WARREN, J. W. and CRAGGS, J. D. Mass spectrometry. Institute of Petroleum, London. 1952. p. 36.

NOTES

EFFECT OF pH ON THE SEDIMENTATION OF SERUM ALBUMINS AND OVALBUMIN[1]

P. A. CHARLWOOD[2] AND ADOLF ENS

Recent density measurements (3) in these laboratories have shown that the change in partial specific volume of ovalbumin between pH 5 and pH 2 is in quantitative agreement with expectation, whereas bovine, human, and horse serum albumins show a change less than that predicted from titration data. If this lack of agreement were due to alterations in molecular configuration, these changes could also affect the sedimentation rate. Since no references to the pH dependence of the sedimentation coefficients of ovalbumin and human serum albumin could be found and published data on horse and bovine serum albumins were inadequate, these four proteins were investigated over the pH range 2 to 10.

The proteins were taken from the batches used in the density studies (3), stock solutions in many cases being identical. Immediately before sedimentation measurements, the protein solutions, which had been dialyzed near pH 5, were mixed with suitable buffers to give a protein concentration of 0.32 to 0.36% and a total ionic strength of 0.2, of which 0.15 was due to potassium chloride. A few samples of bovine serum albumin, after being examined close to pH 2.8, were redialyzed to pH 2.0 or pH 6.6.

Sedimentation measurements were made at 59,780 r.p.m. in a Spinco ultracentrifuge, in the usual way. Ten photographs were taken at 8-minute intervals during each run. The rotor temperature was automatically controlled at 25.0° C.

The results (Fig. 1), corrected to water at 20° C. using the partial specific volume values recently obtained at pH 5 (3), refer to finite protein concentrations, but will differ only slightly from values extrapolated to zero concentration (5, 7), and will show the same variation with changes in pH. Ovalbumin shows a constant value of $s_{20,w}$ in the ranges pH 1.9 to 3.5 and pH 4.0 to 9.7, a barely perceptible increase occurring between pH 3.5 and pH 4.0. The sedimentation coefficients of the three serum albumins show a pronounced rise between pH 2 and pH 5, and then either remain constant or decrease slightly. The results of Svedberg and Sjögren (9) for horse serum albumin show the same trend as those in Fig. 1, but are rather widely scattered, a result partially attributable to their wider range of protein concentration.

An aggregate appeared in bovine serum albumin solutions near pH 2.8, which seemed to dissociate almost reversibly on dialysis to lower or higher pH (Fig. 2). Saroff *et al.* (8) and Bro *et al.* (1), studying 1% solutions of this protein at low pH in the ultracentrifuge, have also observed aggregates. Points shown on the curve in Fig. 1 refer only to the non-aggregated component. Harrington *et al.* (5), working with bovine serum albumin between pH 2 and pH 5, obtained results similar to those recorded in Fig. 1.

Apart from this exception, no evidence for alterations in the molecular weights of the albumins at low pH was found (5, 7, 11, 12). The striking alterations in the sedimentation coefficients of the serum albumins between pH 5 and pH 2 must, therefore, be ascribed

[1]*Issued as N.R.C. No. 4149.*

[2]*Present address: The National Institute for Medical Research, The Ridgeway, Mill Hill, London, N.W.7, England.*

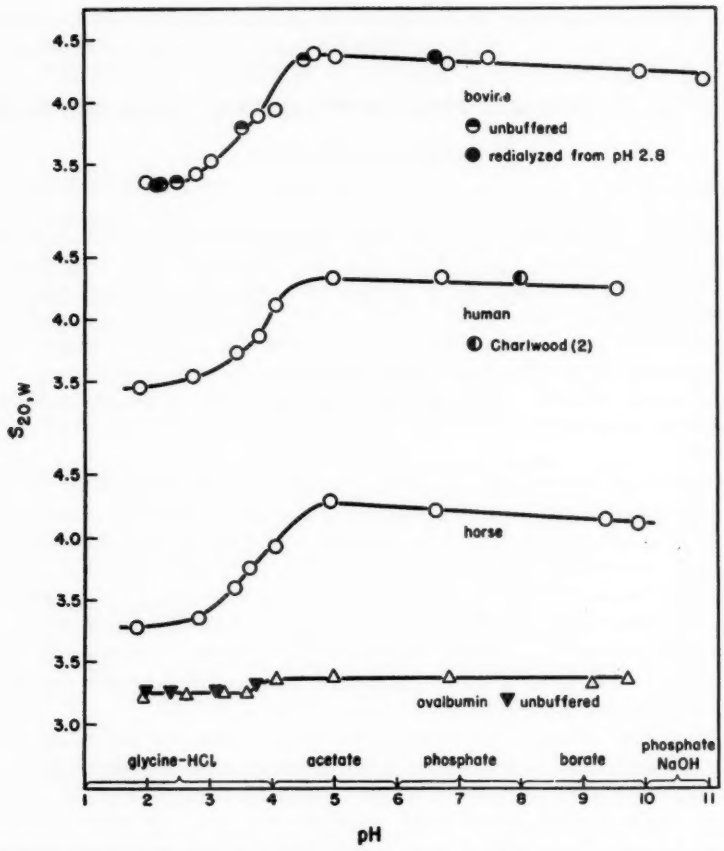

FIG. 1. Sedimentation coefficients of albumins as a function of pH at ionic strength 0.2. (Protein concentration approximately 0.35%.)

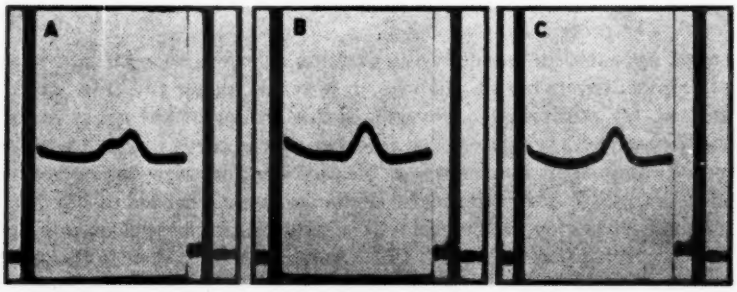

FIG. 2. Ultracentrifuge patterns of bovine serum albumin (0.35%) in ionic strength 0.2 solution, 80 minutes after top speed (59,780 r.p.m.) was reached. Sedimentation is from right to left: (A) pH 2.8; (B) pH 6.6, redialyzed from pH 2.8; (C) pH 2.0, redialyzed from pH 2.8.

to an expansion or unfolding of the molecules, for which evidence has also been adduced on other grounds (10, 11, 12). The exact nature of this molecular alteration is still a matter of discussion (6).

The concept of an extension or expansion of the serum albumin molecules accords with the partial specific volume findings. The increase of $\bar{v}$ between pH 5 and pH 2 is much less than that expected on the basis of titration data. This would be accounted for if the altered configuration of the protein molecules at the lower pH permitted solvent to reach hitherto inaccessible, or "excluded", regions. Between pH 5 and pH 10, where the experimentally observed change in partial specific volume agrees with the calculated value, the change of sedimentation coefficient is small, or possibly zero.

The sedimentation coefficient of ovalbumin appears to be slightly, but significantly, lower in the low pH range. This indicates a small change in the molecular configuration, far less marked than for the serum albumins, and evidently too slight to be detected by density measurements. This behavior is in accord with other evidence indicating that the ovalbumin molecule is a fairly rigid compact structure which usually undergoes major alterations irreversibly (4).

The technical assistance of Mr. D. Muirhead is gratefully acknowledged.

1. Bro, P., Singer, S. J., and Sturtevant, J. M. J. Am. Chem. Soc. **77**, 4924 (1955).
2. Charlwood, P. A. Biochem. J. **51**, 113 (1952).
3. Charlwood, P. A. J. Am. Chem. Soc. (In press).
4. Frensdorff, H. K., Watson, M. T., and Kauzmann, W. J. Am. Chem. Soc. **75**, 5157 (1953).
5. Harrington, W. F., Johnson, P., and Ottewill, R. H. Biochem. J. **62**, 569 (1956).
6. Hill, T. L. J. Phys. Chem. **60**, 358 (1956).
7. Reichmann, M. E. and Charlwood, P. A. Can. J. Chem. **32**, 1092 (1954).
8. Saroff, H. A., Loeb, G. I., and Scheraga, H. A. J. Am. Chem. Soc. **77**, 2908 (1955).
9. Svedberg, T. and Sjogren, B. J. Am. Chem. Soc. **52**, 2855 (1930).
10. Tanford, C. Proc. Iowa Acad. Sci. **59**, 206 (1952).
11. Tanford, C., Buzzell, J. G., Rands, D. G., and Swanson, S. A. J. Am. Chem. Soc. **77**, 6421 (1955).
12. Yang, J. T. and Foster, J. F. J. Am. Chem. Soc. **76**, 1588 (1954).

Received September 9, 1956.
Division of Applied Biology,
National Research Council of Canada,
Ottawa, Canada.

NATURE OF THE ADSORPTION PROCESS RESPONSIBLE FOR JOSHI EFFECT

C. N. Ramachandra Rao

The Joshi effect (2, 3, 4) (Δi) is the instantaneous and reversible variation of the discharge current observed when a gas discharge tube excited by an electric field is irradiated with a light source. This variation can be either a decrease or an increase in the current. On a cathode-ray oscillograph this effect is observed as a variation in the amplitude and/or number of pulses. While a decrease in the current due to irradiation is referred to as the negative Joshi effect ($-\Delta i$), an increase in the current is referred to as the positive Joshi effect ($+\Delta i$). One of the important steps in the mechanism of Joshi effect is the formation of an adsorption layer on the container walls due to adsorption of ions and excited particles. Although there is no direct experimental evidence to show that the adsorption process is fundamental to Joshi effect, many experimental results seem to support such a point of view.

In this note, the nature of the adsorption process which is responsible for Joshi effect is discussed on the basis of a careful examination and analysis of experimental results.

(i) It has been found that in order to initiate Joshi effect in a freshly prepared discharge tube, it is necessary to "age" (maintain the discharge for a period of time) the tube at a constant potential (V) (3, 9). This time-development of the effect has been found to be a rate process, following the first order reaction rates (6). All the stages in the production of Joshi effect are instantaneous and fully reversible and consequently the time-development of Δi under "aging" is determined by the slowest step, the formation of the adsorption layer on the walls of the vessel. (ii) The kinetics of "aging" and the magnitude of $-\Delta i$ depend on the surface of the electrodes and that of the vessel (7). Coatings of polar substances like potassium chloride are found to increase the magnitude of $-\Delta i$ markedly. (iii) The influence of "aging" on the magnitude of Joshi effect is more prominent in soft soda glass vessels rather than in hard glass vessels or Geissler tubes (9). It is interesting to note that formation of surface compounds under discharge on the walls of the vessel (like NaCl in chlorine, NaBr in bromine, NaOH in water vapor, etc., due to combination with Na^+ ions liberated under discharge because of the electrolytic conduction of glass) is also greater on soft soda glass vessels (12). (iv) Δi is observed only at potentials, $V > V_m$, where V_m is the threshold potential of the discharge. The threshold potential of a discharge has been defined as that potential at or above which only chemical reactions can take place under discharge (2).

It has been often stated that physical adsorption is instantaneous and chemisorption takes time. So, physical adsorption of a gas would be complete within the first $\sim$5 minutes after the introduction of the gas into the vessel. Although no definite generalizations can be made about the various possible species of particles produced in a discharge and the nature of their adsorption on glass, it is highly probable that chemisorption associated with large activation energy is fundamental to the formation of the adsorption layer, being particularly favored under discharge conditions (5). Accordingly, Mohanty finds that the energy of activation of the reaction during "aging" is of a high order (8). The non-occurrence of Joshi effect in inert gases is possibly due to their negligible chemisorption on glass under electrical discharge (1).

In the light of the above findings it can be seen that any theory of Joshi effect based on the physical adsorption of gases or vapors on the walls of the discharge tube is not feasible. Ramaiah (10), on the basis of his observation that Joshi effect in water vapor in a cleaned and degassed vessel was appreciable without "aging" and that "aging" disfavored the effect, concludes that physical adsorption of the gas is primary to the production of the Joshi effect. However, "aging" was found necessary to initiate the effect in iodine vapor even in a thoroughly cleaned and degassed vessel, by Saxena and the author (11). Since physical adsorption of a gas is determined by the critical temperature of the gas, it may be considerable in the case of chlorine or water vapor at laboratory temperatures. But the negative Joshi effect is observed (even up to 100% current suppression) in gases like hydrogen, oxygen, nitrogen, etc., the critical temperatures of which are very low compared to that of water vapor. It is therefore not possible to account for these observations on the basis of the physical adsorption of the gases on glass. On the other hand, it can be said that the magnitude of Joshi effect is more pronounced on surfaces favoring chemisorption or surface compound formation. Naturally, any such surface phenomenon as Joshi effect will be affected by the slightest change in the conditions of the surface of the vessel or the electrodes.

ACKNOWLEDGMENT

The author's thanks are due to Professor J. M. Honig, Department of Chemistry, Purdue University, for his helpful suggestions.

1. CAMPBELL, N. R. and WARD, H. Phil. Mag. **43**, 914 (1922).
2. JOSHI, S. S. Presidential Address, Chemistry Sect., Indian Science Congress. 1943.
3. JOSHI, S. S. Current Sci. (India), **8**, 548 (1939); **12**, 535 (1943); **13**, 253 (1944); **14**, 67 (1945); **15**, 281 (1946); **16**, 19 (1947).
4. JOSHI, S. S. Proc. Indian Acad. Sci. **14**, 317 (1945); **22**, 225 (1945); Nature, **154**, 147 (1944).
5. MCBAIN, J. W. The sorption of gases by solids. George Routledge & Sons, Ltd., London. 1932.
6. MOHANTY, S. R. J. Ind. Chem. Soc. **28**, 487 (1951); MURTHY, M. V. R. J. Ind. Chem. Soc. **25**, 255 (1948).
7. MOHANTY, S. R., RAO, T. D. P., and RAMAIAH, R. J. Sci. Ind. Research, **13B**, 144 (1954); MOHANTY, S. R. J. Sci. Ind. Research, **13B**, 145 (1954).
8. MOHANTY, S. R. J. Chem. Phys. **21**, 1908 (1953).
9. RAMAIAH, N. A., KALE, M. N., and SAXENA, A. P. Proc. Indian Sci. Congr., Chem. Sect., A, **92** (1953).
10. RAMAIAH, N. A. J. Sci. Ind. Research, **10A**, 182 (1951).
11. SAXENA, A. P. and RAO, C. N. R. J. Sci. Research Agra Univ. **3**, 207 (1954).
12. WILLOWS, R. S. Phil. Mag. **6**, No. 1, 503 (1901).

RECEIVED JULY 3, 1956.
DEPARTMENT OF CHEMISTRY,
PURDUE UNIVERSITY,
WEST LAFAYETTE, INDIANA, U.S.A.

CANADIAN JOURNAL OF CHEMISTRY

Notes to Contributors

Manuscripts

(i) ***General.*** Manuscripts, in English or French, should be typewritten, double spaced, on paper 8½ × 11 in. **The original and one copy are to be submitted.** Tables and captions for the figures should be placed at the end of the manuscript. Every sheet of the manuscript should be numbered.

Style, arrangement, spelling, and abbreviations should conform to the usage of this journal. Names of all simple compounds, rather than their formulas, should be used in the text. Greek letters or unusual signs should be written plainly or explained by marginal notes. Superscripts and subscripts must be legible and carefully placed.

Manuscripts and illustrations should be carefully checked before they are submitted. Authors will be charged for unnecessary deviations from the usual format and for changes made in the proof that are considered excessive or unnecessary.

(ii) ***Abstract.*** An abstract of not more than about 200 words, indicating the scope of the work and the principal findings, is required, except in Notes.

(iii) ***References.*** References should be listed **alphabetically by authors' names,** numbered, and typed after the text. The form of the citations should be that used in this journal; in references to papers in periodicals, titles should not be given and only initial page numbers are required. The names of periodicals should be abbreviated in the form given in the most recent *List of Periodicals Abstracted by Chemical Abstracts.* All citations should be checked with the original articles and each one referred to in the text by the key number.

(iv) ***Tables.*** Tables should be numbered in roman numerals and each table referred to in the text. Titles should always be given but should be brief; column headings should be brief and descriptive matter in the tables confined to a minimum. Vertical rules should be used only when they are essential. Numerous small tables should be avoided.

Illustrations

(i) ***General.*** All figures (including each figure of the plates) should be numbered consecutively from 1 up, in arabic numerals, and each figure referred to in the text. The author's name, title of the paper, and figure number should be written in the lower left corner of the sheets on which the illustrations appear. Captions should not be written on the illustrations (see Manuscripts (i)).

(ii) ***Line Drawings.*** Drawings should be carefully made with India ink on white drawing paper, blue tracing linen, or co-ordinate paper ruled in blue only; any co-ordinate lines that are to appear in the reproduction should be ruled in black ink. Paper ruled in green, yellow, or red should not be used unless it is desired to have all the co-ordinate lines show. All lines should be of sufficient thickness to reproduce well. Decimal points, periods, and stippled dots should be solid black circles large enough to be reduced if necessary. Letters and numerals should be neatly made, preferably with a stencil (**do NOT use typewriting**) and be of such size that the smallest lettering will be not less than 1 mm. high when reproduced in a cut of suitable size.

Many drawings are made too large; originals should not be more than 2 or 3 times the size of the desired reproduction. In large drawings or groups of drawings the ratio of height to width should conform to that of a journal page but the height should be adjusted to make allowance for the caption.

The original drawings and one set of clear copies (e.g. small photographs) are to be submitted.

(iii) ***Photographs.*** Prints should be made on glossy paper, with strong contrasts. They should be trimmed so that essential features only are shown and mounted carefully, with rubber cement, on white cardboard with no space or only a very small space (less than 1 mm.) between them. In mounting, full use of the space available should be made (to reduce the number of cuts required) and the ratio of height to width should approximate that of a journal page (5½ × 7½ in.); however, allowance must be made for the captions. Photographs or groups of photographs should not be more than 2 or 3 times the size of the desired reproduction.

Photographs are to be submitted in duplicate; if they are to be reproduced in groups one set should be mounted, the duplicate set unmounted.

Reprints

A total of 50 reprints of each paper, without covers, are supplied free. Additional reprints, with or without covers, may be purchased.

Charges for reprints are based on the number of printed pages, which may be calculated approximately by multiplying by 0.5 the number of manuscript pages (double-spaced typewritten sheets, 8½ × 11 in.) and including the space occupied by illustrations. An additional charge is made for illustrations that appear as coated inserts. The cost per page is given on the reprint requisition which accompanies the galley.

Any reprints required in addition to those requested on the author's reprint requisition form must be ordered officially as soon as the paper has been accepted for publication.

Contents

Printed in Canada by University of Toronto Press